MARMARA UNIVERSITY
INSTITUTE FOR GRADUATE STUDIES
IN PURE AND APPLIED SCIENCES

INVESTIGATION OF $PM_{2.5}$ AND HOURLY SEMI VOLATILE ORGANIC COMPOUNDS IN ATMOSPHERIC AEROSOLS

AKIN EMRECAN GÖK

MASTER THESIS
Department of Environmental Engineering

Thesis Supervisor
Assist. Prof. Dr. Rosa FLORES

ISTANBUL, 2017

MARMARA UNIVERSITY
INSTITUTE FOR GRADUATE STUDIES
IN PURE AND APPLIED SCIENCES

INVESTIGATION OF $PM_{2.5}$ AND HOURLY SEMI VOLATILE ORGANIC COMPOUNDS IN ATMOSPHERIC AEROSOLS

AKIN EMRECAN GÖK

(524315821)

MASTER THESIS

Department of Environmental Engineering

Thesis Supervisor

Assist. Prof. Dr. Rosa FLORES

ISTANBUL, 2017

MARMARA UNIVERSITY

INSTITUTE FOR GRADUATE STUDIES IN PURE AND APPLIED SCIENCES

Akın Emrecan GÖK, a Master of Science student of Marmara University Institute for Graduate Studies in Pure and Applied Sciences, defended his thesis entitled "**Investigation of $PM_{2.5}$ and Hourly Semi Volatile Organic Compounds in Atmospheric Aerosols**", on ....17/01/2018..... and has been found to be satisfactory by the jury members.

Jury Members

(Advisor)

Yr. Doç. Dr. Rafa M. Flaes Rangel ..... (SIGN).....
Marmara Üniversitesi

(Jury Member)

Dr. Hüseyin Özdemir ..... (SIGN).....
(İstanbul Teknik Üniversitesi)

(Jury Member)

Doç. Dr. Bülent Oktay Gaga ..... (SIGN).....
Marmara Üniversitesi

APPROVAL

Marmara University Institute for Graduate Studies in Pure and Applied Sciences Executive Committee approves that Akın Emrecan GÖK be granted the degree of Master of Science in Department of Environmental Engineering, Environmental Engineering Program on ..22.01.2018... (Resolution no: 2018/02-02).

Director of the Institute

Prof. Dr. Bülent EKİCİ
Enstitü Müdürü

ACKNOWLEDGMENT

First of all, I would like to thank my advisor Assist. Prof. Rosa FLORES for providing me the chance to study on this topic, her immense knowledge and wise guidance throughout the all processes of this thesis.

I would like to express my deepest gratitude for the constant support and love that I received from my family and my friends.

I also want to thank TUBITAK and BAP for their financial support [Project number: TUBITAK-115Y625, FEN-C-YLP-090217-0060], Bahcesehir University, and IETT (Besiktas) for use of their facilities. I appreciate the data provided by the Ministry of Environment and Urbanization, Department of Transportation, and Turkish State Meteorological Center. Meteorological data was also obtained from Weather Underground.

Last but not least, I must thank to all my teachers from Çukurova University, Department of Environmental Engineering where I learned how to be an engineer.

Akın Emrecan GÖK

October, 2017, Istanbul

TABLE OF CONTENTS

ÖZET

ATMOSFERİK AEROSOLLERDEKİ $PM_{2.5}$ VE SAATLİK YARI UÇUCU ORGANİK BİLEŞİKLERİN İNCELENMESİ

Organik bileşikler kaynaklarına, taşınmasına ve dönüşümüne bağlı olarak atmosferdeki askıda partiküler maddenin (PM) büyük bir bölümünü oluşturur. Organik aerosoller (OA) insan sağlığı, ekosistem ve iklim değişikliğinde önemli bir role sahiptir. Emisyon kaynakları, bileşimlerinin zamana bağlı değişimleri ve kimyasal reaksiyonlara katılımları hakkındaki yetersiz bilgiler, etkileri hakkında belirsizlikler yaratmaktadır. Organik aerosol bileşimleri hakkındaki çalışmalar genellikle 24 saatlik yapılmakta ve bir çok bileşik çalışma dışında kalmaktadır. Turkiye'de organik aerosollerin kimyasal formlarının saptanması konusunda çalışmalar yetersiz durumdadır. Organik bileşimlerin yüksek reaktivitesi sebebiyle çalışmaların kısa zaman aralıklı toplanan örneklerle gerçekleştirilmesi gerekli bir durumdur. Bu çalışmanın ana amaçları yoğun trafiğe sahip bir bölge olan Beşiktaş, İstanbul için yarı uçucu organik bileşiklerin varlıklarının tanımlanması ve 2.5 µm den küçük partiküler maddelerin ($PM_{2.5}$) günlük değişimlerinin anlaşılmasıdır. Bu amaçla, $PM_{2.5}$ numuneleri 2 saatlik aralıklarla 7:00-19:00 saatleri arasında kış mevsiminde toplandı ve toplam 24 numune termal desorpsiyon bağlı gaz kromatografi/kütle spektometresi (TD-GC-MS) sistemi ile analiz edildi. Organik aerosol bileşiminin kalitatif ve kantitatif analizi, hafta sonu/hafta içi ve sıcaklık, solar radyasyon ve hava kütlesi hareketleri gibi meteorolojik şartlar için sunulmuştur. Sonuçlar 11 polisiklik aromatik hidrokarbon (PAH) ve 28 n-alkan için tanımlamaları göstermektedir. Ayrıca, numune alınan bölgenin hafta içi ve hafta sonu, gün boyunca trafik yoğunluğundan son derece etkilendiği görülmüştür.

ABSTRACT

INVESTIGATION OF $PM_{2.5}$ AND HOURLY SEMI VOLATILE ORGANIC COMPOUNDS IN ATMOSPHERIC AEROSOLS

Organic compounds comprise a large fraction of atmospheric suspended particulate matter (PM) according to their origin, transport, and transformation. Organic aerosols (OA) have an important role in human health, ecosystems, and climate change. However, uncertainties of their impacts are large due to gaps in knowledge regarding emission sources, change in composition with respect to time, and participation in chemical reactions. Studies of organic aerosol composition are generally performed every 24 h and many compounds are not included. In Turkey, chemical speciation of organic aerosol has been scarcely studied. Collection of high-time resolved samples is necessary due to high reactivity of the organic compounds. The main objectives of this work are to identify the presence of semi-volatile organic compounds and understand their diurnal variations in PM smaller than 2.5 μm ($PM_{2.5}$) in a traffic-influenced area in Besiktas, Istanbul. For this reason, $PM_{2.5}$ samples were collected for two-hour periods (7:00-19:00h) during the winter. A total of 24 samples were analyzed with thermal desorption coupled to gas chromatography/mass spectrometry (TD-GC-MS). Qualitative and semi-quantitative analysis of OA composition is presented during the weekend and weekdays and with meteorological conditions such as temperature, solar radiation, and air mass trajectories. Results show the identification of 11 PAH and 28 n-alkanes. It was also observed that the receptor site is strongly dependent on traffic density variations during weekend/weekdays and during the day.

ABBREVIATIONS

AAP **:** Ambient Air Pollution

BC **:** Black Carbon

CCN **:** Cloud Condensation Nuclei

EC **:** Elemental Carbon

EI **:** Electron Impact

GC **:** Gas Chromatography

HAP **:** Household Air Pollution

IN **:** Ice Nucleation

MS **:** Mass Spectrometry

OA **:** Organic Aerosol

OC **:** Organic Carbon

PAH **:** Polycyclic Aromatic Hydrocarbons

PCB **:** Polychlorinated Biphenyl

PM **:** Particulate Matter

POA **:** Primary Organic Aerosols

POP **:** Persistent Organic Pollutants

SOA **:** Secondary Organic Aerosols

SVOC **:** Semi Volatile Organic Compounds

TD **:** Thermal Desorption

TSP **:** Total Suspended Particles

VOC **:** Volatile Organic Compounds

LIST OF FIGURES

LIST OF TABLES

1. INTRODUCTION

The main objectives of this work are to identify the presence of semi-volatile organic compounds and understand their diurnal variations in particulate matter smaller than 2.5 μm ($PM_{2.5}$) in a traffic-influenced area in Besiktas, Istanbul. For this reason, $PM_{2.5}$ samples were collected for two-hour periods (7:00-19:00h) during the winter. A total of 24 samples were analyzed with thermal desorption coupled to gas chromatography/mass spectrometry (TD-GC-MS). Qualitative and semi-quantitative analysis of organic aerosol (OA) composition is presented during the weekend and weekdays and with meteorological conditions such as temperature, solar radiation, and air mass trajectories.

In Turkey, continuous measurement of PM_{10} and $PM_{2.5}$ concentrations are available through the Ministry of Environment and Urbanization. In Istanbul, PM_{10} concentrations are available in 28 stations. In contrast, only 6 stations are currently measuring $PM_{2.5}$ concentrations continuously (i.e., Aksaray, Goztepe, Kagithane, Silivri, Umraniye, and Umraniye-MTHM). Currently, the average annual PM_{10} and $PM_{2.5}$ air quality standards are 50 and 12 $\mu g/m^3$, respectively. The air quality in Istanbul considerably improved in 1996 due to the establishment of natural gas pipelines across the country and a regulation to use coal with less than 1.5% sulfur content (Tayanc, 2000). However, it has been reported multiple times that average concentrations of PM_{10} continuously exceed the established limits (Karaca et al., 2005; Unal et al., 2011). In addition to PM_{10} and $PM_{2.5}$ concentrations, criteria pollutants in the gas phase (i.e., NO, NO_2, SO_2, CO, and O_3) are continuously monitored by the Ministry of Environment and Urbanization. However, detailed chemical speciation studies are limited (Karaca et al., 2008). Specially, studies performed at high-time resolved intervals are not available.

Studies about semi-volatile organic compounds (SVOCs) are generally performed every 24 h and many compounds are not included. Short sampling times are important because SVOCs are highly reactive. In Turkey, chemical speciation of organic aerosol has been scarcely studied (Karaca et al., 2008; Ozdemir et al., 2014). OC and EC concentrations in daily PM_{10} were studied for approximately 10 days in July 2008-June 2009 (Theodosi et al., 2010). Concentrations of black carbon (BC) have been also investigated in Istanbul in the spring seasons of 2009 and 2010. Hanedar et al., (2014) and Ozdemir et al., (2014) studied the seasonal variation and sources of 16 PAHs in total suspended particles (TSP).

Kuzu et al., (2014) studied the concentration of 84 PCB during the summer and fall in the gas and particle phases. Understanding sources, transformation, and fate of organic aerosol in the atmosphere is essential to determining effects on human health and global radiation balance (Williams et al., 2007). The hourly measurements of SVOCs associated to $PM_{2.5}$ that can be provided by the method developed in this study will be among the first ones carried out in urban environments on a global level, thus the development and validation of a method have a great importance.

Especially in Turkey, thermal desorption usage in the air quality monitoring is very limited. Using thermal desorption and developing a proper method for air quality monitoring in ambient air of Istanbul is a significant work for literature.

1.1. Atmospheric Aerosols

Atmospheric aerosols are particles that are suspended in the air in liquid or solid phase. The physical and chemical properties of aerosols are important for direct and indirect climate change prediction.

Aerosols also have an important role in radiation balance and in the lifetime and properties of clouds by absorbing and scattering solar radiation (i.e., direct effect) and acting as cloud condensation nuclei, CCN, (i.e., indirect effect), respectively. The physicochemical properties of atmospheric aerosols determine their role at absorbing and scattering radiation. Atmospheric aerosols are in the size range close to the wavelength of the visible radiation (i.e., 0.39-0.7 μm). Thus, due to their longer lifetime in the atmosphere, fine aerosols are expected to have greater impact on climate change due to their interaction with solar radiation and water vapor. Black carbon (BC) absorbs radiation, therefore contributes to the warming of the atmosphere. On the other hand, most organic PM components are considered to cool the atmosphere (Kanakidou et al., 2005).

For all type of climate influence, the most important characteristic of aerosols is the size distribution. Light scattering per unit mass for aerosols that are smaller than micrometer size is higher. In addition, they stay in the atmosphere longer than larger aerosols. Aerosols have a significant negative effect on the total radiative forcing. They have a direct effect because they scatter and absorb atmospheric solar and infrared radiation.

Aerosols increase droplet number and ice particle concentrations and can change the ice, warm, or mixed-phase cloud formation process. They also decrease the precipitation efficiency of warm clouds thus they have indirect radiative effect together with the cloud property changes.

The indirect effect of aerosols is defined as the influence of aerosols on cloud albedo and cloud lifetime. Various physicochemical properties of aerosols determine the magnitude of the aerosol indirect effect. Some of these physicochemical properties include aerosol mass, concentration of organic compounds acting as CCN, concentration of organic compounds acting as ice nucleation (IN), ability of the organic compounds to partition into the water phase, cloud optical depth, among others. Chemical composition of aerosols as a function of size is important for the number of CCN per mass of aerosol (Penner et al., 2001).

Various interdependences and feedbacks for atmospheric aerosols are given in Figure 1.1. The resulting feedback loops of Figure 1.1 are important for environmental pollution and climate change because of quantitative assessment, reliable prediction, and efficient control necessity of natural and anthropogenic aerosol effects on climate and public health.

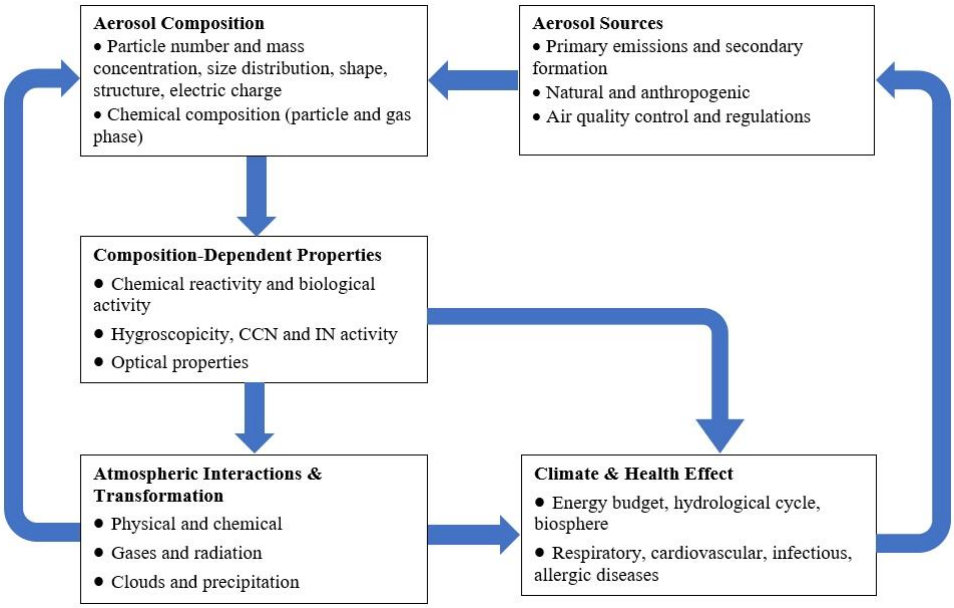

Figure 1.1. Interdependence and feedback between atmospheric aerosol composition, sources, properties, interactions and transformation, and climate and health effects (Poschl, 2005).

1.2. Fine Aerosols

Particulate Matter (PM) term defines the solid or liquid matter in microscopic sizes suspended in the air. Particulate matter can be generated both, through human activities and naturally; however, fine particles emitted by human activities have more important effects on human health and climate change. The $PM_{2.5}$ term defines particles with diameter smaller than 2.5 μm and the increased concentrations are of special concern because these particles move through the respiratory system and accumulate there (Weschler and Nazaroff, 2008). $PM_{2.5}$ particles contain organic and elemental carbon, trace metals, sulphates, nitrates, minerals and oxidized forms of these minerals (Ding et al., 2014). The composition and relative abundance of PM vary according to its origin. Thus, organic compounds comprise a large fraction of the atmospheric aerosol mass in the range 20-90%. These organic compounds can contain numerous complex forms such as aromatics, alcohols, alkanes, and carboxylic acids; most of them toxic for life forms (Hsiao et al., 2000). Some of these compounds are named as semi volatile organic compounds (SVOC) and are generally identified as organic molecules that can be abundant in both the gas phase and condensed phase, represented by vapor pressures between 10^{-14} and 10^{-4} atm. SVOC origins are mainly due to human products such as cleaning agents, food packaging, clothing, furniture, electronics, and pesticides. Some SVOCs cause biological disorders and some kinds of cancer because of their ability to affect hormones in humans and wildlife. In addition, SVOCs can cause neurodevelopmental and behavioral problems and diseases like autism, reproductive abnormalities and metabolic disorders (Weschler and Nazaroff, 2008).

1.2.1. Sources of aerosols

Semi-volatile organic compounds are highly reactive and contribute to the formation of secondary organic aerosol, SOA, (Derwent et al., 2010). Despite their active role on climate change and effects on ecosystems and human health, their sources, reaction mechanisms, removal processes, and climate and health effects are highly uncertain (Jimenez et al., 2009). This lack of understanding is partly due to deficiency of suitable methodologies to quantitatively measure and identify the thousands of compounds with very different physicochemical properties that comprise the organic aerosols. Figure 1.2

shows the sources of aerosol particles that are emitted from natural sources. (Andreae, 2007).

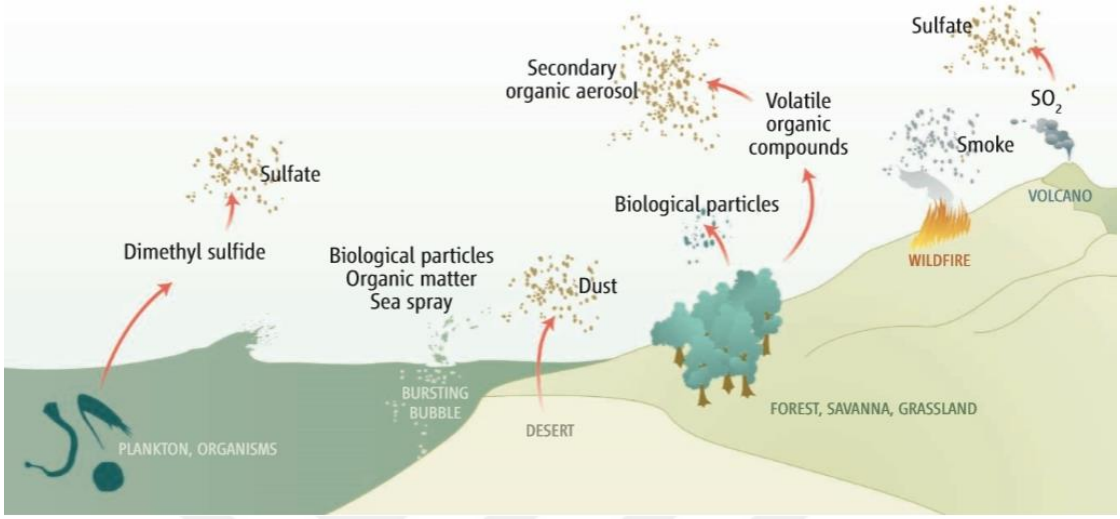

Figure 1.2. Sources of aerosol particles (Andreae, 2007).

1.2.1.1. Vegetation

The first showing of the direct emission of organic particulates by vegetation was in 1970s by Arpino et al., (1972) and Schnell and Vali, (1973). They showed the source is the small particles of epicuticular wax that is emitted by stress in plant leaves. Later Beauford et al., (1975) studied these particles and showed that they have sizes up to a length of 200 nm and a width of 30 nm and they can travel 5000– 6000 km of distance in the atmosphere (Gagosian et al., 1982).

1.2.1.2. Bioaerosol

Bioaerosols are atmospheric particles that are living organisms or released by living organisms. They are large molecules containing living organisms that were released by living organisms, mostly from plants. Bioaerosol particles are plant debris (cuticular waxes, leaf fragments, etc.), pollen, algae, yeast, mold, fungi, bacteria, mycoplasma, viruses, protozoa, and nematodes. These particles can also contain cell fragments which are much smaller than original cells. They may have particle size from 10 nm to 100 µm and widely vary on particle shape (Gelencsér, 2004). Plant substances make the

bioaerosol light absorbing particles in the UV-B region (Havers et al., 1998). (Schnell and Vali, 1976) proved that bioaerosol particles can act both as cloud droplet and ice nuclei.

1.2.1.3. Soil dust

Soil dust is one of the biggest part of aerosol sources, especially in sub-tropical and tropical regions. It contributes to aerosol loading and optical thickness. Dust mainly comes from deserts, dry lake beds and similar areas, but also from surfaces with human activities or with low vegetation. Dust deflation depends on grain size, soil moisture and surface roughness which are main elements of the threshold velocity that generates dust deflation when the surface wind speed exceeds it. Crusting of the surface of the floors and limiting the usability of the particles may reduce dust release from a source region (Gillette, 1978). Dust mobilization can be strongly increased by human activities. Estimations show that up to 50% of the current atmospheric dust load comes from human activities such as disturbed soil surfaces (Tegen and Fung, 1995).

Particle size of the dust determines its atmospheric lifetime. If the particles are large they are removed quickly by gravitational settling, if the particles are small like sub-micron scale they can stay for several weeks in the atmosphere. Some models for regional and global scales of dust mobilization and transport have been developed (Marticorena et al., 1997; Miller and Tegen, 1998).

1.2.1.4. Ocean

Sea salt aerosols are the main aerosols emitted by the ocean. They are generated by physical processes like bursting of mixed air bubbles during whitecap formation that depends on wind speed (Monahan et al., 1986). For regions with marine atmosphere, if the wind speed is high and other aerosol sources weak sea salt aerosols may be the dominant fraction for light scattering and CCN (O'Dowd et al., 1997). For aerosol indirect effects, they are very important because of their high efficiency to act as CCN (Feingold et al., 1999).

Sea salt aerosols have a range of diameter between 0.05 to 10 mm and also wide range of life times at atmosphere. Emissions and distribution at the atmosphere is important and

many model development studies for sea salt aerosols have been done for these reasons (Erickson and Duce, 1988; Gong et al., 1997; Tegen et al., 1997).

Surfactants, such as protein degradation products was found in marine aerosol in 1964 for the first time (Blanchard, 1964). This surface active organic material on the sea-salt aerosol particles is far too much higher than the bulk seawater. Part of this difference is due to the accumulation of the surfactant on the bulk air-water interface, and also the organic material adsorbed or scavenged by the bubbles while the bulk rises to the water surface (Gelencsér, 2004). This ejection height of the bubbles which depends on their kinetic energy can be observed experimentally (Blanchard and Syzdek, 1972).

1.2.1.5. Industrial dust

Primary resources of the industrial dust as primary aerosol particles are industrial and technical activities like transportation, cement factoring, waste incineration, coal combustion and metallurgy. Industrial aerosol particles are the most important anthropogenic aerosol particles because of their hazardous impact on environmental quality. Andreae (1995) estimates the emission of industrial dust aerosol as 100 Tg/yr and Wolf and Hidy, (1997) estimate about 200 Tg/yr. Because of the importance of these particles, they are strictly monitored and regulated. They are generally wider than 1 μm diameter and not optically very active.

1.1.1.1 Carbonaceous aerosols (Soot, Black Carbon, Elemental Carbon)

Carbonaceous aerosols are a very big fraction of atmospheric aerosols and vary largely. Carbonaceous aerosol particles form during combustion, consisting predominantly of organic carbon (>50%), with lesser amounts of oxygen and hydrogen, significant amounts of ash and exhibiting an imperfect graphitic structure. Main sources of these aerosols are fossil fuel burning, biomass burning and atmospheric oxidation of biogenic and anthropogenic VOCs (Penner et al., 2001).

Soot is an incomplete combustion by-product of fossil fuels, biofuels and biomass burning. It is an undesired by-product and its physical properties depend on its source with high variability (Long et al., 2013). It is also named as black carbon (BC), elemental carbon (EC) and graphitic carbon even though there are numerous definitions for these terms.

The black carbon term was applied due to the ability that this aerosol has to absorb visible light. Because of this characteristic of the particle, optical methods are normally used for their determination (Gelencsér, 2004).

Black carbon is a very important atmospheric aerosol because of its solar radiation absorption, influencing on cloud processes (indirect effects), reducing albedo by depositing on snow and ice cover (direct effects) (Bond et al., 2013).

Fossil-fuel soot is generally black because it contains mainly black carbon which is strongly light-absorbing. It is emitted by combustion of diesel, jet fuel, kerosene and coal combustion and consists mainly black carbon and primary organic matter. Meanwhile, biofuel soot particles, which are emitted from burning of wood and organic waste for home heating and cooking, are generally brown colored because the ratio of organic carbon to black carbon that they contain is higher than diesel soot, and organic carbon absorbs short light wavelengths. Also, some particles appear gray or white depending on the hydration of liquid water to ions or solutes within them. Similar to biofuel, biomass burning soot has the same fractions but often higher primary organic matter to black carbon ratio (Jacobson, 2010).

1.3. Semi-Volatile Organic Compounds

SVOCs can be defined as compounds that have boiling points higher than 250 °C, are composed mainly of hydrogen and carbon, and have vapor pressures less than 0.1 mmHg at standard temperature and pressure.

SVOCs can be defined differently depending on their boiling point, vapor pressure or photo-chemical reactivity.

The importance of the SVOCs is their capability of adsorbance onto airborne particles, as well as their presence in the vapor phase. This characteristic makes them important for airborne particle pollution monitoring as much as VOCs even though they have not historically been regarded as being relevant to ambient air monitoring.

However, it is recognized that certain groups of compounds familiar with the components of the material and indoor air emissions may continue to exist within the larger environment.

These compounds, commonly referred to as persistent organic pollutants (POPs), are normally dispersed in soil and water, but are found in air even in "pristine" environments such as polar regions (Hung et al., 2016).

For this reason, SVOCs have become the focal point of various investigations because it is important to understand the physical and chemical mechanisms they play in their global distribution and the possible negative effects on ecosystems.

These semi-volatile contaminants consist of compounds such as aldehydes, ethers, esters, phenols, organic acids, ketones, amines, amides, nitroaromatics, PCBs, PAHs, phthalate esters, nitrosamines and trihalomethanes. They have broad chemical properties and structural features.

PAHs and *n*-alkanes are expected SVOCs to be seen in the sampling area according to their sources.

1.3.1. Polycyclic aromatic hydrocarbons (PAHs)

PAHs are hydrocarbons that consist of various aromatic rings. They occur naturally in coal, petroleum (crude oil), and gasoline. They can result from the incomplete combustion of organic matter. They also are produced when coal, oil, gas, wood, garbage, and tobacco are burned. PAH sources like motor vehicle exhaust, cigarette smoke, wood smoke, high-temperature cooking of meat and similar foods, or fumes from asphalt roads can bind to or form small particles in the air. They have significant contribution to environmental pollution and suspected carcinogenicity (Fetzer, 2007).

Even though, there are natural processes that emit PAHs to the environment, they are mainly anthropogenic because of their sources like coal burning, wood burning or gas and oil burning as in traffic, residential heating, industrial uses, power generation, forest fires, waste incineration processes.

Most important effect of PAHs on human health is their carcinogenicity. Studies on animal models show that they can cause skin, lung, bladder, liver, and stomach cancers and has also been linked with cardiovascular diseases (Boström et al., 2002).

1.3.2. Alkanes

Alkanes are basically defined as acyclic saturated hydrocarbons. They have tree structure with single carbon-carbon bonds consist of only carbon and hydrogen atoms. Their general chemical formula is C_nH_{2n+2}. The simplest alkane form is CH_4, methane which is n=1 (Moss et al., 1995).

In this study, main compounds of interest are C14-C40 *n*-alkanes. *n*-alkanes are linear alkane compounds where there are no branches or cycles.

Alkanes have two main sources as petroleum (oil) and natural gas. Natural gas contains primarily methane and ethane, with some propane and butane. Petroleum is a mixture of liquid alkanes and other hydrocarbons.

Liquid alkanes that are bigger than nonane form the major part of diesel fuel and aviation fuel. Alkanes like hexadecane characterize the diesel fuel. Alkanes that are bigger than hexadecane are important components of fuel oil because they are hydrophobic compounds (Arora, 2006). Most of the alkanes are used like paraffin wax such as candles. Because of this reason, they have been called as *n*-paraffins, years before they named correctly.

Organic air pollutant compounds are produced by anthropogenic and natural sources (Rogge et al., 1993a, 1993b). Typical sources of *n*-alkanes from human activities are mainly combustion of fossil fuels, wood and agricultural debris or leaves. Also, direct suspension of pollen, micro-organisms, insects and plant particles like epicuticular waxes are natural sources (Simoneit et al., 1977). At the same time with their contribution as *n*-alkane sources, anthropogenic activities such as wood and coal burning, automobile exhaust, heat and power generation and incomplete combustion of fossil fuels are also really important PAH sources.

1.4. Air pollution in Megacities

Megacities are defined as cities that have a population exceeding 10 million (UN, 2014). They have become a worldwide problem with their rapidly growing populations. In 1970, there were only two megacities in the world which were New York and Tokyo with more than 10 million residents. In 2011, the total number became 23 megacities in the world. As of 2017 there are 37 megacities with more than 10 million population and a total of

84 urban areas have more than 5 million population. This shows an accelerated trend of growth in megacity urbanization. Today megacities have 10 percent of the world's population despite covering 0.2 percent of the world's surface area (Demographia, 2017). Most of the megacities are in undeveloped and developing countries. This is making the disadvantages of megacities such as pollution, lack of resources, unplanned urbanization etc. worse when compared to developed countries. When it considered that the more than half of the population of the world is living in the urbans instead of rural areas, the importance of urban areas becomes clearly visible.

Megacities have a wide range of influences on the environment. The dense population of these cities releases sufficiently great amounts of emissions to pollute the air. This air pollution is not a problem for only the city that emits but also for a wide range of the city area. For primary particulate matter (PM) and black carbon average transportation distance is up to 200 km and the maximum distance more than 2000 km (Butler and Lawrence, 2009). A study for Mexico City showed that ozone and aerosol particles production were distributed for hundreds of kilometers (Molina et al., 2010). Also, these pollutants can distribute over national borders and transport between continents. This makes the air pollution of megacities a global problem including climate change (Molina et al., 2004). This shows that the impacts of megacities are not just local but can be regional and more than that global (Baklanov et al., 2016).

Figure 1.3 is a **s**chematic showing the work of Baklanov et al. in 2010 that was a European research project. Baklanov et al., suggested these linkages between megacities, air quality and climate. In addition to the overall connections between these three main subjects, the figure also shows the main feedbacks, ecosystem, health and weather impact pathways, and mitigation routes which was investigated in their project that was named as MEGAPOLI (Megacities: Emissions, urban, regional and Global Atmospheric POLlution and climate effects, and Integrated tools for assessment and mitigation) (Baklanov et al., 2010). According to this study wood burning during winter and cooking activities during both summer and winter made strong contributors to primary organic aerosol, in addition to traffic-related emissions. The major organic aerosol fraction during summer was secondary organic aerosol that was mostly of biogenic origin and secondary aerosol build-up due to anthropogenic emissions has been observed (Stock et al., 2013).

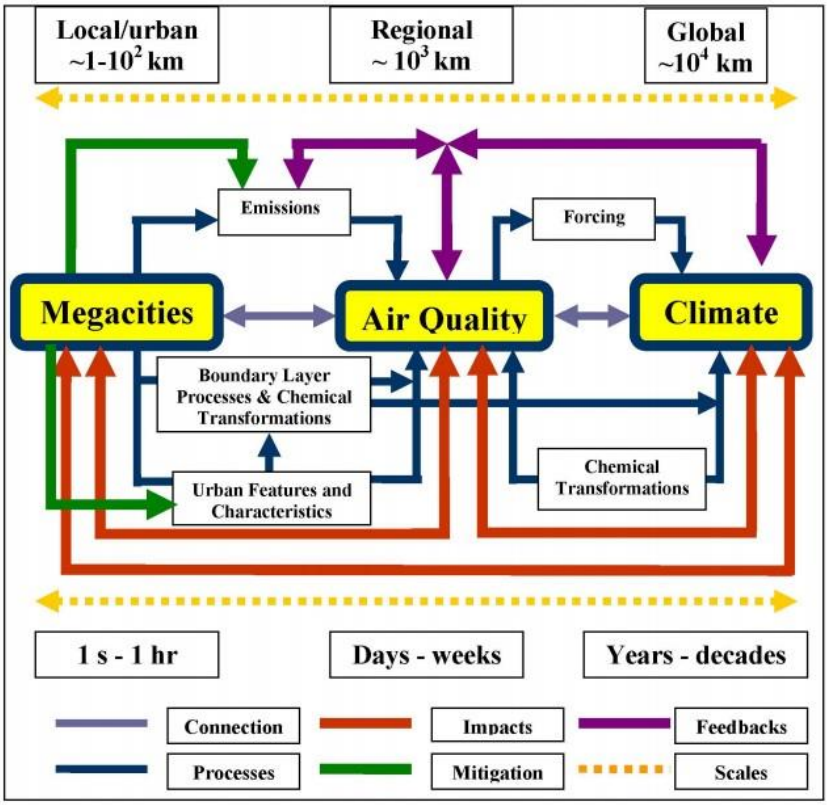

Figure 1.3. Schematic showing the main linkages between megacities, air quality and climate (Baklanov et al., 2010).

Megacities have impacts of air quality that can have significant effects on human health, natural environment, visibility, haze, or smog. Ambient air pollution (AAP) caused 3.7 million deaths only in 2012, while 4.3 million deaths are caused by household air pollution (HAP) in the same year (WHO, 2016). Ambient air pollution is one of the biggest megacity problems and the most harmful pollutants are $PM_{2.5}$ which are emitted by diesel vehicles and coal fire (Zhu et al., 2012). Each year, ambient air pollution causes 350,000 to 500,000 premature deaths in China (Chen et al., 2013).

Istanbul is the biggest city of Turkey and as of 2016 the city has 14,804,116 inhabitants (TurkStat, 2016). With this population, it is the twenty-third biggest megacity of the world (Demographia, 2017). As a megacity, Istanbul has problems as much as other megacities including air pollution. Effects like unplanned urbanization, industrialization, atmospheric conditions, meteorological parameters, construction, and population density are the reasons for the rise of air pollution of the city. Istanbul is the most important city in Turkey and one of the most important cities of the world due to its geological

transcontinental location, grandness on population, and industry. The main reasons of air pollution in Istanbul are (1) the excessive use of low quality fossil fuels for residential heating and transportation, (2) continuous expansion on industrial areas, (3) rising vehicle number and traffic, (4) insufficient green areas, and (5) unplanned urbanization (Tayanc, 2000).

According to "Institute for Health Metrics and Evaluation" data, 23,602 people in 2005, 21,921 people in 2010 and 26,675 people in 2015 died prematurely from ambient PM exposure in Turkey (IHME, 2016). Figure 1.4 shows the premature death counts from ambient PM exposure on a global scale (approximately 7.5%) and in Turkey (approximately 8% since 2010).

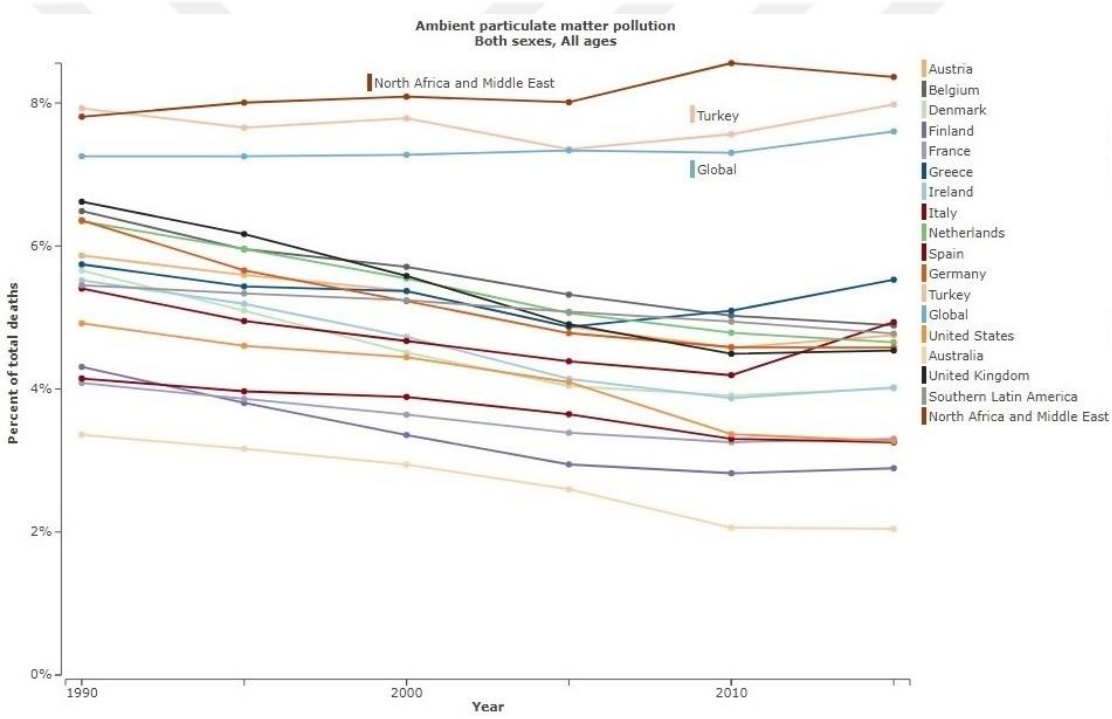

Figure 1.4. Percentage of all causes of deaths attributable solely to ambient particulate matter pollution by years in global scale and in Turkey (IHME, 2017).

Even though this specific kind of air pollution has all these risks and hazards, there are not any scientific research about the concentrations of these compounds in the air or how to analyze the samples accurately. It is important to study the biggest city of the Turkey in this topic to understand its air pollution problems at the same time with developing the correct method to achieve this.

2. MATERIALS

The main work of the study was the part of developing a method for investigation of organic compounds in ambient air samples. For this reason, more than 200 analyses were made with mixtures of target analytes. The method used by (Bates et al., 2008) was used as an example for the study. Except that their method was used only for 7 polycyclic aromatic hydrocarbons (PAH) but this study has approximately 70 target compounds to investigate. Due to the wide range of volatilities in the target compounds a new TD-GC-MS method has been developed as a quantitative and reproducible method, also it is a method that is recovering as much as possible from the PM samples.

Basically, the method can be summarized as: A predetermined piece of the filter that is used as a sorbent for collecting ambient air is punched and put inside a sample tube. Inside of this sample tube is plugged with glass wool for retaining the filter and preventing it from moving through the system. Then the tube is placed into the tube desorption oven where the tube is heated rapidly (~150°C/min).

In this heating process, there is helium flow through the tube to the cold trap. The sample that is released from the adsorbed filter goes to the cold trap with this flow and traps the compounds at a colder temperature. After this step, the cold trap heats and releases the compounds through the transfer line to GC (Figure 2.1).

The GC has an inlet that connects its column to the transfer line that is coming from thermal desorber. After compound mixture reaches the inlet they go through the column where they are separated according to their volatilities. While more volatile compounds move faster through the column less volatile compounds move slower. That makes the mixture of compounds separate and leave the column one by one. Once a compound leaves the column it reaches the mass spectrometer where it is ionized and identified according to their signature ions.

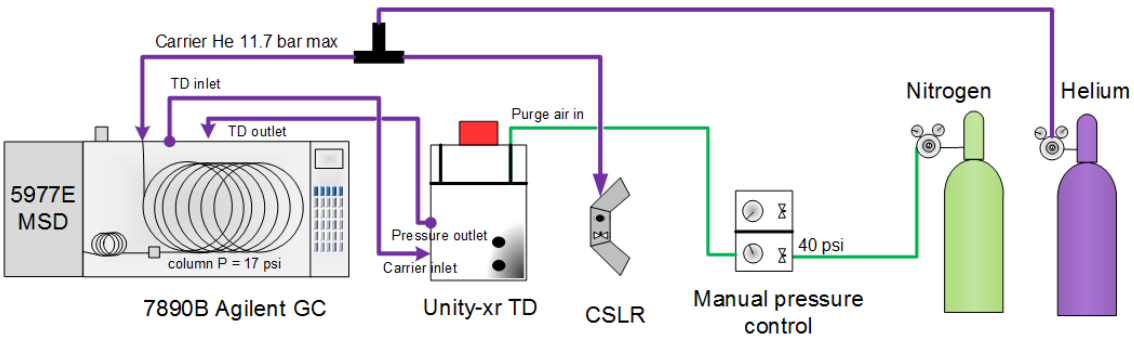

Figure 2.1. Diagram of TD-GC-MS system that was used in the study.

2.1. Chemicals

A total of 69 target SVOC analytes were selected as representative for a broad range of SVOCs based on their functional groups and availability. Table 2.1 shows the physical properties that aid in the identification of these target analytes.

Table 2.1. Target compounds and their physical properties.

Target compound name	Functional group	Formula	Molecular weight	BP (°C)
Methyltertbutylether[1]	straight alkane, O	$C_5H_{12}O$	88,148	55
Benzene[1]	aromatic	C_6H_6	78,11	80,1
Heptane[3]	n-alkane	C_7H_{16}	100,2	98
Toluene[1]	branched aromatic	C_7H_8	92,138	110
Octane[3]	n-alkane	C_8H_{18}	114,23	125,7
Ethylbenzene[1]	branched aromatic	C_8H_{10}	106,17	135
p,m,o-xylene[1]	branched aromatic	C_8H_{10}	106,17	140
Nonane[3]	n-alkane	C_9H_{20}	128,26	150,8
1,3,5-trimethylbenzene[1]	branched aromatic	C_9H_{12}	120,19	165
1,2,4-trimethylbenzene[1]	branched aromatic	C_9H_{12}	120,19	169
Decane[3]	n-alkane	$C_{10}H_{22}$	142,28	174
1,3-diethylbenzo[l]	branched aromatic	$C_{10}H_{14}$	134,22	182
Undecane[3]	n-alkane	$C_{11}H_{24}$	156,31	195
Dodecane[3]	n-alkane	$C_{12}H_{26}$	170,33	216
Naphthalene[1]	PAH	$C_{10}H_8$	128,17	217
Naphthalene[2]	PAH	$C_{10}H_8$	128,17	218
Tridecane[3]	n-alkane	$C_{13}H_{28}$	184,36	234
Tetradecane[3]	n-alkane	$C_{14}H_{30}$	198,39	250
Pentadecane[3]	n-alkane	$C_{15}H_{32}$	212,41	267
Acenaphthene[2]	PAH	$C_{12}H_{10}$	154,21	279,2
Acenaphthylene[2]	PAH	$C_{12}H_8$	152,19	280,2

Table 2.1. Target compounds and their physical properties (continued).

Target compound name	Functional group	Formula	Molecular weight	BP (°C)
Hexadecane[3]	n-alkane	$C_{16}H_{34}$	226,44	281
Fluorene[2]	PAH	$C_{13}H_{10}$	166,22	298,2
Heptadecane[3]	n-alkane	$C_{17}H_{36}$	240,47	302
Heneicosane[3]	n-alkane	$C_{21}H_{44}$	296,57	306
Octadecane[3]	n-alkane	$C_{18}H_{38}$	254,49	316,3
Nonadecane[3]	n-alkane	$C_{19}H_{40}$	268,52	330
Phenanthrene[2]	PAH	$C_{14}H_{10}$	178,23	336,2
Anthracene[2]	PAH	$C_{14}H_{10}$	178,23	340,2
Eicosane[3]	n-alkane	$C_{20}H_{42}$	282,55	343,2
Docosane[3]	n-alkane	$C_{22}H_{46}$	310,6	368,8
Fluoranthene[2]	PAH	$C_{16}H_{10}$	202,25	375
Tricosane[3]	n-alkane	$C_{23}H_{48}$	324,63	380,2
Tetracosane[3]	n-alkane	$C_{24}H_{50}$	338,65	391
Pyrene[2]	PAH	$C_{16}H_{10}$	202,25	393
Pentacosane[3]	n-alkane	$C_{25}H_{52}$	352,68	402,1
Hexacosane[3]	n-alkane	$C_{26}H_{54}$	366,71	412
Heptacosane[3]	n-alkane	$C_{27}H_{56}$	380,73	422
Octacosane[3]	n-alkane	$C_{28}H_{58}$	394,76	431,8
Benz[a]anthracene[2]	PAH	$C_{18}H_{12}$	228,29	437,8
Nonacosane[3]	n-alkane	$C_{29}H_{60}$	408,79	441
Chrysene[2]	PAH	$C_{18}H_{12}$	228,29	448,2
Triacontane[3]	n-alkane	$C_{30}H_{62}$	422,81	450
Hentriacontane[3]	n-alkane	$C_{31}H_{64}$	436,84	458
Dotriacontane[3]	n-alkane	$C_{32}H_{66}$	450,87	467,2
Tritriacontane[3]	n-alkane	$C_{33}H_{68}$	464,89	474
Benzo[k]fluoranthene[2]	PAH	$C_{20}H_{12}$	252,31	480,2
Tetratriacontane[3]	n-alkane	$C_{34}H_{70}$	478,92	483
Pentatriacontane[3]	n-alkane	$C_{35}H_{72}$	492,95	490,2
Benzo[a]pyrene[2]	PAH	$C_{20}H_{12}$	252,31	495,2
Hexatriacontane[3]	n-alkane	$C_{36}H_{74}$	506,97	497
Benzo[ghi]perylene[2]	PAH	$C_{22}H_{12}$	276,33	500
Nonatriacontane[3]	n-alkane	$C_{39}H_{80}$	549,05	517,5
Dibenz[a,h]anthracene[2]	PAH	$C_{22}H_{14}$	278,35	524,2
Indeno[1,2,3-cd]pyrene[2]	PAH	$C_{22}H_{12}$	276,33	164 (Melting °C)
Benzo[b]fluoranthene[2]	PAH	$C_{20}H_{12}$	252,31	166 (Melting °C)
Heptatriacontane[3]	n-alkane	$C_{37}H_{76}$	521	77 (Melting °C)
Octatriacontane[3]	n-alkane	$C_{38}H_{78}$	535,03	79 (Melting °C)
Tetracontane[3]	n-alkane	$C_{40}H_{82}$	563,08	81 (Melting °C)

[1]PVOC Mixture 3 (Wisconsin),
[2]PAH Calibration Mix TraceCERT,
[3]C7-C40 Saturated Alkane Mixture.

Analytical standards obtained as commercial neat chemicals with the highest purity available (> 97%) from LGC standards, Alpha Aesar, Acros Organics, Sigma Aldrich, and Supelco. Multi-compound dilution mixtures were prepared in the range 10^{-3}-10^{2} ng. There were total of 3 mixture solutions which are PVOC Mixture 3 (Wisconsin), PAH Calibration Mix TraceCERT, C7-C40 Saturated Alkane Mixture as calibration mixtures and other compounds were separate.

Acenaphthene

Acenaphthylene

Anthracene

Benz[a]anthracene

Benzo[a]pyrene

Benzo[b]fluoranthene

Benzo[ghi]perylene

Benzo[k]fluoranthene

Chrysene

Dibenz[a,h]anthracene

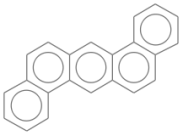

Fluoranthene

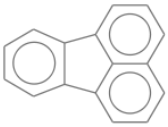

Fluorene

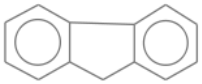

Indeno[1,2,3-cd]pyrene

Naphthalene

Phenanthrene

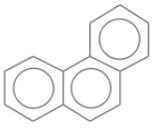

Pyrene

n-alkanes[1]

Figure 2.2. Chemical structures of target compounds.

[1]all *n*-alkanes have the same linear structure except their length is the only difference.

2.1.1. Solubility predictions of the target compounds

Mixtures of solvents are investigated and the solvent that provides optimum solubility are chosen. Methanol, dichloromethane, and iso-octane are initially considered as solvents. For choosing which one of these three solvents is the best for solubility of a target compound, Abraham's general solvation model is used to predict the solubility of each target compounds.

The Abraham method assumes that the partition coefficient between water and a solvent, P_s, is given by the ratio of solubilities of a solute in the solvent, S_s, and in water, S_w,

$$P_S = \frac{S_S}{S_w} \tag{2-1}$$

If this assumption is reasonable for the solute and solvent in question, then the solubility of the solute in the solvent can be calculated from the predicted partition coefficient,

$$\log P_S = c + eE + sS + aA + bB + vV \tag{2-2}$$

where the continually refined (as more experimental data becomes available) coefficients c, e, s, b, and v vary by solvent and E, S, A, B, and V are solute descriptors, described as follows (Mintz, 2009):

E is the solute excess molar refractivity in units of (cubic cm per mol)/10. It represents the solute's polarizability and gives a measure of the ability of a solute to interact with a solvent through n- and π- electron pairs.

S is the solute dipolarity/polarizability. It gives a measure of the solute's ability to stabilize a charge or dipole

A is the overall (summation) hydrogen bond acidity. The hydrogen bond acidity descriptor measures the extent of hydrogen bonding by the solute in a basic solvent.

B is the overall (summation) hydrogen bond basicity. The hydrogen bond basicity descriptor measures of the extent of hydrogen bonding by the solute in an acidic solvent.

V is the McGowan characteristic volume in units of (cubic cm per mol)/100.

Abraham et al., (2010) is used for getting measured Abraham descriptors of target compounds. Table 2.2 shows the Abraham descriptors for each target compounds.

Table 2.2. Abraham descriptors of the target compounds.

Compound name	E	S	A	B	V	L
Methyltertbutylether	0,024	0,22	0	0,55	0,872	2,372
Benzene	0,61	0,52	0	0,14	0,716	2,786
Heptane	0	0	0	0	1,095	3,173
Toluene	0,601	0,52	0	0,14	0,857	3,325
Octane	0	0	0	0	1,236	3,677
Ethylbenzene	0,613	0,51	0	0,15	0,998	3,778
P-xylene	0,613	0,52	0	0,16	0,998	3,839
M-xylene	0,623	0,52	0	0,16	0,998	3,839
O-xylene	0,663	0,56	0	0,16	0,998	3,939
Nonane	0	0	0	0	1,377	4,182
1,3,5-trimethylbenzene	0,649	0,52	0	0,19	1,139	4,344
1,2,4-trimethylbenzene	0,677	0,56	0	0,19	1,139	4,441
Decane	0	0	0	0	1,518	4,686
1,3-diethylbenzol	0,637	0,5	0	0,18	0,979	-
Undecane	0	0	0	0	1,659	5,191
Dodecane	0	0	0	0	1,799	5,696
Naphthalene	1,326	0,791	0	0,205	1,085	-
Naphthalene	1,326	0,791	0	0,205	1,085	-
Tridecane	0	0	0	0	1,94	6,2
Tetradecane	0	0	0	0	2,081	6,705
Pentadecane	-	-	-	-	-	-
Acenaphthene	1,781	0,982	0	0,237	1,259	-
Acenaphthylene	1,54	1,122	0	0,21	1,216	-
Hexadecane	0	0	0	0	2,363	7,714
Fluorene	1,604	1,06	0	0,248	1,357	-
Heptadecane	-	-	-	-	-	-
Heneicosane	0	0	0	0	3,068	10,236
Octadecane	-	-	-	-	-	-
Nonadecane	-	-	-	-	-	-
Phenanthrene	2,122	1,344	0	0,171	1,454	-
Anthracene	2,12	1,376	0	0,25	1,454	-
Eicosane	0	0	0	0	2,927	9,731
Docosane	0	0	0	0	3,208	10,74
Fluoranthene	3,127	1,664	0	0,296	1,585	-
Tricosane	0	0	0	0	3,349	11,252
Tetracosane	0	0	0	0	3,49	11,758
Pyrene	3,13	1,528	0	0,327	1,585	-
Pentacosane	0	0	0	0	3,631	12,264
Hexacosane	0	0	0	0	3,772	12,77
Heptacosane	0	0	0	0	3,913	13,276
Octacosane	0	0	0	0	4,054	13,78
Benz[a]anthracene	2,992	1,7	0	0,33	1,823	10,291
Nonacosane	-	-	-	-	-	-
Chrysene	3,027	1,73	0	0,36	1,823	10,33

Table 2.2. Abraham descriptors of the target compounds (continued).

Compound name	E	S	A	B	V	L
Triacontane	-	-	-	-	-	-
Hentriacontane	-	-	-	-	-	-
Dotriacontane	0	0	0	0	4,617	15,79
Tritriacontane	-	-	-	-	-	-
Benzo[k]fluoranthene	3,19	1,91	0	0,33	1,954	11,607
Tetratriacontane	-	-	-	-	-	-
Pentatriacontane	-	-	-	-	-	-
Benzo[a]pyrene	3,625	1,96	0	0,37	1,954	11,736
Hexatriacontane	0	0	0	0	5,181	17,74
Benzo[ghi]perylene	4,073	1,9	0	0,48	2,084	13,26
Nonatriacontane	-	-	-	-	-	-
Dibenz[a,h]anthracene	4	2,04	0	0,44	2,192	12,96
Indeno[1,2,3-cd]pyrene	-	-	-	-	-	-
Benzo[b]fluoranthene	3,194	1,82	0	0,4	1,954	11,632
Heptatriacontane	-	-	-	-	-	-
Octatriacontane	-	-	-	-	-	-
Tetracontane	-	-	-	-	-	-

Table 2.3 shows the predicted solubilities of target compounds for methanol, dichloromethane and iso-octane.

Table 2.3. Predicted solubilities of target compounds for methanol, dichloromethane and iso-octane.

Compound name	methanol	dichloromethane	iso-octane
Methyltertbutylether	10.748	2,407	4.223
Benzene	9.065	2.408	2.161
Heptane	9.921	11.946	1.284
Toluene	14.226	3.834	2.645
Octane	13.575	16.834	1.356
Ethylbenzene	18.523	5.273	2.758
P-xylene	16.785	4.541	2.513
M-xylene	16.825	4.594	2.532
O-xylene	17.083	4.220	2.502
Nonane	17.078	21.700	1.326
1,3,5-trimethylbenzene	18.433	5.029	2.307
1,2,4-trimethylbenzene	18.662	4.554	2.258
Decane	5,273.618	6,866.174	318.446
1,3-diethylbenzol	0.865	0.247	0.144
Undecane	69.469	92.677	3.262
Dodecane	127.983	174.918	4.681
Naphthalene	7.398	1.449	1.082
Naphthalene	7.398	1.449	1.082

Table 2.3. Predicted solubilities of target compounds for methanol, dichloromethane and iso-octane (continued).

Compound name	methanol	dichloromethane	iso-octane
Tridecane	267.200	374.191	7.598
Tetradecane	584.145	838.208	12.916
Pentadecane	-	-	-
Acenaphthene	1.956	0.297	0.224
Acenaphthylene	0.452	0.035	0,04
Hexadecane	3,514.704	5,295.047	46.983
Fluorene	2.077	0.204	0.169
Heptadecane	-	-	-
Heneicosane	783,986.709	1,334,027.554	2,978.422
Octadecane	-	-	-
Nonadecane	-	-	-
Phenanthrene	1.417	0.098	0,079
Anthracene	0.938	0.051	0.058
Eicosane	231,539.291	384,508.372	1,131.299
Docosane	2,689,482.359	4,688,401.541	7,958.776
Fluoranthene	0.467	0.023	0.030
Tricosane	9,535,702.648	17,032,711.876	21,940.944
Tetracosane	34,596,861.262	63,320,276.117	61,896.245
Pyrene	0.085	0.006	0.007
Pentacosane	131,437,926.722	246,491,416.180	182,840.879
Hexacosane	476,875,158.888	916,348,767.380	515,801.143
Heptacosane	1,853,910,226.073	3,650,226,385.061	1,559,162.210
Octacosane	7,375,181,286.375	14,879,173,228.208	4,822,811.635
Benz[a]anthracene	0.141	0.005	0.006
Nonacosane	-	-	-
Chrysene	0.113	0.004	0.005
Triacontane	-	-	-
Hentriacontane	-	-	-
Dotriacontane	1,871,477,887,232.825	4,161,173,269,418.304	448,112,749.048
Tritriacontane	-	-	-
Benzo[k]fluoranthene	0.475	0.011	0.013
Tetratriacontane	-	-	-
Pentatriacontane	-	-	-
Benzo[a]pyrene	0.089	0.002	0.003
Hexatriacontane	490,818,247,013,165	1,202,961,698,741,938	42,955,947,211
Benzo[ghi]perylene	0.099	0.004	0.004
Nonatriacontane	-	-	-
Dibenz[a,h]anthracene	0.216	0.006	0.006
Indeno[1,2,3-cd]pyrene	-	-	-
Benzo[b]fluoranthene	0.267	0.007	0.009

Predicted solubility values show that dichloromethane is the best solvent option to choose. It has the optimum values for all compounds.

2.2. Sample Tubes

Empty glass thermal desorption tubes with 89 mm body length, 6.4 mm outer diameter and 4 mm internal diameter were used for insertion of the samples. Thermal desorption glass tubes were conditioned by thermal cleaning with temperatures that range 250-350 ℃ during 10-20 min under a flow rate of high purity Helium. The conditioning of the tubes is a 4-stage process: (1) conditioning at 250 ℃ for 20 min, (2) conditioning at 300 ℃ for 20 min, (3) conditioning at 330 ℃ for 20 min, (4) conditioning at 350 ℃ for 20 min. 4 stages take place in order. Also for subsequent uses, preconditioning at 320 ℃ for 10 min was applied to the sample tubes. A figure of the empty glass thermal desorption tubes can be seen as figure 2.3.

Figure 2.3. A thermal desorption glass tube.

2.3. Glass wool

Glass wool is made up of short non-flammable glass fibers. Glass wool are used as plugs inside of the thermal desorption tubes to keep non-volatile material from entering the system. It can also be used in packed GC columns, solvent desorption tubes, thermal desorption tubes, and purge traps to retain adsorbent beds. It is widely considered as a thermal insulation material in ships, automobiles, air conditioning ducts and water supply pipes (Japan, 2012).

2.3.1. Cleaning the glass wool

“Supelco Silanized Glass Wool” was used in the study as plugs inside the thermal desorption tubes. Due to the high peaks of silane compounds in the chromatography of the glass wool, a necessity of combustion appeared. A method for cleaning the glass wool

was developed. Firstly, the glass wool was cleaned by immersing in methanol 3 times then in dichloromethane also 3 times. After this immersing step glass wool was conditioned by thermal cleaning with 290 ℃ for 30 minutes. This process was repeated for two times and the cleaned glass wool as the final product is used for analysis. Figure 2.4 shows the chromatograms of newly unpacked dirty glass wool (analysis of "glasswool1a" as black line) and cleaned glass wool (analysis of "glasswool5blank1" as blue). It can be seen clearly that the cleaning method is working well for cleaning the silane group peaks.

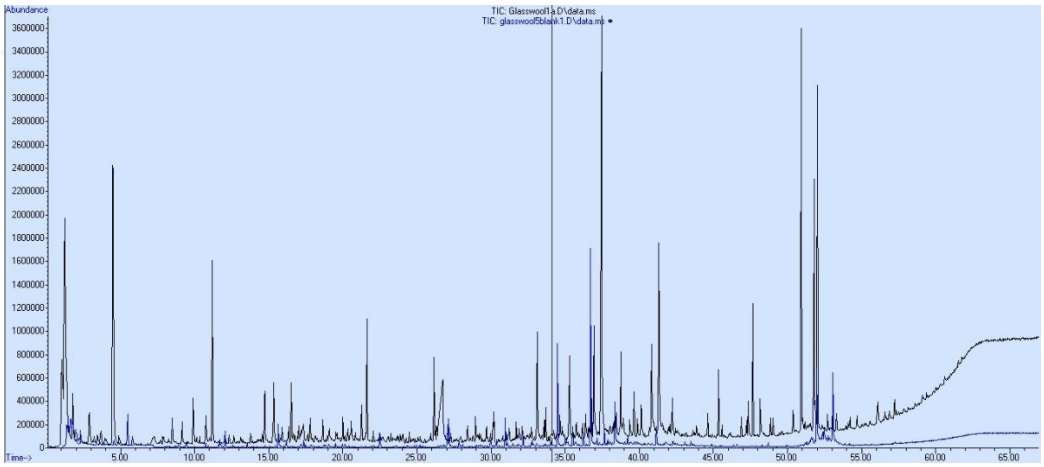

Figure 2.4. Overlaid chromatograms of newly unpacked dirty glass wool.
*(analysis of "glasswool1a" as black line) and cleaned glass wool (analysis of "glasswool5blank1" as blue).

2.4. Sampler

Ambient air particle sampling was performed with a "Tisch TE-PNY1123 Mass Flow Controlled High Volume Air Sampler". Figure 2.5 shows the scheme of the high volume ambient air sampler.

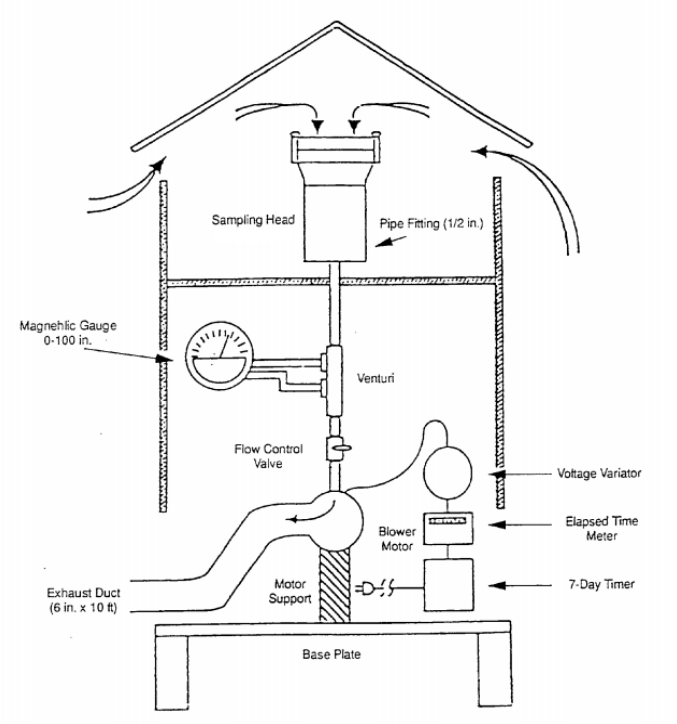

Figure 2.5. Scheme of the high-volume sampler used in the study.

The sampler that was used in this study is a high volume ambient air sampler. The difference between high and low volume air samplers is the amount of air sampled. High volume air samplers generally sample more than 1500 m^3 of air over a period of 24 hours, while low volume air samplers maximum sampling capacity is only 24 m^3 of air.

Mass flow controlled samplers use a hot wire anemometer probe to control the flow rate. The hot wire anemometer probe is inserted into the flow stream and automatically adjusts the motor speed as the filter begins to collect particulate. Flow can be controlled manually with the flow controller to adjust vacuum power of the motor for the voltage changes of the system during the day.

2.4.1. Calibration of the sampler

Total suspended particulate samplers such as our Tisch high volume ambient air sampler have wide range of air flow operating limits. A mass flow controller is used to sense the changes of air flow through motor and increases the voltage to the blower which increases the motor speed for equalization.

"Tisch TE-5028 Variable Orifice Calibrator" (Figure 2.6) is used for the calibration of the high-volume sampler. Calibration procedures of the company's operation manual are implemented with the exact order of the steps. Orifice calibration worksheet of the operation manual of the sampler is used for calculations.

Figure 2.6. "Tisch TE-5028 Calibrator" attached to the sampler for calibration process.

2.4.2. Impactor

"Tisch Environmental TE-231 Single Stage Fine (40CFM $PM_{2.5}$ Single Stage)" special model high-volume cascade impactor is used in the sampler system for $PM_{2.5}$ sample collections. The impactor stage is a slotted aluminium plate with outside dimensions of 15.24 centimeters to 17.78 centimeters. It has total 10 ten slots and each slot has 0.127 centimeters width.

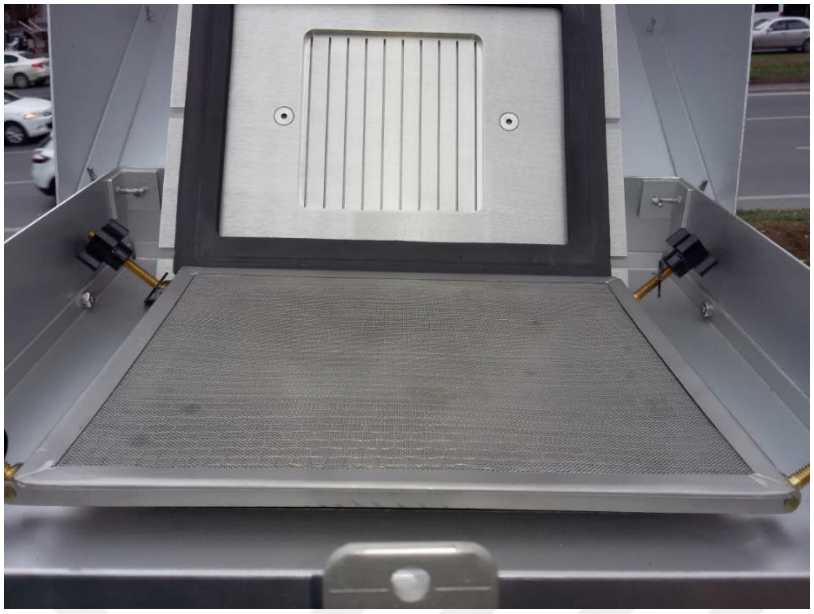

Figure 2.7. Filter holder (base part) and the cascade impactor head (upper part) while open.

Figure 2.8. Appearance of the sampler at the sampling station.

2.4.3. Sampling

$PM_{2.5}$ Samples were collected for four continuous days between 28 and 31 of January, 2017. Each sample was collected for 2 hours. First sample was taken at 07:00-09:00 hours

on 28 January 2017. Total of 24 samples were collected and analyzed. Sampling period for two-hour samples is shown at table 2.4.

Table 2.4. Sampling period.

Days	Sampling Period					
	Sample 1	Sample 2	Sample 3	Sample 4	Sample 5	Sample 6
28.1.2017	07:00-09:00	09:00-11:00	11:00-13:00	13:00-15:00	15:00-17:00	17:00-19:00
29.1.2017	07:00-09:00	09:00-11:00	11:00-13:00	13:00-15:00	15:00-17:00	17:00-19:00
30.1.2017	07:00-09:00	09:00-11:00	11:00-13:00	13:00-15:00	15:00-17:00	17:00-19:00
31.1.2017	07:00-09:00	09:00-11:00	11:00-13:00	13:00-15:00	15:00-17:00	17:00-19:00

2.5. Filters

The filter is basically a sorbent for adsorption of the compounds that are particulate matter in the ambient air. For the collection of ambient air samples, Whatman QMA quartz microfiber filters with the sizes of 203 mm to 254 mm were used. While these filters are used on sampler for collecting $PM_{2.5}$, slotted filters are used on impactor head for filtering the particles that are larger than 2.5 microns.

Figure 2.9. Slotted filters for the impactor head of the sampler.

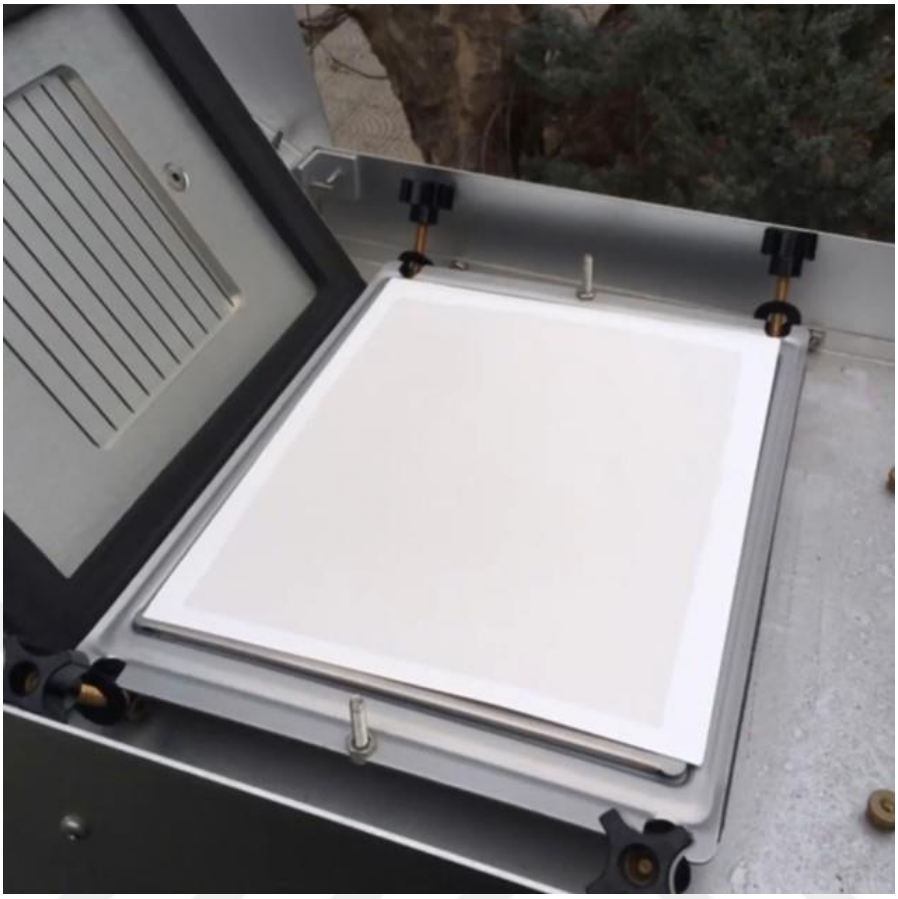

Figure 2.10. A filter on its position of sampling after collecting the sample (Impactor head is open).

2.5.1. Combustion of the filters

All of the filters were wrapped individually in aluminium foil, baked at 450 ℃ for 5 hours for prior to sampling to combust carbon impurities, and stored at -24 ℃ until sampling. Immediately after sampling, filters were wrapped in same aluminium foil and stored at -24 ℃ to avoid loses of any adsorbed compounds.

2.6. Thermal Desorption Unit

Thermal desorption (TD) process is used for releasing the adsorbed compounds from a material with heating. It is a pre-concentration technique for gas chromatography that makes gas chromatography compatible with low concentration analytes which otherwise would not be detectable.

"Markes International UNITY-xr" thermal desorption unit is used in the study as the thermal desorber. Figure 2.11 shows the front view of the thermal desorber with its cover and the figure 2.12 shows the upper view of the thermal desorber without the cover.

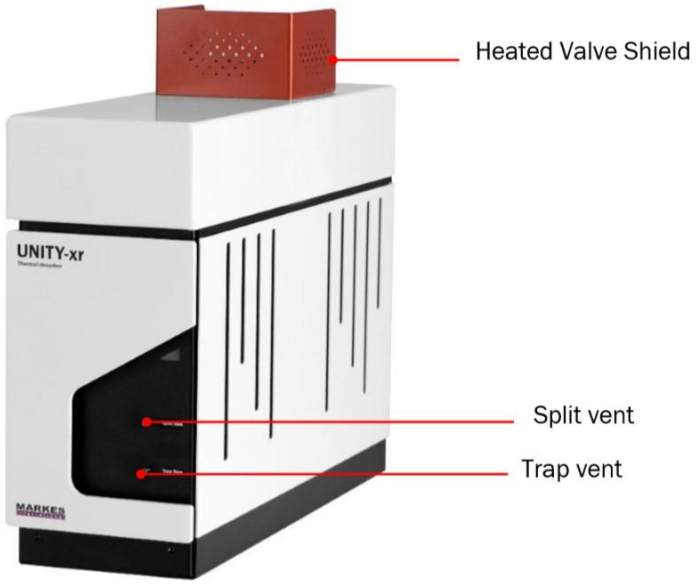

Figure 2.11. Front view of the UNITY-xr thermal desorption unit.

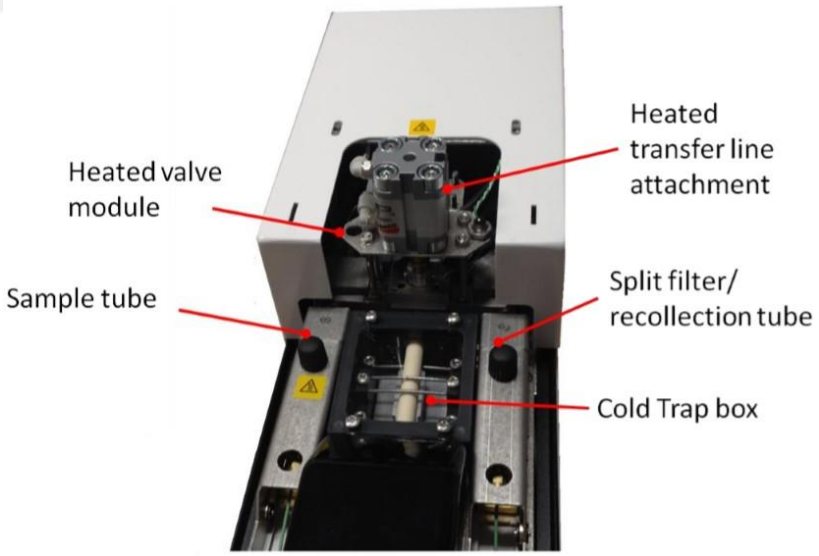

Figure 2.12. Upper view of the UNITY-xr thermal desorption unit.

Thermal desorption is a heating process that is used for releasing the adsorbed compounds from a sorbent material which is a quartz filter in this study. This heating process of thermal desorption releases the collected compounds of filter to an inert gas flow as

carrier gas. Helium was used as the inert gas in this study. Then the compounds are concentrated in the cold trap into a smaller volume in colder temperature. After this step, cold trap gets heat and release the compounds through transfer line to GC.

A purging process takes place before the heating of the sample tube and the cold trap to remove any air from the system. UNITY-xr TD uses nitrogen gas for the purge process.

Some thermal desorption units use single-stage operation, where the volatiles collected on a sorbent tube are released by heating the tube in a flow of gas, from where they passed directly into the GC. In the two-stage operation of thermal desorption process, compounds that are released from the sorbent material are concentrated in the cold trap with smaller volume in colder temperature and this provide improved sensitivity and better GC peak shape in the chromatography.

"Markes International General Purpose Cold Trap" was used as the cold trap in UNITY-xr.

Figure 2.13. Cold trap.

UNITY-xr TD comes with its own software to control the system on computer. Figure 2.14 shows the interactive schematic of the UNITY-xr on the software.

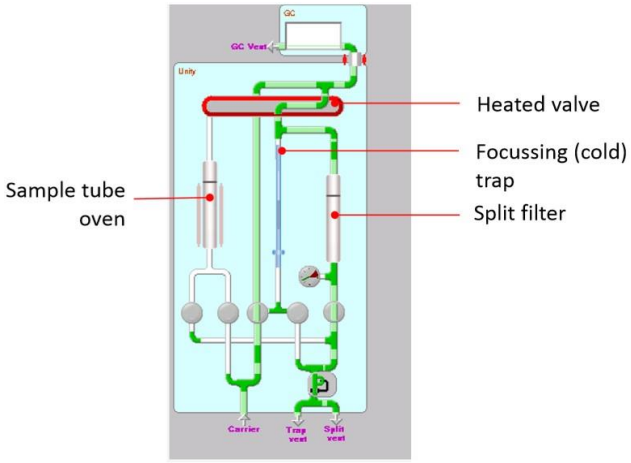

Figure 2.14. UNITY-xr interactive schematic from the software.

2.7. Gas Chromatography and Mass Spectrometry Unit

Gas Chromatography and Mass Spectrometry (GC/MS) is widely used for identification, characterization and structure analysis of substances separated in a gas chromatographic column. In GC/MS combinations, MS works as detector. Chromatograms of the compounds separated from GC are taken and sent to the mass spectrometer and the mass spectrum of each compound can be drawn and the qualitative determination can be made more precisely. With the MS detector, the entire chromatogram of the sample is followed, the retention time is observed and most importantly, the mass spectrum of each peak can be determined. It has important advantages such as high speed, high separation power, qualitative-quantitative analysis and high sensitivity.

In this study, an "Agilent 7890B GC" instrument is used with "5977 Series MSD" system as can be observed in Figure 2.15.

Figure 2.15. 5977 Series GC/MS system, shown with Agilent 7890B GC.

2.7.1. Gas chromatography

Gas chromatography is a separation process of injected vaporized sample which is a mixture of compounds. Gas chromatography instrument (GC) has different parts such as inlet, oven, and control panel as it can be seen in figure 2.15.

The oven is the most important part of the GC since the analytical column is located in there. Figure 2.16 shows the inside of the GC oven.

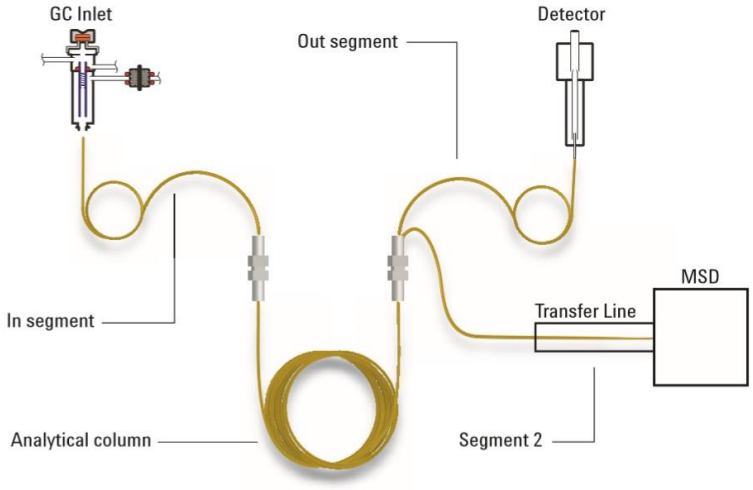

Figure 2.16. Inside scheme of the Agilent 7890B GC oven.

GC has an inlet that transfers the sample to column or that works as a connection of its column to the transfer line that is coming from thermal desorber. After compound mixture reaches the inlet they go to the column where they are separated by their volatilities. While more volatile compounds move faster through the column less volatile compounds move slower. That makes the mixture of compounds separate and leave the column one by one. Once a compound leaves the column it reaches to mass spectrometer where it is ionized and identified by their ions.

2.7.2. Mass spectrometry

Mass spectrometry is an ionization technique for individual molecules and it provides measurement of the ions based on their mass-to-charge ratio (m/z).

A mass spectrometer has three main functions as; (1) ionization of a sample by losing its one electron by “the ion source”, (2) sortation and separation of the ions according to their m/z by “the mass analyzer”, and (3) measurement and result display of the separated ions by “the detector”. Ion source is the most important part of the mass spectrometer. EI (electron-impact) source is used in the study and the EI source is the technique of bombardment of the sample molecules by electrons in the ion source (Griffiths, 2008).

GC/MS system can be controlled manually by the operating panel in the front side of the instrument and also by the software in a computer that is connected to it.

2.7.3. Calibration of the GC/MS system

Quantification of the ambient air samples are made by the GC/MS software by using the calibration curves that are prepared with calibration solutions. For this study, two different mixtures of target analytes (PAH Calibration Mix TraceCERT, C7-C40 Saturated Alkane Mixture) were used as calibration solutions.

For preparing the calibration curves, mixtures of target analytes were spiked on quartz fiber filters and inserted into thermal desorption tubes. Tubes were desorbed with the developed TD-GC-MS method and quantification method was prepared with the "ChemStation" software. The process was repeated 12 times with different amounts of solutions.

Table 2.5. Amount of solutions used for calibration.

Sample	Amount of each solution
Sample 1	5 ng
Sample 2	5 ng
Sample 3	5 ng
Sample 4	5 ng
Sample 5	15 ng
Sample 6	15 ng
Sample 7	15 ng
Sample 8	15 ng
Sample 9	20 ng
Sample 10	20 ng
Sample 11	20 ng
Sample 12	20 ng

2.8. Study area

Beşiktaş is one of the municipalities of Istanbul city which is located on the European shore of the Bosphorus (Figure 2.17). Even though it is a small municipality both on population and area, it is a lively area with many universities and business centres. An average of 2 million people pass daily because the Bosphorus and Fatih Sultan Mehmet bridges connect the two continents (Asia and Europe) and Istanbul's shores. The sampling area of this study is near the shore side of Beşiktaş as can be observed in Figure 2.18.

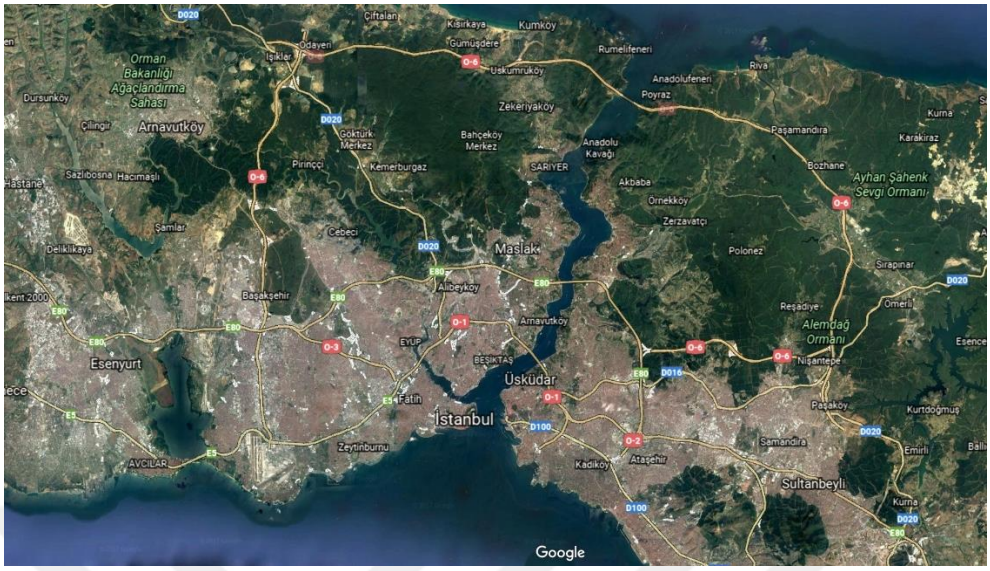

Figure 2.17. Map of Istanbul.

Figure 2.18. Location of sampling station in Beşiktaş.

The dense population of the city and its traffic, especially in the sampling area of Beşiktaş, make that the expected results are high concentrations of SVOCs according to their sources. Because of this reason, some compounds were chosen as target compounds to see in the ambient air samples.

2.9. Meteorological Data

Meteorological data for the sampling days was obtained for every 20 min from “Weather Underground”. The data also compared with a meteorological observation station near to the sampling station.

Next three figures show three charts for temperature, solar radiation and wind speed data. Every dot represents the average value of each two-hour sampling for four days.

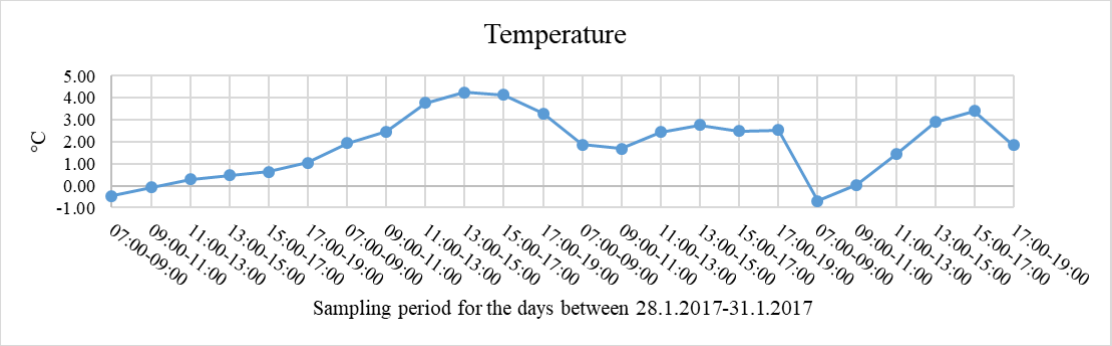

Figure 2.19. Chart of average temperature values (°C) for each sample time for four days.

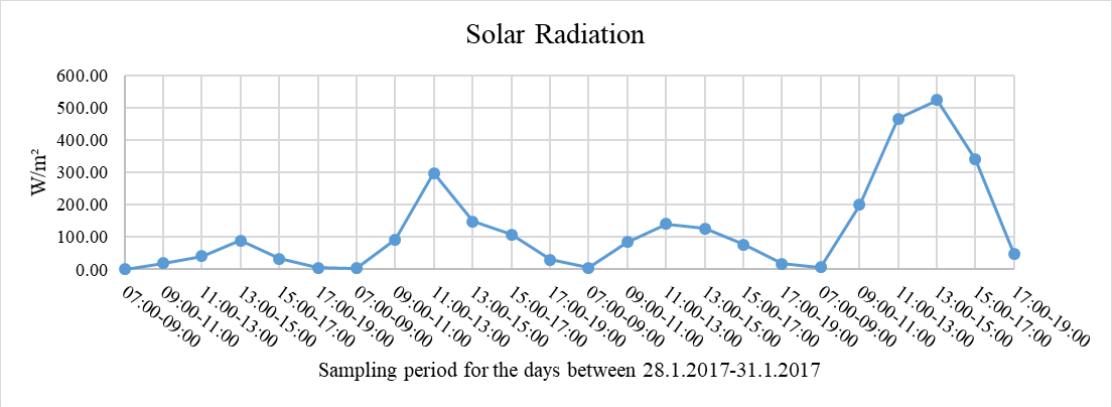

Figure 2.20. Chart of average solar radiation values (W/m^2) each sample time for four days.

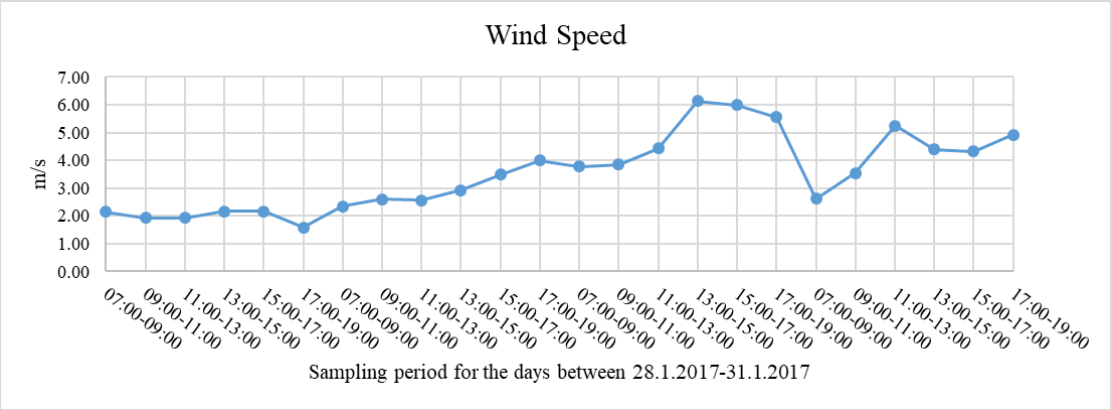

Figure 2.21. Chart of average wind speed values (m/s) for each sample time for four days.

Wind rose figures were used for showing the wind speed values and wind directions together as it can be seen in the next four figures. Dominant wind direction in Istanbul is from Northeast as can be observed in Figures 2.22-2.25. On 28/Jan/17 the dominant wind direction was from northwest.

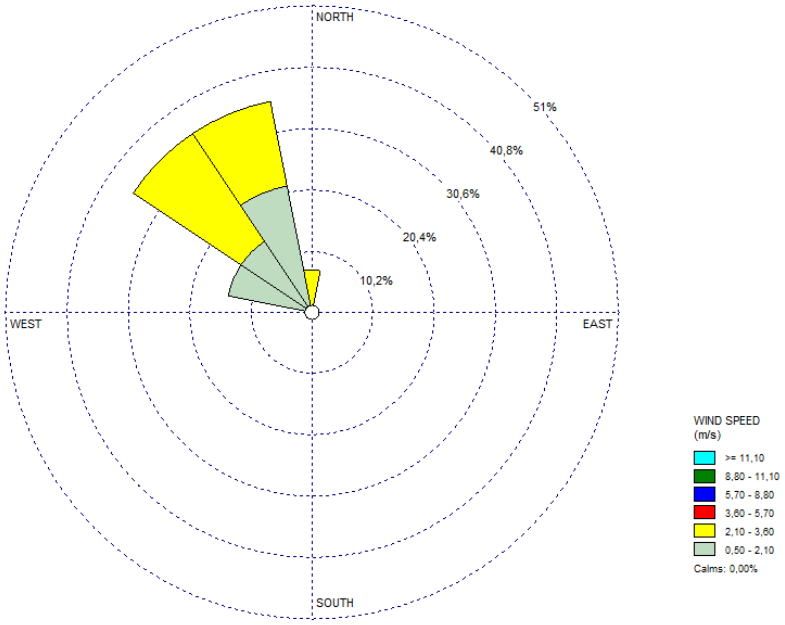

Figure 2.22. Wind rose for the sample day 28.1.17, from 7:00 to 20:00.

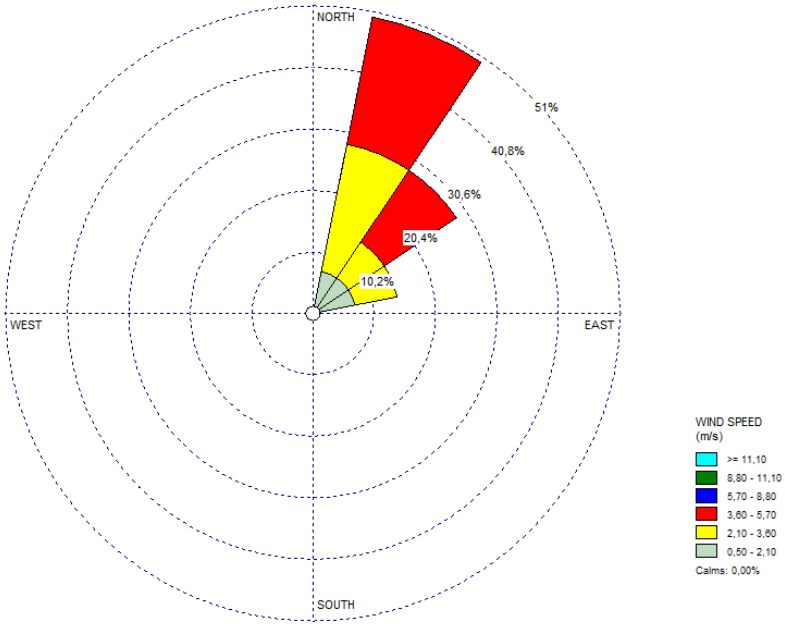

Figure 2.23. Wind rose for the sample day 29.1.17, from 7:00 to 20:00.

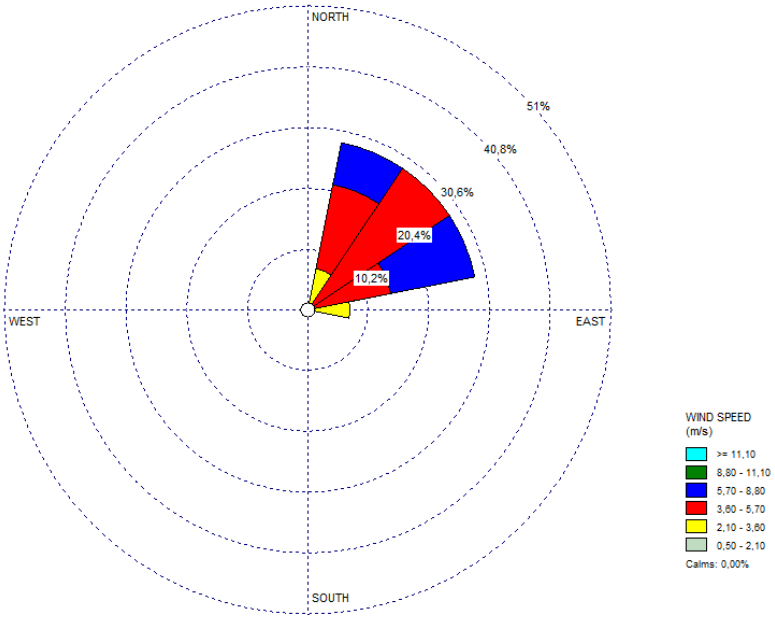

Figure 2.24. Wind rose for the sample day 30.1.17, from 7:00 to 20:00.

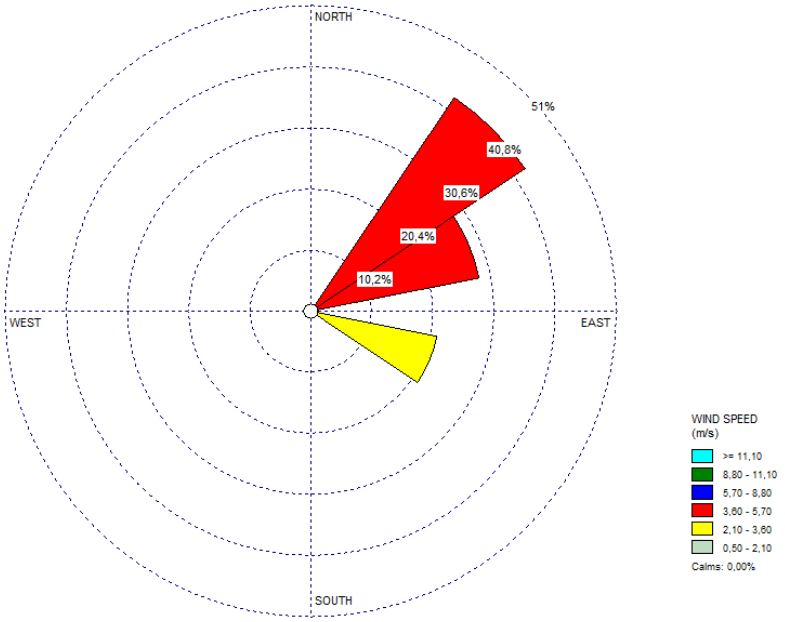

Figure 2.25. Wind rose for the sample day 31.1.17, from 7:00 to 20:00.

2.10. Traffic Data

Traffic data for the sampling time was obtained from "Directorate of Traffic, Department of Transportation of Istanbul Metropolitan Municipality (İstanbul Büyükşehir Belediyesi Ulaşım Daire Başkanlığı Trafik Müdürlüğü)". The closest sensor to the sampling station that named as "Sensor 263" which is located on Barbaros Boulevard is used to keep track of the traffic for the sampling area every minute. For each sampling period, total number of vehicles are calculated and shown in the table below.

Table 2.6. Traffic data from the Sensor No 263.

Sample Hours	28.1.2017	29.1.2017	30.1.2017	31.1.2017
07:00-09:00	3748	2353	5942	6392
09:00-11:00	6155	4481	6377	8532
11:00-13:00	6153	5597	7170	8434
13:00-15:00	7778	6737	8906	9027
15:00-17:00	7315	7624	9496	7550
17:00-19:00	6894	7149	7448	6865
Daily total	38043	33941	45339	46800

Next figure of "Figure 2.26" shows the traffic count of the Sensor No 263.

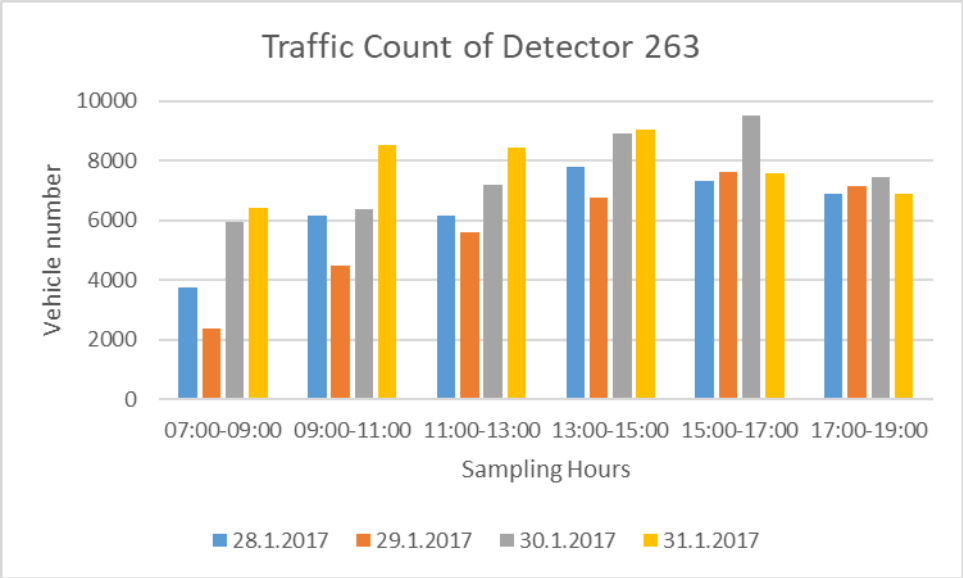

Figure 2.26. Traffic data from the Sensor No 263.

3. RESULTS

3.1. Method Development

Method development section as the most important part of the study was a process of developing a valid TD-GC-MS method for analysis and quantification of the target compounds in the ambient air samples. The laboratory system that was used in the study was a TD-GC-MS system which was described in the previous section.

Basic reasons of the method development for a specific compound detection are getting fast, simple and sensitive analysis and precise quantification.

Every setting in every step of TD-GC-MS unit can be changed to the wanted values.

For thermal desorption unit, these are:

- Sample tube desorption settings
  - Desorption temperature
  - Desorption time
- Cold trap settings
  - Cold trap low temperature
  - Cold trap high temperature
  - Cold trap hold time
- Flow settings
  - Trap flow
  - Split flow
- Transfer line temperature

For gas chromatography unit:

- GC column settings
  - Pressure/flow mode changes
  - Flow value
  - Pressure value
- GC oven settings
  - Initial temperature
  - Holding time at the initial temperature
  - Temperature increase rate (Ramp rate)

- Final temperature
- Holding time at the final temperature

For mass spectrometer unit:

- Mass-to-charge ratio (m/z)
- SIM (Selected Ion Monitoring) number
- Scan/s ratio

As a controlled experiment, analysis were made to check the results according to each variable. In total, there were more than 200 analyses only for method development part of the study.

After each change, the optimum setting was selected for the best method for the analysis of target compounds. It was needed to develop the method for analysis before creating the quantitation method. Thus, the chromatograms were used for choosing the best setting for the method. Each target compound peak on the chromatograms were integrated and the area of the peaks gave representative quantity for each compound. Mainly the biggest area for a compound is the best option for a setting. So, the comparison of areas for each setting change gives the best method. For this reason, the comparison charts for every change to select the method are shown in this section.

For this developing process, mixtures of target analytes were used by spiking them on quartz fiber filters and inserted into thermal desorption glass tubes. Then the tube is inserted to thermal desorption oven to analyze the sample. After analysis, the results are used as abundance values that were given by MSD. The graphs in the method development section are based on this abundance values.

Many studies have been compared for the method developing process. Similar works for the analysis of similar compounds and samples have been considered as the base works for our study. Some of the comparable studies have been given in the table 3.1 which is based on the table of Chow et al. (2007).

Table 3.1. Similar studies with the experimental details.

Reference	Sample type	Sample preparation	TD unit	Analytical instrument	TD program	Desorbent focusing path	GC column	GC program
This study	$PM_{2.5}$ aerosol collected onto quartz-fiber filter on Istanbul	6 cm^2 filter strip cut and placed inside a glass sample tube and held with glass wool	Markes Unity-xr desorber used for glass tubes	Agilent 7890B GC/5977 MSD	From ambient to 320 ℃ for 20 min	0 ℃ cold trapping to 310 ℃ for 10 min onto column head	DB-5MS (30 m x 0.25 mm x 0.25 µm)	40 ℃ for 5 min, 40-325 ℃ at 5 ℃/min, held at 325 ℃ for 7 min
(Voorhees et al., 1991)	$PM_{0.6}$ and PM>0.45 collected on quartz-fiber in pristine regions of Colorado	Filters were first extracted in sequence with methanol, dichloroethane, acetone, and hexane. The resulting in soluble material was introduced to a tube furnace	A tube furnace directly interfaced to an GC/MS	Extrel Simulscan GC/MS, 35–450 amu scan range	550 ℃ for 10 min	Cold trapping onto column head	DB-5 (25 m x 0.25 mm)	35-220 ℃ at 8.5 ℃/min
(Jeon et al., 2001)	High-volume PM10 samples collected along the US/Mexico Border	A filter strip cut and placed inside a glass tube lined with a ferromagnetic foil	Curie point pyrolizer	HP 5890 GC/5792 MSD	From ambient to 315 ℃, 10s	Cold trapping onto column head	HP-5MS (25 m x 0.20 mm x 0.33 µm)	50 ℃ to 320 ℃ 3-15 ℃/min
(Blanchard et al., 2002)	Aerosol samples collected on quartz-and glass-fiber filters in Ontario	A 1 cm diameter section of sample filter was punched and transferred into a GC liner spiked with internal standards	A GC injection port was added with three minor components, including a small T-connector, 3-way valve, and needle valve.	HP 5890GC/5972A MS in EI mode	Isocratic desorption at 300 ℃, 15 min	Cold trapping onto column head	HP-5MS (25 m x 0.20 mm x 0.33 µm)	30 ℃ for 0.75 min, 30-175 ℃ at 7.5 ℃/min, 175-295 ℃ at 10 ℃/min, held at 295 ℃ for 5 min
(Blazsó et al., 2003)	$PM_{2.6}$ collected on quartz-fiber filters and size-segregated aerosol samples collected on Al foils in Brazil	The collection substrates were spiked with derivatization agents, dried, and introduced into a pyrolysis sample holder	A pyrolizer	Agilent 6890 GC/5793 MSD	400 ℃ for 20 s	Cold trapping onto column head	HP-5 (30 m x 0.25 mm)	50 ℃ for 1 min, 50-300 ℃ at 10 ℃/min, held at 300 ℃ for 4 min
(Hamilton et al., 2004)	$PM_{2.5}$ aerosol collected in London	The filter strip (with 10 µg loading) was inserted into the GC liner and directly introduced into the GC injector	Conventional GC injection port	Agilent 6890 GC/LECO, Pegasus III TOF/MS with a LECO Pegasus 4D GCxGC modulator, 20 to 350 amu scan range	40-300 ℃ at 20 ℃/min for 13 min	Cold trapping onto column head	HP-5 (10 m x 0.18 mm x 0.18 µm) followed by DB17 (1.66 m x 0.1 mm x 0.1 µm)	40 ℃ for 5 min, 40-270 ℃ at 3.5 ℃/min, held at 270 ℃ for 10 min

Table 3.1. Similar studies with the experimental details (continued).

Reference	Sample type	Sample preparation	TD unit	Analytical instrument	TD program	Desorbent focusing path	GC column	GC program
(Yang et al., 2005)	Ambient aerosol samples collected on Teflon impregnated glass-fiber filters in Hong Kong and on quartz-filters at Nanjing, China	Two pieces of 1.45 cm^2 filter samples were spiked with deuterated internal standards, placed in the GC inject liner and held with glass wool	Conventional GC injection port without any modification	HP 5890GC/5791 MSD, 50-650 amu scan range	100-275 ℃ within 7-8 min	Cold trapping onto column head	HP-5MS (25 m x 0.20 mm x 0.33 μm)	30 ℃ for 2 min, 30-120 ℃ at 20 ℃/min, 120-300 ℃ at 10 ℃/min, held at 300 ℃ for 10 min
(Williams et al., 2006)	In-situ aerosol samples collected in Berkeley, CA	The aerosols were collected into the collection-TE cell, thermally desorbed and transferred into the GC injector	Collection-TE cell with conventional GC injection port	Agilent 6890 GC/5793 MSD, 29–550 amu scan range	50-300 ℃ at 30-40 ℃/min for 10 min	Cold trapping onto column head	Rtx-5MS (30 m x 0.25 mm x 0.25 μm)	45 ℃ for 12 min, 45-300 ℃ at 8.5 ℃/min, held at 300 ℃ for ~7 min
(Bates et al., 2008)	Airborne 4-6 ring PAHs collected onto quartz filters	The filter was inserted into sample tube then to the thermal desorption oven	Markes TD unit	TD-GC/MS system	From ambient to 320 ℃ for 10 min	30 ℃ cold trapping to 360 ℃ for 4 min	DB-XLB (30 m x 0.25 mm x 0.25 μm)	50 ℃ for 0.5 min, 50-160 ℃ at 20 ℃/min, 160-325 ℃ at 10 ℃/min, 325-340 ℃ at 25 ℃/min, held at 340 ℃ for 5 min
(Elorduy et al., 2016)	Short-term particulate concentrations of 13 PAHs in PM_{10} in Bilbao, Spain	Filter samples were randomly cut into 8 portions of 1 cm^2 and put into stainless-steel tubes	Turbomatrix 150 ATD	Agilent 5973	From ambient to 320 ℃ for 10 min	-10 ℃ cold trapping to 325 ℃ for 6 min	Meta X5 (30 m x 0.25 mm x 0.25 μm)	100 ℃ for 3 min, 100-250 ℃ at 10 ℃/min, 160-325 ℃ at 10 ℃/min, 250-320 ℃ at 5 ℃/min, held at 320 ℃ for 10 min
(Wang et al., 2016b)	$PM_{2.5}$ collected onto quartz filters (PAHs and OPAHs)	The filters were cut into small pieces and inserted into TD tube	In-injection port TD-GC/MS	Agilent 7890A GC/5975C MS system	From 50 ℃ to 275 ℃	In-injection port	HP-5MS (25 m x 0.20 mm x 0.25 μm)	30 ℃ for 2 min, 30-120 ℃ at 10 ℃/min, 120-310 ℃ at 8 ℃/min, held at 310 ℃ for 20 min

3.1.1. Effect of trap sorption (low) temperature

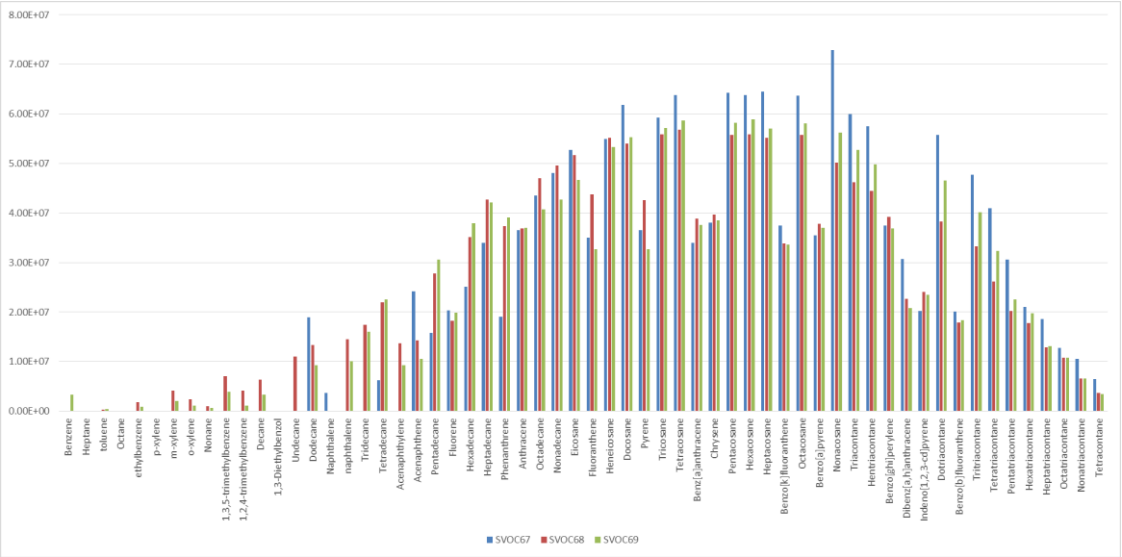

Figure 3.1. Comparison chart of trap sorption (low) temperature values (SVOC67: 0 °C; SVOC68: -15 °C; SVOC69: 20 °C).

Figure 3.1 shows instrumental responses and the effect of trap sorption temperature at 0 ℃, -15 ℃ and 20 ℃. All experiments were performed at trap desorption temperature of 310 ℃ for 10 min and GC column pressure 23 psi.

Three different traps low (holding) temperature values (0 ℃, -15 ℃ and 20 ℃) were used with the names as SVOC67, SVOC68 and SVOC69, respectively. It was seen that 0 ℃ value of SVOC67 analysis is the best option for *n*-alkane group between C20-C40. The figure shows that the selection of the trap low temperature value depends on which compounds will be investigated. Overall, it can be observed that the studied temperatures do not considerably influence the sorption recoveries. In this experiment, better recoveries of light aromatics and C14 and C15 n-alkanes were obtained at a temperature of -15 ℃. Similar results were obtained at a trapping temperature of 0 ℃ with average recoveries of 106% and 100% for n-alkanes and PAH, respectively. Therefore, a trapping temperature of 0 ℃ was chosen.

3.1.2. Effect of trap desorption (high) temperature

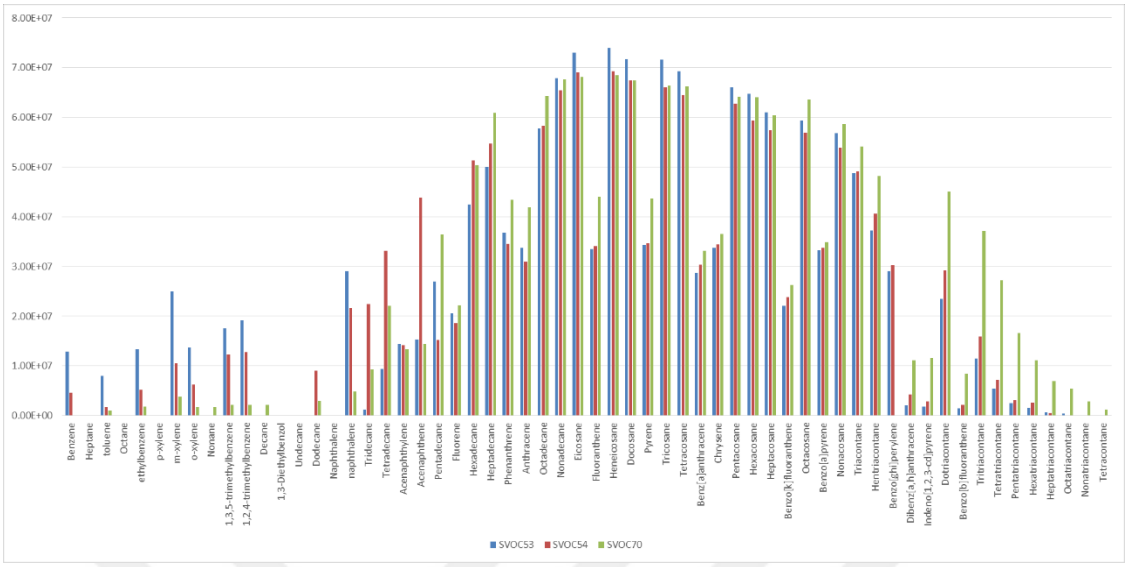

Figure 3.2. Comparison chart of trap desorption (high) temperature values (SVOC53: 310 °C; SVOC54: 320 °C; SVOC70: 360 °C).

Figure 3.2 shows the instrument response of 10 ng light aromatics, 10 ng n-alkanes, and 10 ng PAH at general conditions of 17 psi and three different trap desorption (high) temperature values (310 ℃, 320 ℃ and 360 ℃) that were used with the names as SVOC53, SVOC54 and SVOC70 respectively, for 5 min at sample desorption flow rates of 50 ml/min.

It was seen that 310 ℃ value of SVOC53 analysis is the best option for the target compounds together with in order to preserve lifetime of the carbon trap.

It was observed that the 310 ℃ trap desorption temperature value in the SVOC53 analysis provided better results for all VOCs, whereas the 360 ℃ trap desorption temperature value in the SVOC70 analysis was observed to be better for the compounds that have higher boiling point as C24-C40 range and also for the same range of PAHs.

Higher responses are obtained for aromatic compounds as desorption temperature decreases, this may be due to thermal degradation. Normal desorption temperatures are 275 ℃. Average recoveries of n-alkanes and PAH did not considerably differ at 310 ℃ and 320 ℃. On the other hand, average recoveries of SVOCs improved 30-40% and 3-6 times for n-alkanes and PAH larger than C30 at high temperatures of 360 ℃ for 5 min. However, in order to preserve lifetime of the carbon trap, we chose 310 ℃.

3.1.3. Effect of trap desorption time

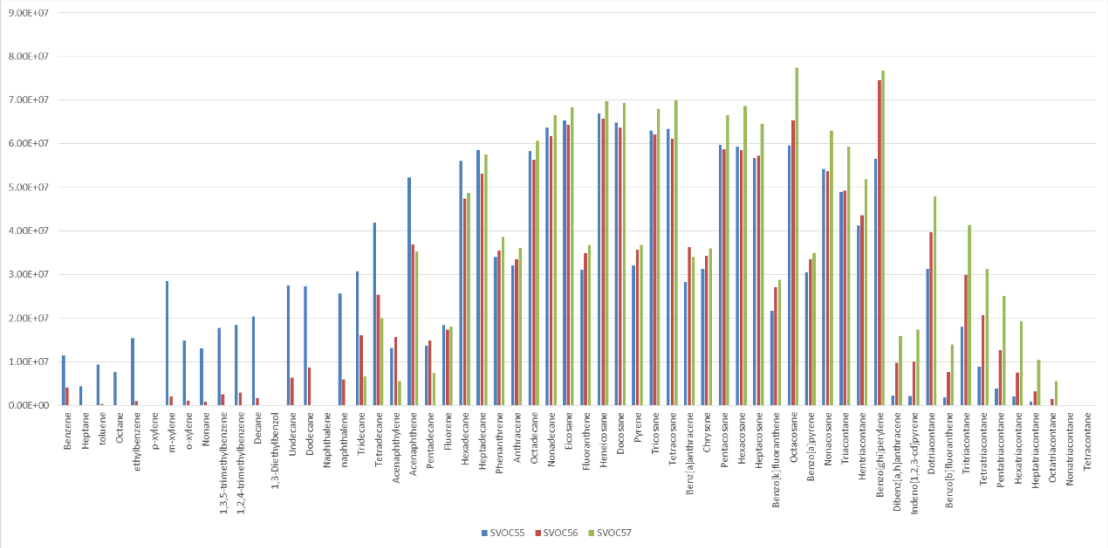

Figure 3.3. Comparison chart of trap desorption times (SVOC55: 5 min; SVOC56: 7 min; SVOC57: 10 min).

Figure 3.3 shows the instrument response of 10 ng light aromatics, 10 ng n-alkanes, and 10 ng PAH at general conditions of 17 psi and desorption temperature 310 ℃ at three different trap holding time values (5 min, 7 min and 10 min) that were used with the names as SVOC55, SVOC56 and SVOC57, respectively at sample desorption flow rates of 50 ml/min. Desorption time is one of the parameters that shows the highest selectivity of SVOCs. It was seen that 5-min trap desorption time value of SVOC55 analysis is the best option for the VOCs and C7-C16, while SVOC57 is the best for C16-C40 and PAHs with 10 min trap desorption time value. Desorption time of 5 minutes provides the highest recovery of lighter SVOCs such as light aromatics and n-alkanes below C17. N-alkanes lighter than C14 are not typically present in the aerosol phase, therefore, SVOC57 analysis with 10-min trap desorption time should be selected according to the type of the main compounds of interest in this study.

3.1.4. Effect of trap desorption flowrate

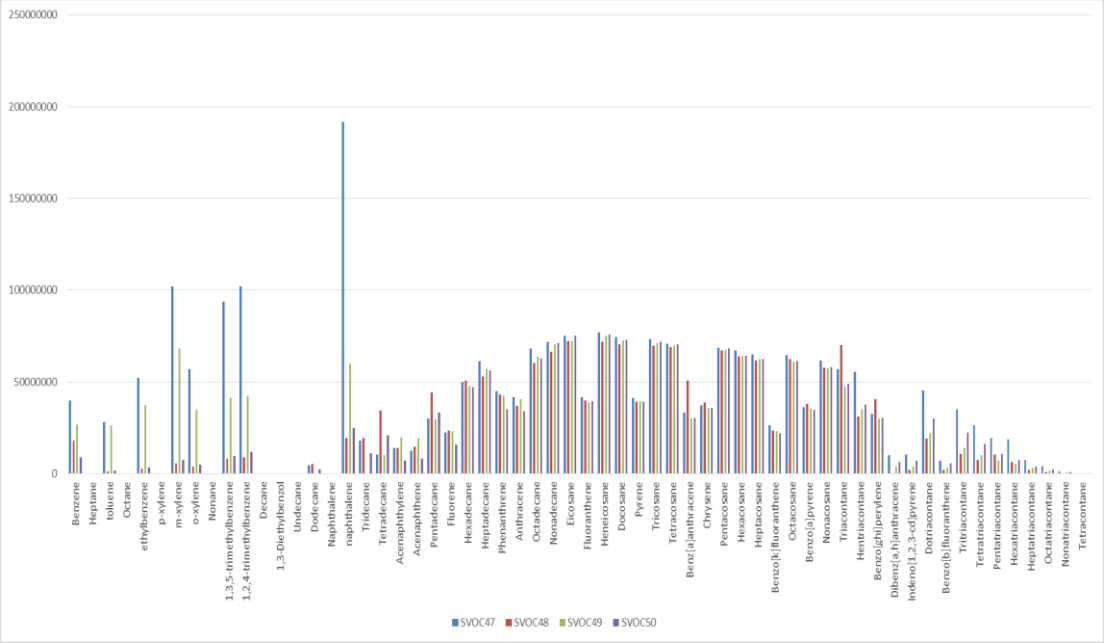

Figure 3.4. Comparison chart of trap flows (SVOC47: 50 ml/min; SVOC48: 70 ml/min; SVOC49: 30 ml/min; SVOC50: 20 ml/min).

Figure 3.4 shows the instrument response of 20 ng light aromatics, 10 ng n-alkanes, and 10 ng PAH at general conditions of 17 psi and desorption temperature 310 °C for 5 min with four different trap flow values (20 ml/min, 30 ml/min, 50 ml/min and 70 ml/min) that were used with the names as SVOC50, SVOC49, SVOC47 and SVOC48, respectively. Sample desorption flowrates are the same flowrates going through the trap (i.e., trap sorption flowrate). It can be seen much more larger aromatics peaks because the number of aromatics spiked is 2 times more than the n-alkanes and PAH. The best recoveries of lighter SVOCs was obtained at average flowrates of 30 and 50 ml/min. It was seen that 50 ml/min flow value of SVOC47 analysis is the best option for the target compounds. Middle volatility SVOCs did not show considerable improvements in recoveries. Better recoveries were observed for C32-C36 n-alkanes at 50 ml/min, however, C37-C40 n-alkanes and heavy PAH were poorly recovered. In this study, 50 ml/min was selected to get the highest recoveries of selected compounds.

3.1.5. Effect of GC pressure and flow

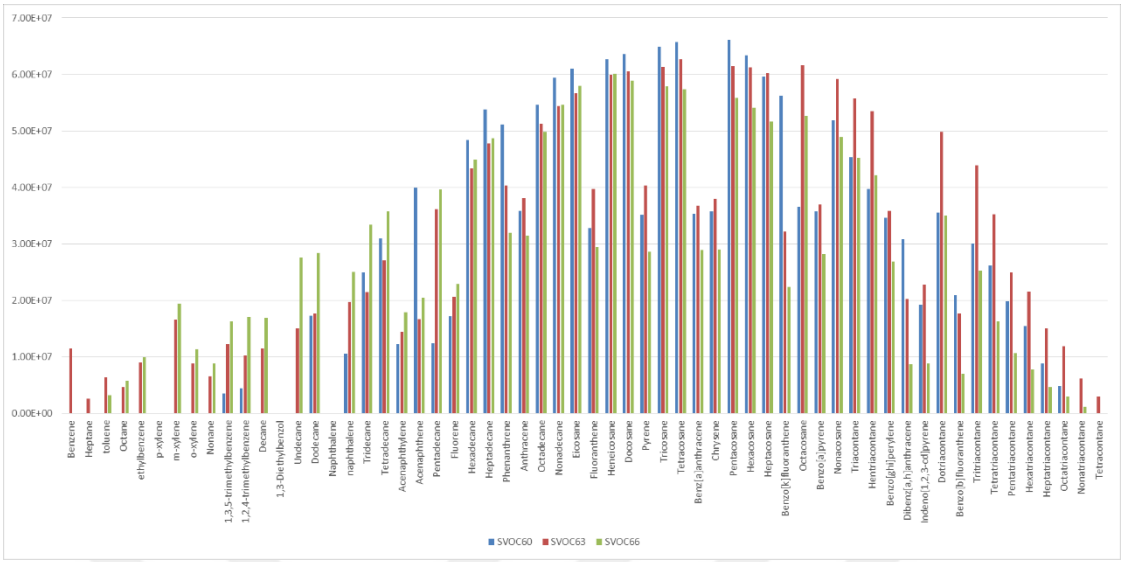

Figure 3.5. Comparison chart of GC constant pressure and constant flow modes (SVOC60: constant pressure 17 psi; SVOC63: constant pressure 23 psi; SVOC66: constant flow 1.2 ml/min).

Figure 3.5 shows the effect of GC column pressure on recovery of SVOCs. All experiments were performed at trap desorption 310 °C for two different GC mode with total of three different values (constant pressure 17 psi, constant pressure 23 psi and constant flow 1.2 ml/min) that were used with the names as SVOC60, SVOC63 and SVOC66, respectively.

The TD-GC-MS system pressure and flow through the TD-GC transfer line are determined by the GC column pressure and column flow, respectively.

It was seen that 5-min trap desorption time value of SVOC55 analysis is the best option for the VOCs and C7-C16, while SVOC57 is the best for C16-C40 and PAHs with 10 min trap desorption time value. It was understood that SVOC57 analysis with 10-min trap desorption time should be selected according to the type of the main of interest in this study.

3.1.6. Effect of GC initial temperature

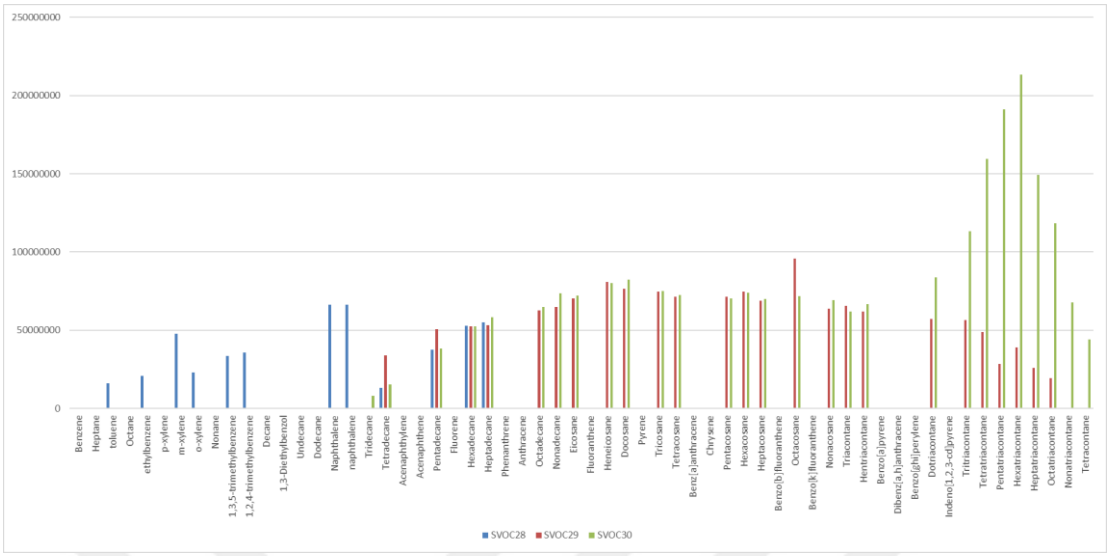

Figure 3.6. Comparison chart of GC initial temperature values (SVOC28: 50 °C; SVOC29: 32 °C; SVOC30: 40 °C).

Three different GC initial temperature values (50 ℃, 32 ℃ and 40 ℃) were used with the names as SVOC28, SVOC29 and SVOC30, respectively. It was seen that 40 ℃ value of SVOC30 analysis is the best option for the target compounds.

It was observed that the 50 ℃ GC initial temperature value in the SVOC28 analysis provided better results for all VOCs, whereas the 40 ℃ GC initial temperature value in the SVOC30 analysis was observed to be better for high boiling point compounds.

3.2. Analysis Results

Collected ambient air samples were analysed as the next step after method development process. In order to evaluate the developed TD-GC-MS method, $PM_{2.5}$ samples were collected every two hours from 07:00h to 19:00h during four days in the winter season. A total of 11 PAH and 28 n-alkanes (C12-C40) were identified and quantified in 24 samples. Analysis results have been given as concentrations of the compounds in the ambient air as ng/m^3.

Concentrations of the identified and quantified compounds are shown in the Table 3.2 with minimum, maximum and average values. Also, some similar studies have been shown in the Table 3.2 for comparison of the concentrations of similar studies.

Table 3.2. Comparison of the concentration results with similar studies (ng/m^3).

	This Study			(Wang et al., 2016a)			(Elorduy et al., 2016)	(Schnelle-Kreis et al., 2007)			(Mugica et al., 2010)	(Bourotte et al., 2005)	(Viana et al., 2008)	(Cincinelli et al., 2007)	(Cotham and Bidleman, 1995)	
Compound Name	Min	Max	Avg	Min	Max	Avg	Avg	Min	Max	Avg	Avg	Avg	Avg	Avg	chicago center	uwgb rural
Acenaphthylene	0.92	63.82	11.03	0.06	26.5	5.1	-	-	-	-	0.64	0.09	0.50	-	-	-
Acenaphthene	0.33	21.11	4.52	0.03	14.2	1.9	-	-	-	-	0.49	0.35	0.00	-	-	-
Fluorene	0.00	9.91	2.59	0	19.3	1.7	0.12	-	-	-	0.29	0.00	0.17	-	92.00	4.10
Phenanthrene	0.00	2.61	0.63	0.07	71.3	3.9	0.39	-	-	-	0.74	0.18	0.33	21.70	159.00	9.60
Anthracene	0.00	11.60	3.50	0.06	2.7	1.1	0.09	-	-	-	0.67	0.00	0.03	4.48	15.00	0.05
Fluoranthene	2.33	22.15	6.54	0.66	29.7	9.2	0.74	-	-	-	0.86	0.68	0.37	5.85	56.00	1.70
Pyrene	0.00	0.18	0.02	0.66	38.2	9.9	0.76	-	-	-	0.96	0.52	0.23	5.49	36.00	0.76
Benz[a]anthracene	3.74	32.75	10.67	0.23	39.6	9.6	0.64	0.1	2.62	1.26	1.08	0.46	0.29	0.93	21.00	0.16
Chrysene	9.15	42.38	19.43	0.88	59	18.8	0.69	0.23	6.25	3.24	1.18	0.51	0.33	1.80	-	-
Benzo[b]fluoranthene	0.17	7.73	2.88	1.1	50.1	14.9	2.12	0.6*	7.46*	4.03*	1.83	1.23	0.48	0.89	39.00*	0.57*
Benzo[k]fluoranthene	0.00	1.29	0.27	0.81	21.6	9.2	0.56				0.81	0.76	0.27	2.10		
Dodecane	15.21	52.31	30.53													
Tridecane	14.82	43.93	27.89													
Tetradecane	1.54	34.93	20.03													
Pentadecane	1.56	13.41	6.06													
Hexadecane	8.76	27.42	18.39													
Heptadecane	1.25	12.24	5.80													
Octadecane	6.45	21.11	14.34													
Nonadecane	5.02	12.79	8.68													
Eicosane	0.00	7.74	2.39					0.3	9.12	4.71						
Heneicosane	0.11	10.02	3.05					0.19	17.71	8.95						
Docosane	0.26	15.52	7.78					1.02	23.46	12.24						
Tetracosane	2.92	16.45	6.99					2.05	25.55	13.8						
Pentacosane	0.38	14.65	7.01					0.93	23.15	12.04						
Hexacosane	0.32	9.72	3.22					0.62	20.92	10.77						
Heptacosane	0.00	9.67	1.84					1.82	24.48	13.15						
Octacosane	0.00	9.87	4.34					0.66	17.44	9.05						
Nonacosane	1.93	10.85	4.72					1.23	17.47	9.35						
Triacontane	0.47	10.20	3.99					0.12	9.3	4.71						
Hentriacontane	0.93	10.85	5.04					0.84	15.96	8.4						
Dotriacontane	1.14	6.78	2.80					1.9	2.7	2.3						
Tritriacontane	1.09	5.86	2.45					0.26	4.34	2.3						
Tetratriacontane	0.54	3.03	1.34					0.02	0.94	0.48						
Pentatriacontane	0.75	2.38	1.20													
Hexatriacontane	0.85	1.98	1.24													
Heptatriacontane	1.49	2.39	1.74													
Octatriacontane	1.57	2.44	1.84													
Nonatriacontane	0.00	0.00	0.00													

(*Total of Benzo[b]fluoranthene and Benzo[k]fluoranthene)

Table 3.2 shows that some values are similar with this study while some others look very different. Also, most of the studies are about PAHs while there is not much work done for n-alkanes analysis on $PM_{2.5}$. All samples were taken during winter period for all these studies.

The study of Wang et al. has the ambient air samples of Xian, China on December 2013. It was a central place on the city with many influences like this study so the analysis results show similar values of PAHs except the almost 5-10 times higher concentrations of Phenanthrene, Pyrene, Benzo[b]fluoranthene and Benzo[k]fluoranthene than this study (Wang et al., 2016a).

Elorduy et al. have a similar study in Bilbao city, northern Spain during 2013 but the Table 3.2 only shows the results of December 2013. The city is a smaller metropolitan area than Istanbul. Samples were taken by 8 hours period for PM_{10}. They have 10-20 times smaller PAHs concentrations except the almost same Benzo[b]fluoranthene concentrations (Elorduy et al., 2016).

Schnelle-Kreis et al. collected $PM_{2.5}$ samples in Augsburg, Germany from January 2003 through December 2004. Winter period of the study is shown in the Table 3.2. It can be seen that the concentration values of 4 PAHs and 14 n-alkanes are similar to this study except lower Benz[a]anthracene and Chrysene concentrations and higher Hexacosane and Heptacosane concentrations (Schnelle-Kreis et al., 2007).

Mugica et al. studied PAHs in $PM_{2.5}$ and PM_{10} in Mexico City, Mexico from April 2006 to March 2007. Not only winter season but average values of all sampling period is shown in the Table 3.2. Concentrations of the PAHs are much more lower than this study except Phenanthrene, Pyrene and Benzo[k]fluoranthene (Mugica et al., 2010).

Bourotte et al. collected 24 h PM samples from May 2002 to July 2002 at Sao Paulo city, Brazil and made PAH analysis. They have similar results just as the study of Mugica et al. (2010). Also, Viana et al. (2008) studied the PM in Valencia, Spain between 2004 and 2005 and have similar results with Bourotte et al. (2005) and Mugica et al. (2010).

Cotham and Bidleman collected air samples at an urban (Chicago, USA) and a rural (University of Wisconsin at Green Bay, UWGB) site during February 1988. It is an important study to see the difference of the PAH concentrations between urban and rural

cites and it has the highest PAH concentration among all these studies, also urban PAH concentration values are much more higher than this study (Cotham and Bidleman, 1995).

3.2.1. $PM_{2.5}$ concentrations

Hourly $PM_{2.5}$ concentration data was obtained from the stations of "Ministry of Environment and Urbanization of Turkey" for Kagithane, Silivri, and Umraniye. Data for Catladikapi was not available on 28-31 January. Umraniye station also missed some of the data, however, it appears to follow similar concentrations and behavior as Kagithane. Both Kagithane and Umraniye have a population of approximately 400,000 and 700,000, respectively. Lower population of 150,000 live in Silivri, thus lower concentrations of $PM_{2.5}$ are expected during the winter.

World Health Organization (WHO) established the 24-hour air quality standard as 25 $\mu g/m^3$ and United States Environmental Protection Agency (US-EPA) established it as 35 $\mu g/m^3$ (WHO, 2016; US-EPA, 2017). European Union and Turkish authorities have not been established any standard for $PM_{2.5}$ daily averages. Yearly averages are 10, 12, and 25 $\mu g/m^3$ according to WHO, EPA, and EU, respectively. The 24-hour WHO air quality standard of 25 $\mu g/m^3$ was exceeded five times during the study period, mainly in Kagithane and Umraniye (Table 3.3). On the other hand, the 24-hour US-EPA air quality standard of 35 $\mu g/m^3$ was exceeded on 28-Jan on all three sampling stations, possibly due to the absence of vertical atmospheric motion (Figure 3.10).

During the study period, hourly $PM_{2.5}$ concentrations were below 30 $\mu g/m^3$, except a few spikes of maximum concentrations of approximately 50-65 $\mu g/m^3$ observed at noon. The diurnal pattern of $PM_{2.5}$ concentrations is variable in Kagithane and Silivri. Overall, both of the stations show a decreasing trend from Saturday to Monday that increases on Tuesday afternoon. However, the maximum concentrations occur at different times during the day. This may be due to a combination of traffic/industrial emissions in Kagithane and residential heating emissions in both sampling stations.

Table 3.3. Daily average $PM_{2.5}$ concentrations ($\mu g/m^3$).

Date	Kağıthane	Silivri	Ümraniye
28/01/2017	47.29	38.25	65.00
29/01/2017	21.00	18.71	21.14
30/01/2017	20.29	12.78	26.29
31/01/2017	27.13	17.00	19.09

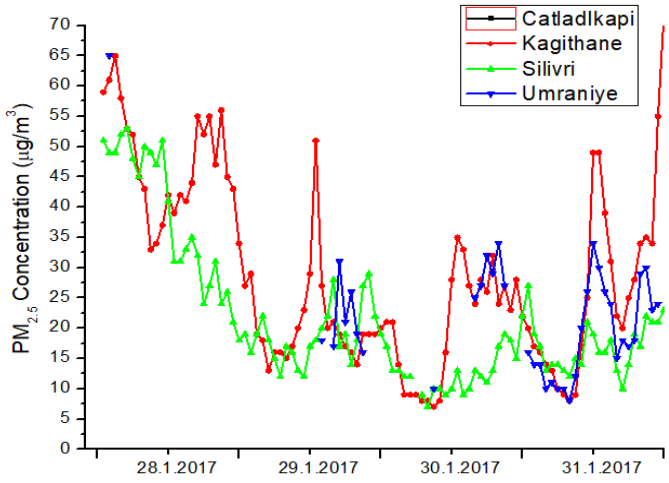

Figure 3.7. Hourly $PM_{2.5}$ concentration ($\mu g/m^3$).

Figure 3.8 shows the diurnal variations of SVOC concentrations in $PM_{2.5}$ as ng/m^3 for four sampling days. A similar trendline between Figures 3.7 and 3.8 can be observed. For 28-Jan, concentrations are a bit higher than the 29-Jan which are weekend days and trendline increases for the next two days which are 30-Jan Monday and 31-Jan Tuesday. Highest concentrations are observed on Tuesday morning hours. In total, the biggest difference between weekend and weekdays can be observed as traffic dependent compounds in this figure.

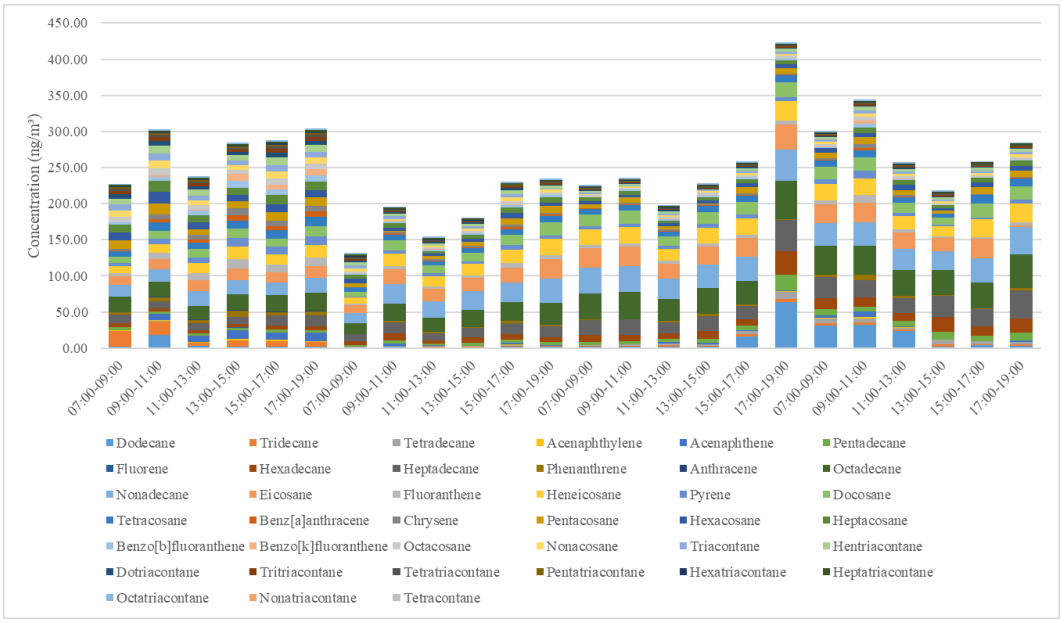

Figure 3.8. Diurnal variation of SVOCs in $PM_{2.5}$ (ng/m^3).

3.2.2. Effect of traffic density

Traffic density data for the sampling time was obtained from “Directorate of Traffic, Department of Transportation of Istanbul Metropolitan Municipality”. Total vehicle counts were calculated for all six lanes of Barbaros Bulvari for every 2-hour sample (Table 2.6). This data is organized according to sampling time and consecutively from 28-31 Jan (Figure 2.26 and 3.9).

The traffic density has various movements and interesting behaviour for the different days of the week and times of the day according to people activities, as can be observed on Figure 3.9. The samples reported here were collected on 4 days starting from the Saturday (Saturday-Sunday-Monday-Tuesday) in order to evaluate the effect of traffic during weekend and weekdays on air pollutant levels. Overall, the lowest counts are on Saturday and Sunday between 07:00-15:00h hours. After 15:00h, vehicle density reaches higher values similar to Monday and Tuesday for the same hours.

On weekdays (Monday and Tuesday), traffic density is higher than on weekends and shows an increasing trend from 07:00-13:00h until 15:00-17:00h on Monday and until 13:00-15:00h for Tuesday. After this point it starts to show a slow decreasing trend (Figure 3.9).

The total vehicle count observed for the 2-hour periods were between 2,353-9,496 on Sunday 07:00-09:00h (minimum) and Monday 15:00-17:00h (maximum), respectively. Over the sampling period, vehicle density shows an increasing trend at 07:00 and reaches a maximum at 13:00h or 15:00h. The total vehicle counts registered at this point were 38,043-33,941 on Saturday-Sunday, respectively, and 45,339-46,800 on Monday-Tuesday, respectively.

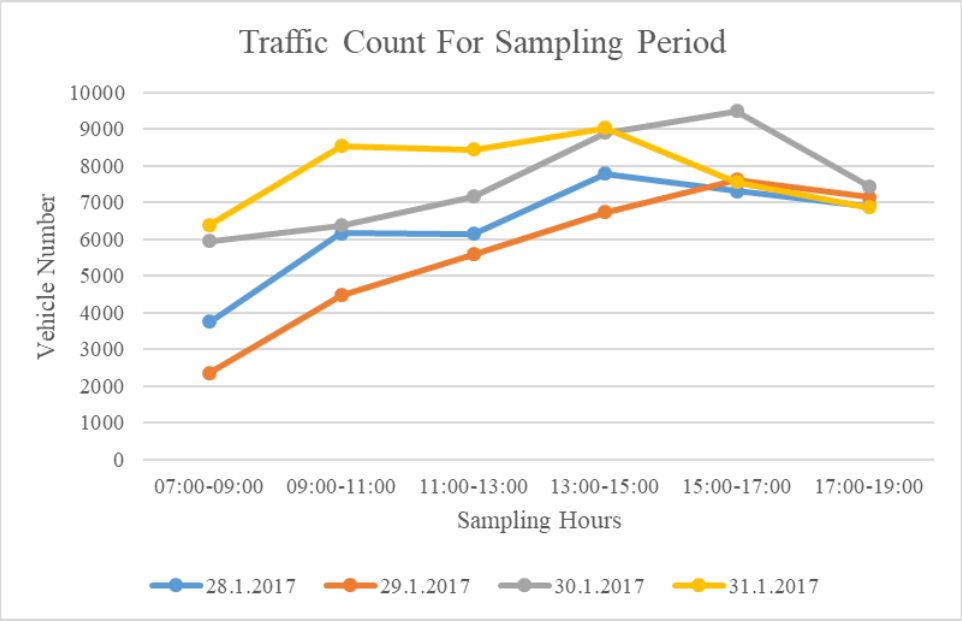

Figure 3.9. Traffic count for sampling for each 2h sample.

3.2.3. Effect of meteorology

Figures 2.19, 2.20 and 2.21 show temperature, solar radiation, wind speed, and figure 3.10 shows air mass trajectories observed during each 2-hour sample on January 28-31, 2017, respectively. Air mass backward trajectories were obtained from NOAA-HYSPLIT. During the sampling days, typical winter weather conditions of low temperatures, wind speed, and solar radiation were observed.

The temperature had an increasing trendline from the beginning of the sampling period to the 29-Jan 13:00-15:00h which was the highest temperature point that was observed (4.25 ℃). After this point a slow decreasing trend was observed until 31-Jan 07:00-09:00h which was the lowest temperature point (-0.7 ℃). Another increasing in the trendline was observed after this point during the last sampling day (Figure 2.19).

Due to low temperatures, low wind speeds were observed during these sampling dates. Wind speed was in stable trend for the 28-Jan with 2 m/s average speed and showed a very slowly increasing trendline for 29-Jan with 3 m/s average speed. On 30-Jan, wind speed reached to its maximum point 6.14 m/s at 13:00-15:00h then started decreasing until next morning. Last sampling day 31-Jan showed an increasing trendline until 11:00-13:00h then remain almost stable with 4.73 m/s average speed from 11:00-13:00h to 17:00-19:00h. The average wind speed for the whole sampling period was observed as

3.53 m/s which was corresponding to between light air and gentle breeze according to Beaufort wind scale (Figure 2.21).

Solar radiation was in stable trend for the 28-Jan with 89.58 W/m^2 peak point on 13:00-15:00h and increased on 29-Jan to 298.36 W/m^2 peak point on 11:00-13:00h. On 30-Jan, solar radiation was in stable trend again with 75.37 W/m^2 average value. Last sampling day, 31-Jan showed the highest trendline with the highest point with 524.50 W/m^2 peak at 13:00-15:00h. In comparison, radiation during the summer may be 600-800 W/m^2. With these values we can say very low solar radiation was observed on 28-30 Jan (Figure 2.20).

Wind direction varied from NNW to NE on 28-29 Jan and remained from NE on 30-31 Jan (Figures from 2.22 to 2.25).

Stable conditions in the atmosphere were observed on 28-Jan due to very low radiation and low temperatures. This is shown in Figure 3.10 due to the lack of vertical motion in air mass trajectories. Similar behavior is observed on 30-Jan (Figure 3.10C) with air mass trajectories arriving from maximum a couple hundred meters above ground level. Greater vertical motion, and possible dispersion of pollutants, can be observed on 29 and 31 of January with air masses arriving from approximately 500-1000 m above ground level (Figure 3.10B and 3.10D).

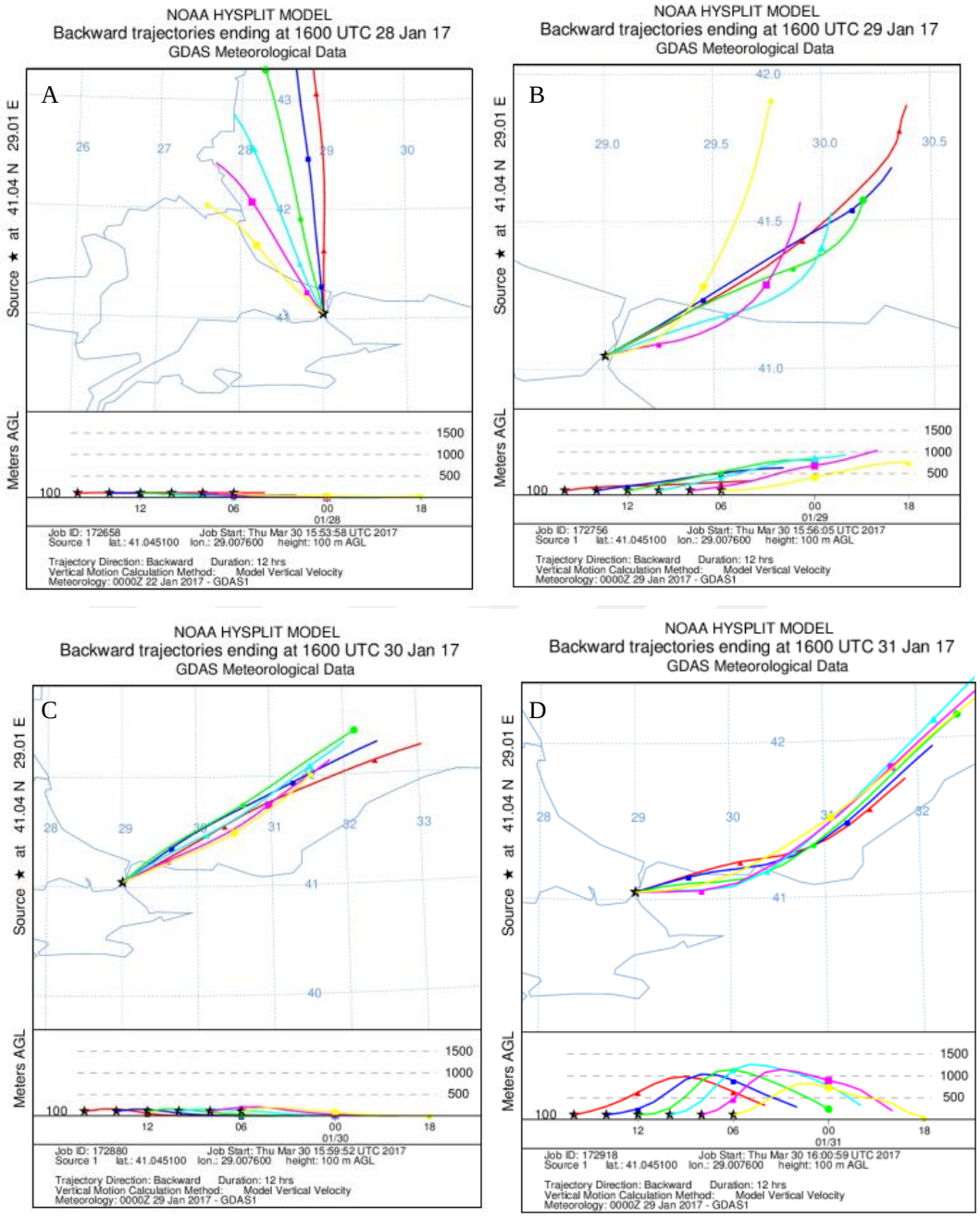

Figure 3.10. HYSPLIT simulations of air mass backward trajectories for each 2h sample. (A) 28.1.2017, (B) 29.1.2017, (C) 30.1.2017, (D) 31.1.2017.

3.2.4. Daily composition

Next four figures are given to show the daily composition of the compounds and the changes of them between sampling periods. To show this, each figure is prepared for every compound for each day.

Traffic density and meteorological conditions such as temperature, solar radiation, wind speed, wind direction, and stability of the atmosphere play a very big role on the diurnal variations. Figure 3.11 shows high concentration values for all compounds, unlike the next three figures. 28-Jan Saturday has the lowest temperature and lowest wind speed amongst sampling days. Also, only this day wind direction was different (NW). Probably for these reasons, high volatility compounds have higher values on this day.

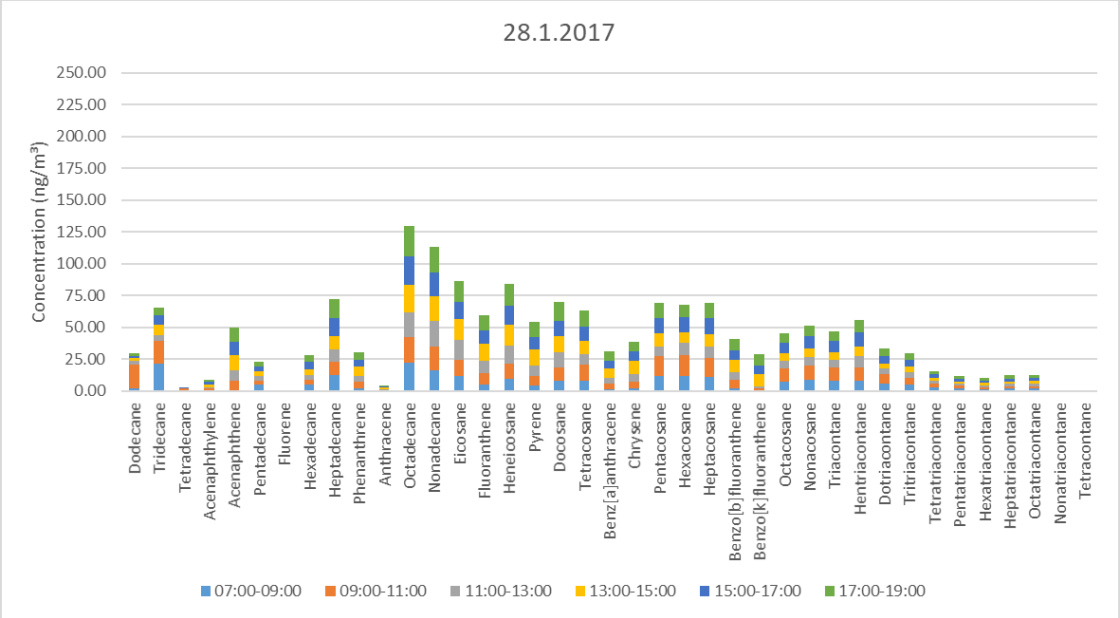

Figure 3.11. Daily composition of the compounds for 28.1.2017 (ng/m^3).

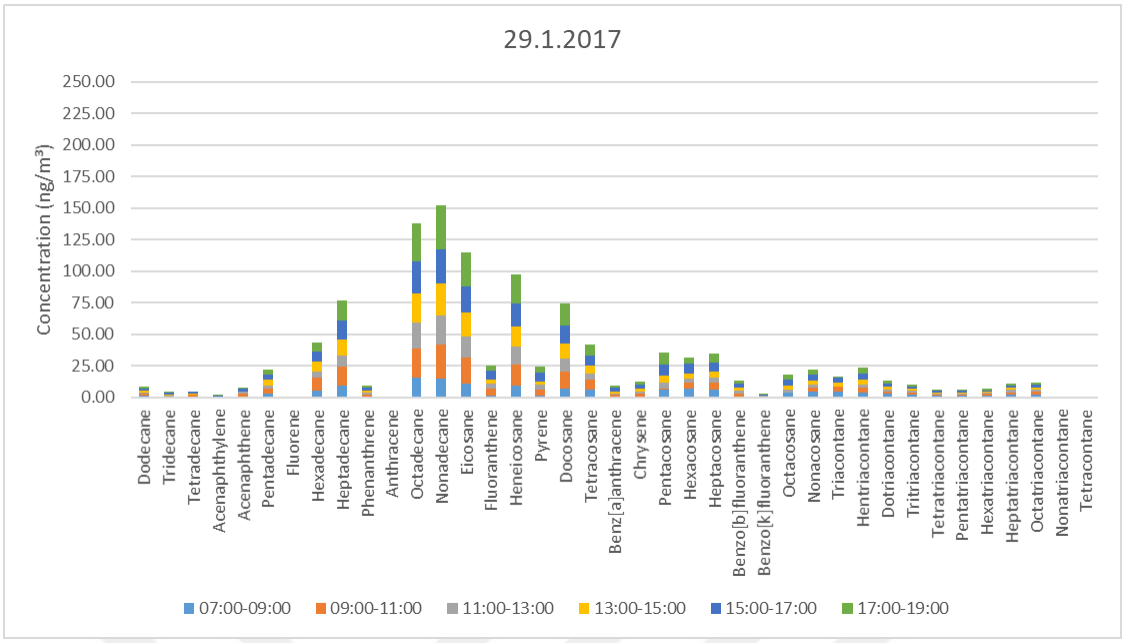

Figure 3.12. Daily composition of the compounds for 29.1.2017 (ng/m^3).

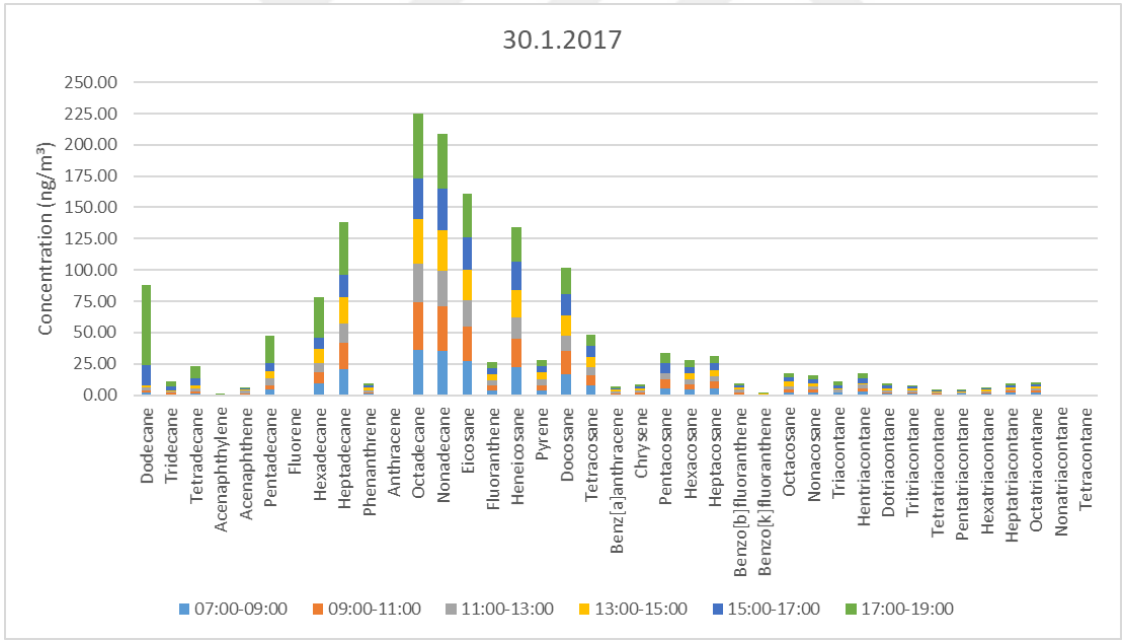

Figure 3.13. Daily composition of the compounds for 30.1.2017 (ng/m^3).

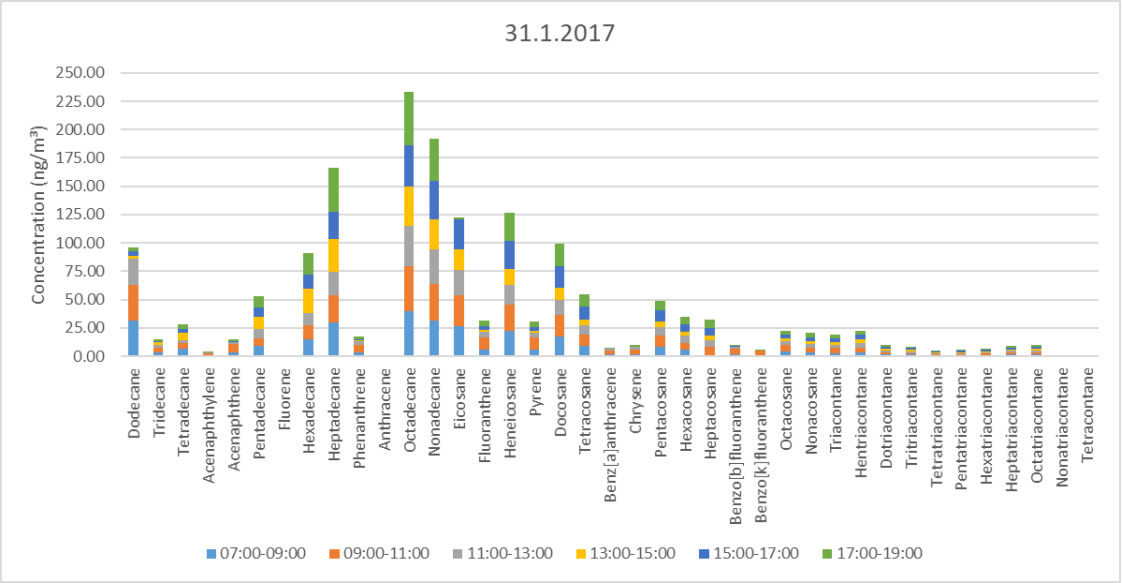

Figure 3.14. Daily composition of the compounds for 31.1.2017 (ng/m^3).

3.2.5. Hourly comparisons

Concentrations of the compounds for each four days of sampling are compared to each other for every 2-hour sampling periods. Results are used as percentage to show the differences of the concentrations between days on the same sampling hours. Next figures are important to see these differences.

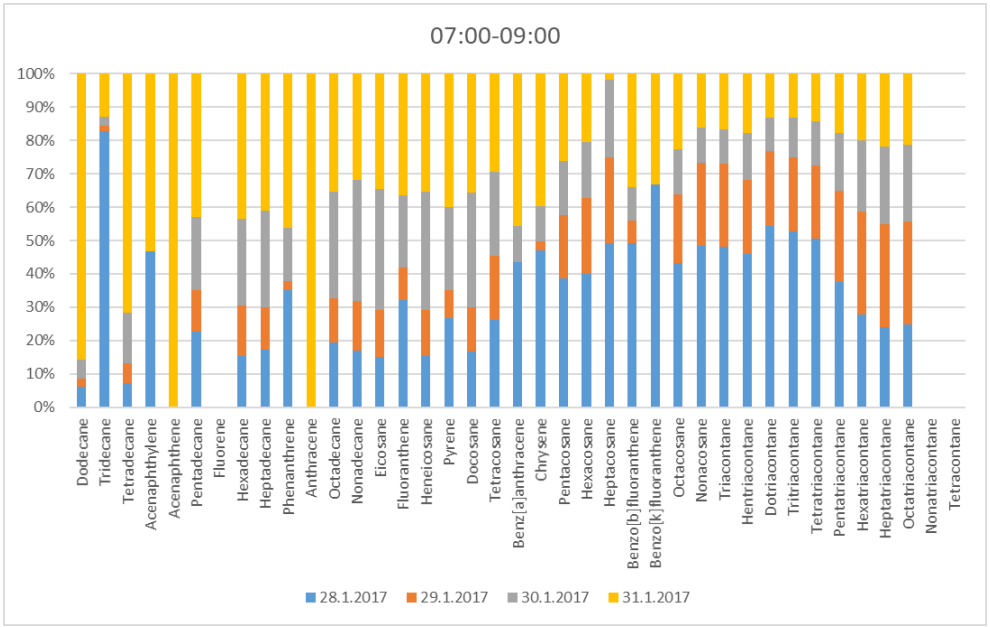

Figure 3.15. Hourly composition comparison of the compounds for 07:00-09:00 period.

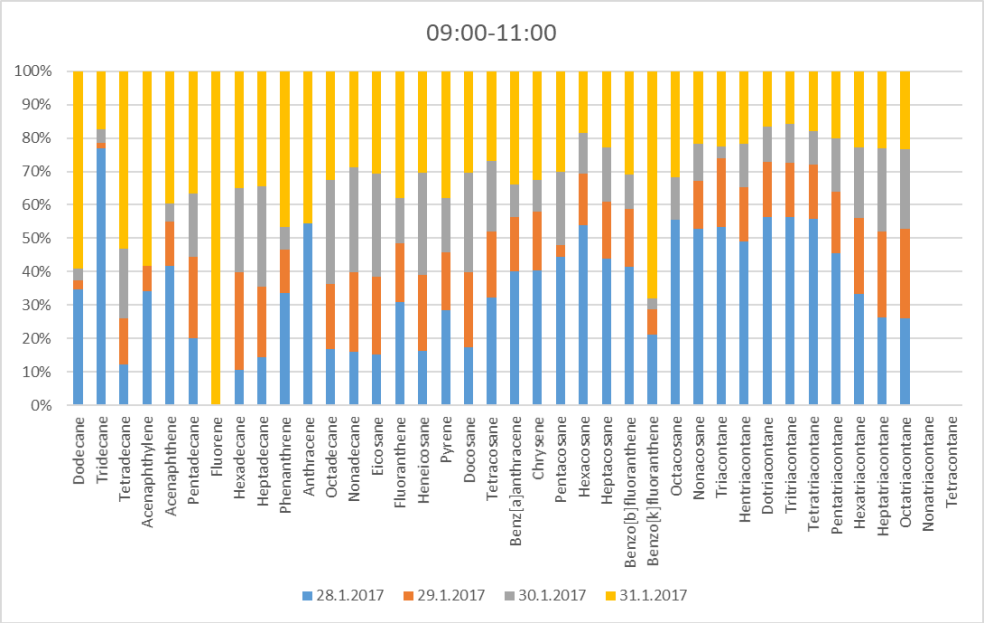

Figure 3.16. Hourly composition comparison of the compounds for 09:00-11:00 period.

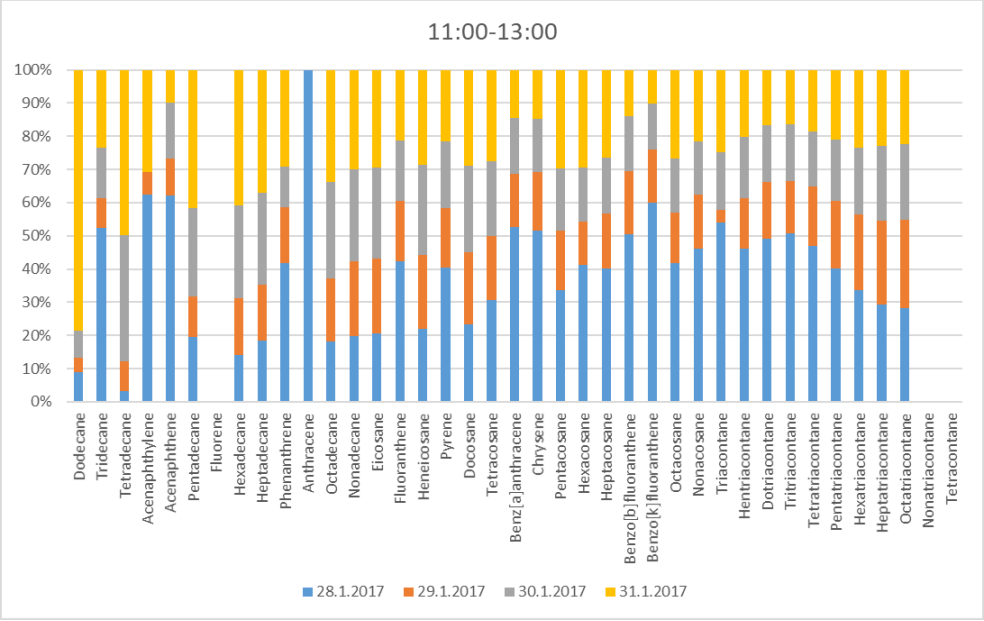

Figure 3.17. Hourly composition comparison of the compounds for 11:00-13:00 period.

While morning hours have higher low volatility compounds for weekdays, it was seen that weekend days have higher high volatility compounds. Also, 28-Jan Saturday have an increasing trendline for all compounds during the day.

29-Jan Sunday, has the lowest concentrations amongst all four sampling days. It is the day that has the lowest traffic count among sampling days.

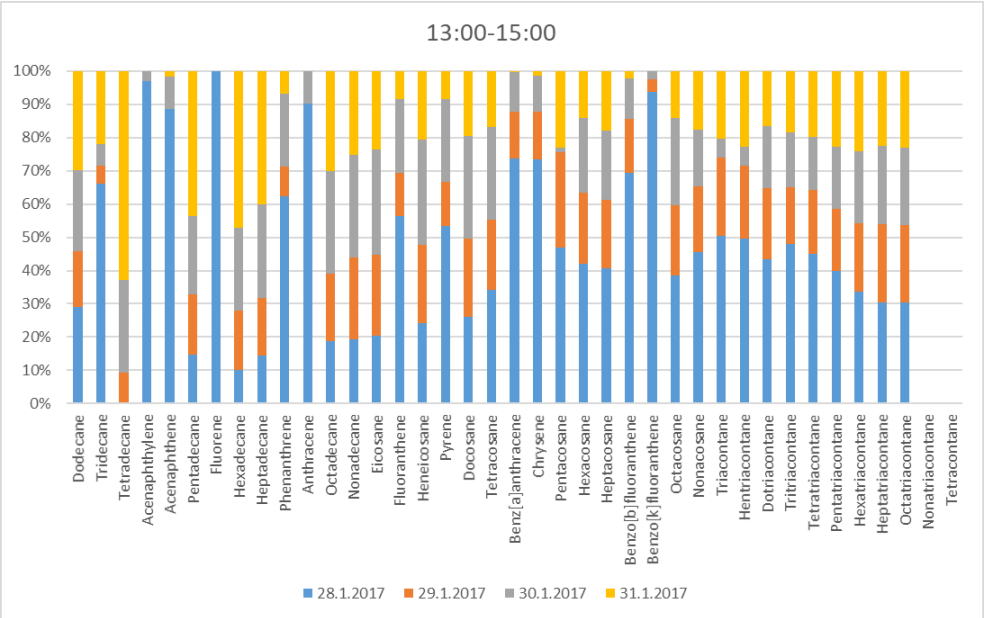

Figure 3.18. Hourly composition comparison of the compounds for 13:00-15:00 period.

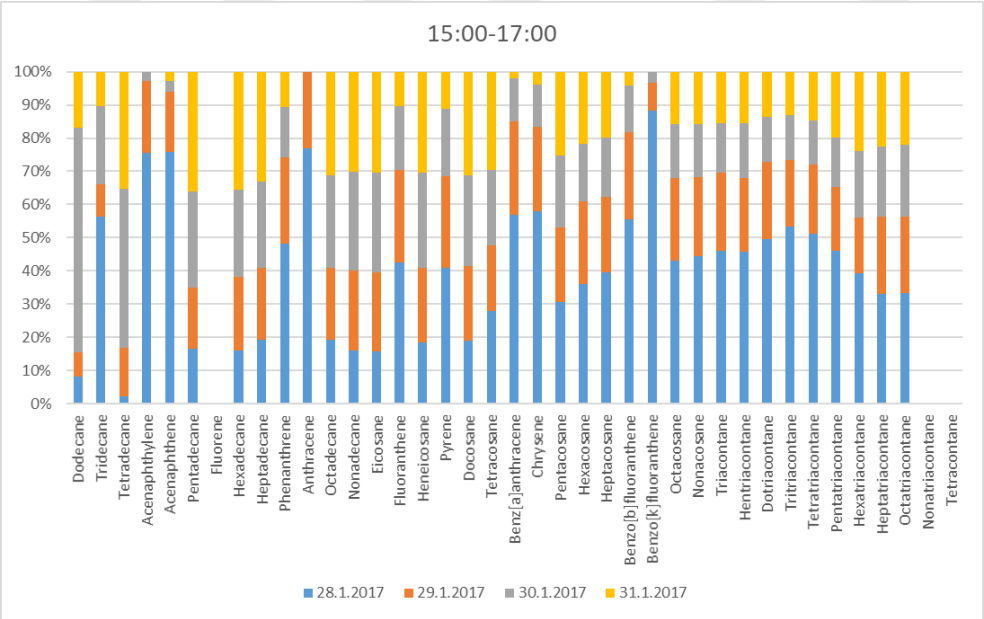

Figure 3.19. Hourly composition comparison of the compounds for 15:00-17:00 period.

After 15:00h-17:00h, 30-Jan Monday shows increasing concentration values on low volatility compounds which are traffic dependent compounds.

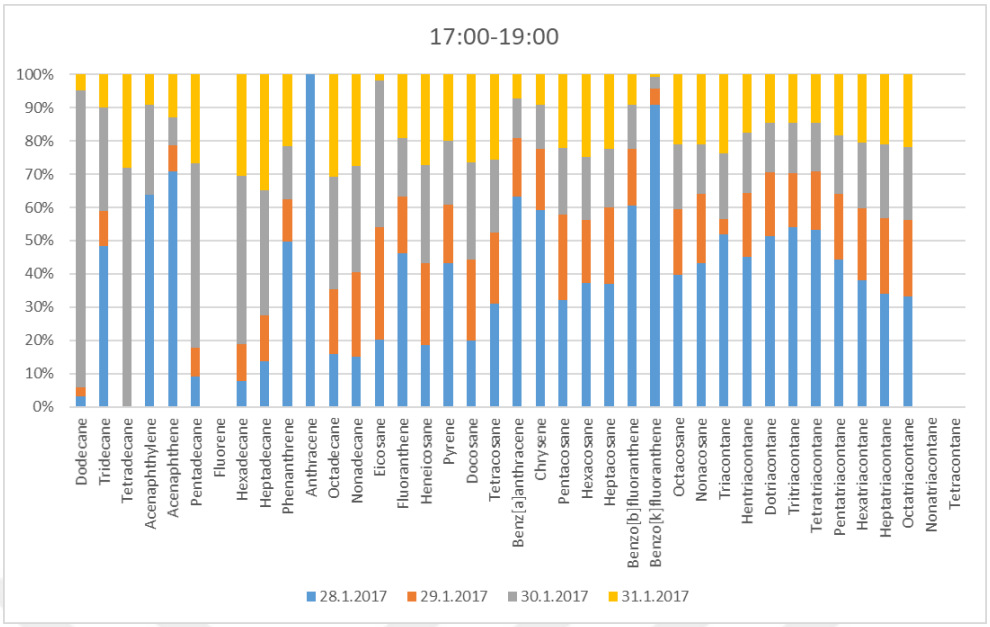

Figure 3.20. Hourly composition comparison of the compounds for 17:00-19:00 period.

4. CONCLUSIONS

A thermal desorption method was developed and applied to identify and quantify 11 PAH and 28 n-alkanes in 2-hour $PM_{2.5}$ samples with gas chromatography – mass spectrometry (TD-GC-MS). The samples were collected in a traffic-influenced area for four days to compare the impact of traffic over the weekend and weekdays. A high correlation between concentration of SVOCs and traffic was found ($R^2 = 0.5$). However, stability of the atmosphere also influenced the concentration of SVOCs in the particle phase, particularly on Saturday, when no vertical motion was observed. The use of the developed thermal desorption method will allow the analysis of highly-time resolved samples for better apportionment of sources and understanding of transport and transformation of organic compounds in the atmosphere.

The study of organic compounds in high-time resolved samples presented here is reported for the first time in Turkey and has been scarcely reported in the world. Concentrations of organic compounds in the atmosphere depend on physicochemical properties that determine reactivity and volatility, sources, and transport or dispersion through the atmosphere. Therefore, traffic density and meteorological conditions such as temperature, solar radiation, wind speed, wind direction, and stability of the atmosphere play a very big role on their diurnal variations.

The main sources of organic compounds in the atmosphere have been identified as coal combustion mostly for residential heating (20-29%), vehicle emissions (13-15%), and secondary organic carbon (15-17%). The distribution of these sources varies during the winter and summer and includes additional contributions from cooking (11-13%) and biomass burning (3-8%) (Wang et al., 2016b). In our work we found a strong correlation between total concentration of SVOCs and traffic ($R^2 = 0.5$) that can be observed in Figure 3.8 and Figure 3.9. An inverse correlation was found with temperature ($R^2 = -0.35$), relative humidity ($R^2 = -0.24$), and solar radiation ($R^2 = -0.19$). These small correlations will require the use of multivariate factor analysis to better understand the complex relationship among various factors.

REFERENCES

Abraham, M.H., Smith, R.E., Luchtefeld, R., Boorem, A.J., Luo, R. and Acree, W.E., Jr. (2010) Prediction of solubility of drugs and other compounds in organic solvents. J Pharm Sci 99(3), 1500-1515.

Andreae, M.O., (1995) Climatic effects of changing atmospheric aerosol levels. In: Henderson-Sellers, A. (Ed.), World Survey of Climatology. Future Climates of the World, vol. 16. Elsevier, Amsterdam, pp. 341–392.

Andreae, M.O. (2007) Atmosphere. Aerosols before pollution. Science 315(5808), 50-51.

Arora, A. (2006) Hydrocarbons (Alkanes, Alkenes And Alkynes), Discovery Publishing House Pvt. Limited.

Arpino, P., Albrecht, P. and Ourisson, G. (1972) Advances in Organic Geochemistry. von Gaertner, H.R. and Wehner, H. (eds), pp. 173-187, Pergamon Press, Oxford.

Baklanov, A., Lawrence, M., Pandis, S., Mahura, A., Finardi, S., Moussiopoulos, N., Beekmann, M., Laj, P., Gomes, L., Jaffrezo, J.L., Borbon, A., Coll, I., Gros, V., Sciare, J., Kukkonen, J., Galmarini, S., Giorgi, F., Grimmond, S., Esau, I., Stohl, A., Denby, B., Wagner, T., Butler, T., Baltensperger, U., Builtjes, P., van den Hout, D., van der Gon, H.D., Collins, B., Schluenzen, H., Kulmala, M., Zilitinkevich, S., Sokhi, R., Friedrich, R., Theloke, J., Kummer, U., Jalkinen, L., Halenka, T., Wiedensholer, A., Pyle, J. and Rossow, W.B. (2010) MEGAPOLI: concept of multi-scale modelling of megacity impact on air quality and climate. Advances in Science and Research 4, 115-120.

Baklanov, A., Molina, L.T. and Gauss, M. (2016) Megacities, air quality and climate. Atmospheric Environment 126, 235-249.

Bates, M., Bruno, P., Caputi, M., Caselli, M., de Gennaro, G. and Tutino, M. (2008) Analysis of polycyclic aromatic hydrocarbons (PAHs) in airborne particles by direct sample introduction thermal desorption GC/MS. Atmospheric Environment 42(24), 6144-6151.

Beauford, W., Barber, J. and Barringer, A.R. (1975) Heavy metal release from plants into the atmosphere. Nature 256(5512), 35-37.

Bernard, S.M., Samet, J.M., Grambsch, A., Ebi, K.L. and Romieu, I. (2001) The Potential Impacts of Climate Variability and Change on Air Pollution-Related Health Effects in the United States. Environmental Health Perspectives 109, 199.

Blanchard, D.C. (1964) Sea-to-Air Transport of Surface Active Material. Science 146(3642), 396-397.

Blanchard, D.C. and Syzdek, L.D. (1972) Concentration of bacteria in jet drops from bursting bubbles. Journal of Geophysical Research 77(27), 5087-5099.

Blanchard, P., Brook, J.R. and Brazal, P. (2002) Chemical characterization of the organic fraction of atmospheric aerosol at two sites in Ontario, Canada. Journal of Geophysical Research: Atmospheres 107(D21), ICC 10-11-ICC 10-18.

Blazsó, M., Janitsek, S., Gelencsér, A., Artaxo, P., Graham, B. and Andreae, M.O. (2003) Study of tropical organic aerosol by thermally assisted alkylation-gas chromatography mass spectrometry. Journal of Analytical and Applied Pyrolysis 68, 351-369.

Bond, T.C., Doherty, S.J., Fahey, D.W., Forster, P.M., Berntsen, T., DeAngelo, B.J., Flanner, M.G., Ghan, S., Kärcher, B., Koch, D., Kinne, S., Kondo, Y., Quinn, P.K., Sarofim, M.C., Schultz, M.G., Schulz, M., Venkataraman, C., Zhang, H., Zhang, S., Bellouin, N., Guttikunda, S.K., Hopke, P.K., Jacobson, M.Z., Kaiser, J.W., Klimont, Z., Lohmann, U., Schwarz, J.P., Shindell, D., Storelvmo, T., Warren, S.G. and Zender, C.S. (2013) Bounding the role of black carbon in the climate system: A scientific assessment. Journal of Geophysical Research: Atmospheres 118(11), 5380-5552.

Boström, C.-E., Gerde, P., Hanberg, A., Jernström, B., Johansson, C., Kyrklund, T., Rannug, A., Törnqvist, M., Victorin, K. and Westerholm, R. (2002) Cancer risk assessment, indicators, and guidelines for polycyclic aromatic hydrocarbons in the ambient air. Environmental Health Perspectives 110(Suppl 3), 451-488.

Bourotte, C., Forti, M., Taniguchi, S., Bicego, M. and Lotufo, P. (2005) A wintertime study of PAHs in fine and coarse aerosols in Sao Paulo City, Brazil.

Butler, T.M. and Lawrence, M.G. (2009) The influence of megacities on global atmospheric chemistry: a modelling study. Environmental Chemistry 6(3), 219.

Chen, Z., Wang, J.N., Ma, G.X. and Zhang, Y.S. (2013) China tackles the health effects of air pollution. Lancet 382(9909), 1959-1960.

Chow, J.C., Yu, J.Z., Watson, J.G., Ho, S.S., Bohannan, T.L., Hays, M.D. and Fung, K.K. (2007) The application of thermal methods for determining chemical composition of carbonaceous aerosols: a review. J Environ Sci Health A Tox Hazard Subst Environ Eng 42(11), 1521-1541.

Cincinelli, A., Bubba, M.D., Martellini, T., Gambaro, A. and Lepri, L. (2007) Gas-particle concentration and distribution of n-alkanes and polycyclic aromatic hydrocarbons in the atmosphere of Prato (Italy). Chemosphere 68(3), 472-478.

Cotham, W.E. and Bidleman, T.F. (1995) Polycyclic aromatic hydrocarbons and polychlorinated biphenyls in air at an urban and a rural site near lake michigan. Environ Sci Technol 29(11), 2782-2789.

Demographia World Urban Areas. 13th Annual Edition, 13th ed., Demographia, 2017, www.demographia.com/db-worldua.pdf., (01.04.2017).

Derwent, R.G., Jenkin, M.E., Utembe, S.R., Shallcross, D.E., Murrells, T.P. and Passant, N.R. (2010) Secondary organic aerosol formation from a large number of reactive man-made organic compounds. Sci Total Environ 408(16), 3374-3381.

Ding, L., Chan, T.W., Ke, F. and Wang, D.K.W. (2014) Characterization of chemical composition and concentration of fine particulate matter during a transit strike in Ottawa, Canada. Atmospheric Environment 89, 433-442.

Elorduy, I., Elcoroaristizabal, S., Durana, N., García, J. and Alonso, L. (2016) Diurnal variation of particle-bound PAHs in an urban area of Spain using TD-GC/MS: Influence of meteorological parameters and emission sources.

Erickson, D.J. and Duce, R.A. (1988) On the global flux of atmospheric sea salt. Journal of Geophysical Research: Oceans 93(C11), 14079-14088.

Feingold, G., Frisch, A.S., Stevens, B. and Cotton, W.R. (1999) On the relationship among cloud turbulence, droplet formation and drizzle as viewed by Doppler radar, microwave radiometer and lidar. Journal of Geophysical Research: Atmospheres 104(D18), 22195-22203.

Fetzer, J.C. (2007) The Chemistry and Analysis of the Large Polycyclic Aromatic Hydrocarbons. Polycyclic Aromatic Compounds 27(2), 143-162.

Gagosian, R.B., Zafiriou, O.C., Peltzer, E.T. and Alford, J.B. (1982) Lipids in aerosols from the tropical North Pacific: Temporal variability. Journal of Geophysical Research: Oceans 87(C13), 11133-11144.

Gelencsér, A. (2004) Carbonaceous aerosol, p. 352, Springer Science & Business Media, Netherlands.

Gillette, D. (1978) A wind tunnel simulation of the erosion of soil: Effect of soil texture, sandblasting, wind speed, and soil consolidation on dust production. Atmospheric Environment (1967) 12(8), 1735-1743.

Gong, S.L., Barrie, L.A. and Blanchet, J.P. (1997) Modeling sea-salt aerosols in the atmosphere: 1. Model development. Journal of Geophysical Research: Atmospheres 102(D3), 3805-3818.

Griffiths, J. (2008) A Brief History of Mass Spectrometry. Analytical Chemistry 80(15), 5678-5683.

Hamilton, J.F., Webb, P.J., Lewis, A.C., Hopkins, J.R., Smith, S. and Davy, P. (2004) Partially oxidised organic components in urban aerosol using GCXGC-TOF/MS. Atmos. Chem. Phys. 4(5), 1279-1290.

Hanedar, A., Alp, K., Kaynak, B. and Avsar, E. (2014) Toxicity evaluation and source apportionment of Polycyclic Aromatic Hydrocarbons (PAHs) at three stations in Istanbul, Turkey. Sci Total Environ 488-489, 437-446.

Havers, N., Burba, P., Lambert, J. and Klockow, D. (1998) Spectroscopic Characterization of Humic-Like Substances in Airborne Particulate Matter. Journal of Atmospheric Chemistry 29(1), 45-54.

Hsiao, W.L., Mo, Z.Y., Fang, M., Shi, X.M. and Wang, F. (2000) Cytotoxicity of PM(2.5) and PM(2.5--10) ambient air pollutants assessed by the MTT and the Comet assays. Mutat Res 471(1-2), 45-55.

Hung, H., Katsoyiannis, A.A., Brorström-Lundén, E., Olafsdottir, K., Aas, W., Breivik, K., Bohlin-Nizzetto, P., Sigurdsson, A., Hakola, H., Bossi, R., Skov, H., Sverko, E., Barresi, E., Fellin, P. and Wilson, S. (2016) Temporal trends of Persistent Organic Pollutants (POPs) in arctic air: 20 years of monitoring under the Arctic Monitoring and Assessment Programme (AMAP). Environmental Pollution 217, 52-61.

Institute for Health Metrics and Evaluation (2013) The Global Burden of Disease (GBD) Visualizations: GBD compare. Institute for Health Metrics and Evaluation, Seattle, USA (https://vizhub.healthdata.org/gbd-compare/) (Retrieved 25/04/17).

Jacobson, M.Z. (2010) Short-term effects of controlling fossil-fuel soot, biofuel soot and gases, and methane on climate, Arctic ice, and air pollution health. Journal of Geophysical Research: Atmospheres 115(D14), n/a-n/a.

Japan, T.o. (2012) Advanced Ceramic Technologies & Products, Springer, Japan.

Jeon, S.J., Meuzelaar, H.L., Sheya, S.A., Lighty, J.S., Jarman, W.M., Kasteler, C., Sarofim, A.F. and Simoneit, B.R. (2001) Exploratory studies of PM10 receptor and source profiling by GC/MS and principal component analysis of temporally and spatially resolved ambient samples. J Air Waste Manag Assoc 51(5), 766-784.

Jimenez, J.L., Canagaratna, M.R., Donahue, N.M., Prevot, A.S., Zhang, Q., Kroll, J.H., DeCarlo, P.F., Allan, J.D., Coe, H., Ng, N.L., Aiken, A.C., Docherty, K.S., Ulbrich, I.M., Grieshop, A.P., Robinson, A.L., Duplissy, J., Smith, J.D., Wilson, K.R., Lanz, V.A., Hueglin, C., Sun, Y.L., Tian, J., Laaksonen, A., Raatikainen, T., Rautiainen, J., Vaattovaara, P., Ehn, M., Kulmala, M., Tomlinson, J.M., Collins, D.R., Cubison, M.J., Dunlea, E.J., Huffman, J.A., Onasch, T.B., Alfarra, M.R., Williams, P.I., Bower, K., Kondo, Y., Schneider, J., Drewnick, F., Borrmann, S., Weimer, S., Demerjian, K., Salcedo, D., Cottrell, L., Griffin, R., Takami, A., Miyoshi, T., Hatakeyama, S., Shimono, A., Sun, J.Y., Zhang, Y.M., Dzepina, K., Kimmel, J.R., Sueper, D., Jayne, J.T., Herndon, S.C., Trimborn, A.M., Williams, L.R., Wood, E.C., Middlebrook, A.M., Kolb, C.E., Baltensperger, U. and Worsnop, D.R. (2009) Evolution of organic aerosols in the atmosphere. Science 326(5959), 1525-1529.

Kanakidou, M., Seinfeld, J.H., Pandis, S.N., Barnes, I., Dentener, F.J., Facchini, M.C., Van Dingenen, R., Ervens, B., Nenes, A., Nielsen, C.J., Swietlicki, E., Putaud, J.P., Balkanski, Y., Fuzzi, S., Horth, J., Moortgat, G.K., Winterhalter, R., Myhre, C.E.L., Tsigaridis, K., Vignati, E., Stephanou, E.G. and Wilson, J. (2005) Organic aerosol and global climate modelling: a review. Atmos. Chem. Phys. 5(4), 1053-1123.

Karaca, F., Alagha, O. and Erturk, F. (2005) Statistical characterization of atmospheric PM10 and PM2.5 concentrations at a non-impacted suburban site of Istanbul, Turkey. Chemosphere 59(8), 1183-1190.

Karaca, F., Alagha, O., Ertürk, F., Yılmaz, Y.Z. and Özkara, T. (2008) Seasonal Variation of Source Contributions to Atmospheric Fine and Coarse Particles at Suburban Area in Istanbul, Turkey. Environmental Engineering Science 25(5), 767-782.

Kuzu, S.L., Saral, A., Summak, G., Coltu, H. and Demir, S. (2014) Ambient polychlorinated biphenyl levels and their evaluation in a metropolitan city. Sci Total Environ 472, 13-19.

Long, C.M., Nascarella, M.A. and Valberg, P.A. (2013) Carbon black vs. black carbon and other airborne materials containing elemental carbon: Physical and chemical distinctions. Environmental Pollution 181, 271-286.

Marticorena, B., Bergametti, G., Aumont, B., Callot, Y., N'Doumé, C. and Legrand, M. (1997) Modeling the atmospheric dust cycle: 2. Simulation of Saharan dust sources. Journal of Geophysical Research: Atmospheres 102(D4), 4387-4404.

Miller, R.L. and Tegen, I. (1998) Climate Response to Soil Dust Aerosols. Journal of Climate 11(12), 3247-3267.

Mintz, C. (2009) Predicting chemical and biochemical properties using the Abraham general solvation model. Ph.D. Thesis, University of North Texas, USA.

Molina, L.T., Madronich, S., Gaffney, J.S., Apel, E., de Foy, B., Fast, J., Ferrare, R., Herndon, S., Jimenez, J.L., Lamb, B., Osornio-Vargas, A.R., Russell, P., Schauer, J.J., Stevens, P.S., Volkamer, R. and Zavala, M. (2010) An overview of the MILAGRO 2006 Campaign: Mexico City emissions and their transport and transformation. Atmospheric Chemistry and Physics 10(18), 8697-8760.

Molina, M.J., Ivanov, A.V., Trakhtenberg, S. and Molina, L.T. (2004) Atmospheric evolution of organic aerosol. Geophysical Research Letters 31(22), n/a-n/a.

Monahan, E.C., Spiel, D.E. and Davidson, K.L. (1986) Oceanic Whitecaps: And Their Role in Air-Sea Exchange Processes. Monahan, E.C. and Niocaill, G.M. (eds), pp. 167-174, Springer Netherlands, Dordrecht.

Moss, G.P., Smith, P.A.S. and Tavernier, D. (1995) Glossary of class names of organic compounds and reactivity intermediates based on structure (IUPAC Recommendations 1995), p. 1307.

Mugica, V., Torres, M., Salinas, E., Gutierrez, M. and García, R. (2010) Air Pollution. Villanyi, V. (ed), p. Ch. 4, InTech, Rijeka.

O'Dowd, C.D., Smith, M.H., Consterdine, I.E. and Lowe, J.A. (1997) Marine aerosol, sea-salt, and the marine sulphur cycle: a short review. Atmospheric Environment 31(1), 73-80.

Ozdemir, H., Pozzoli, L., Kindap, T., Demir, G., Mertoglu, B., Mihalopoulos, N., Theodosi, C., Kanakidou, M., Im, U. and Unal, A. (2014) Spatial and temporal analysis of black carbon aerosols in Istanbul megacity. Sci Total Environ 473-474, 451-458.

Penner, J.E., Andreae, M.O., Annegarn, H., Barrie, L., Feichter, J., Hegg, D., Jayaraman, A., Leaitch, R., Murphy, D., Nganga, J. and Pitari, G. (2001) Climate Change 2001: The Scientific Basis. Contribution of Working Group I to the Third Assessment Report of the Intergovernmental Panel on Climate Change. Houghton, J.T., Ding, Y., Griggs, D.J., Noguer, M., van der Linden, P.J., Dai, X., Maskell, K. and Johnson, C.A. (eds), pp. 289 - 348, Cambridge University Press, Cambridge, UK, and New York, NY, USA.

Poschl, U. (2005) Atmospheric aerosols: composition, transformation, climate and health effects. Angew Chem Int Ed Engl 44(46), 7520-7540.

Schnell, R.C. and Vali, G. (1973) World-wide Source of Leaf-derived Freezing Nuclei. Nature 246(5430), 212-213.

Rogge, W.F., Hildemann, L.M., Mazurek, M.A., Cass, G.R. and Simoneit, B.R.T. (1993a) Sources of fine organic aerosol. 2. Noncatalyst and catalyst-equipped automobiles and heavy-duty diesel trucks. Environmental Science & Technology 27(4), 636-651.

Rogge, W.F., Hildemann, L.M., Mazurek, M.A., Cass, G.R. and Simoneit, B.R.T. (1993b) Sources of fine organic aerosol. 3. Road dust, tire debris, and organometallic brake lining dust: roads as sources and sinks. Environmental Science & Technology 27(9), 1892-1904.

Schnell, R.C. and Vali, G. (1976) Biogenic Ice Nuclei: Part I. Terrestrial and Marine Sources. Journal of the Atmospheric Sciences 33(8), 1554-1564.

Schnelle-Kreis, J., Sklorz, M., Orasche, J., Stölzel, M., Peters, A. and Zimmermann, R. (2007) Semi Volatile Organic Compounds in Ambient PM2.5. Seasonal Trends and Daily Resolved Source Contributions. Environmental Science & Technology 41(11), 3821-3828.

Simoneit, B.R.T., Chester, R., Eglinton, G. (1977) Biogenic lipids in particulates from the lower atmosphere over the eastern Atlantic, Nature, 267, 682-685.

Stock, S.Z., Russo, M., Butler, T.M., Archibald, A., Lawrence, M., Telford, P., Abraham, N.L. and Pyle, A.J. (2013) Modelling the impact of megacities on local, regional and global tropospheric ozone and the deposition of nitrogen species. Atmospheric Chemistry and Physics 13, 12215–12231.

Tayanc, M. (2000) An assessment of spatial and temporal variation of sulfur dioxide levels over Istanbul, Turkey. Environmental Pollution (107), 61-69.

Tegen, I. and Fung, I. (1995) Contribution to the atmospheric mineral aerosol load from land surface modification. Journal of Geophysical Research: Atmospheres 100(D9), 18707-18726.

Tegen, I., Hollrig, P., Chin, M., Fung, I., Jacob, D. and Penner, J. (1997) Contribution of different aerosol species to the global aerosol extinction optical thickness: Estimates from model results. Journal of Geophysical Research: Atmospheres 102(D20), 23895-23915.

Theodosi, C., Im, U., Bougiatioti, A., Zarmpas, P., Yenigun, O. and Mihalopoulos, N. (2010) Aerosol chemical composition over Istanbul. Sci Total Environ 408(12), 2482-2491.

Turkish Statistical Institute (TurkStat), Adrese Dayalı Nüfus Kayıt Sistemi Sonuçları, 2016 (in Turkish), http://www.turkstat.gov.tr/, Retrieved 1 April 2017.

United Nations, Department of Economic and Social Affairs, Population Division (2015). World Urbanization Prospects: The 2014 Revision, (ST/ESA/SER.A/366).

Unal, Y.S., Toros, H., Deniz, A. and Incecik, S. (2011) Influence of meteorological factors and emission sources on spatial and temporal variations of PM10 concentrations in Istanbul metropolitan area. Atmospheric Environment 45(31), 5504-5513.

United States Environmental Protection Agency (US-EPA), National Ambient Air Quality Standards (NAAQS) Table, 2017 (in website), https://www.epa.gov/criteria-air-pollutants/naaqs-table, Retrieved 1 October 2017.

Viana, M., Querol, X., Alastuey, A., Ballester, F., Llop, S., Esplugues, A., Fernández-Patier, R., García dos Santos, S. and Herce, M.D. (2008) Characterising exposure to PM aerosols for an epidemiological study. Atmospheric Environment 42(7), 1552-1568.

Voorhees, K.J., Schulz, W.D., Kunen, S.M., Hendricks, L.J., Currie, L.A. and Klouda, G.A. (1991) Analysis of insoluble carbonaceous materials from airborne particles collected in pristine regions of colorado. Journal of Analytical and Applied Pyrolysis 18(3), 189-205.

Wang, J., Hang Ho, S.S., Huang, R., Gao, M., Liu, S., Zhao, S., Cao, J., Wang, G., Shen, Z. and Han, Y. (2016a) Characterization of parent and oxygenated-polycyclic aromatic hydrocarbons (PAHs) in Xi'an, China during heating period: An investigation of spatial distribution and transformation. Chemosphere 159, 367-377.

Wang, J., Ho, S.S., Ma, S., Cao, J., Dai, W., Liu, S., Shen, Z., Huang, R., Wang, G. and Han, Y. (2016b) Characterization of PM2.5 in Guangzhou, China: uses of organic markers for supporting source apportionment. Sci Total Environ 550, 961-971.

Weschler, C.J. and Nazaroff, W.W. (2008) Semivolatile organic compounds in indoor environments. Atmospheric Environment 42(40), 9018-9040.

Williams, B.J., Goldstein, A.H., Kreisberg, N.M. and Hering, S.V. (2006) An In-Situ Instrument for Speciated Organic Composition of Atmospheric Aerosols: Thermal Desorption Aerosol GC/MS-FID (TAG). Aerosol Science and Technology 40(8), 627-638.

Williams, B.J., Goldstein, A.H., Millet, D.B., Holzinger, R., Kreisberg, N.M., Hering, S.V., White, A.B., Worsnop, D.R., Allan, J.D. and Jimenez, J.L. (2007) Chemical speciation of organic aerosol during the International Consortium for Atmospheric Research on Transport and Transformation 2004: Results from in situ measurements. Journal of Geophysical Research: Atmospheres 112(D10).

Wolf, M.E. and Hidy, G.M. (1997) Aerosols and climate: Anthropogenic emissions and trends for 50 years. Journal of Geophysical Research: Atmospheres 102(D10), 11113-11121.

World Health Organization. Department of Public Health, E. and Health, S.D.o. (2016) Ambient Air Pollution: A Global Assessment of Exposure and Burden of Disease, World Health Organization.

World Health Organization (WHO), Ambient (Outdoor) Air Quality And Health Fact Sheet, 2016 (in website), http://www.who.int/mediacentre/factsheets/fs313/en/, Retrieved 1 October 2017.

Yang, H., Yu, J.Z., Ho, S.S.H., Xu, J., Wu, W.-S., Wan, C.H., Wang, X., Wang, X. and Wang, L. (2005) The chemical composition of inorganic and carbonaceous materials in PM2.5 in Nanjing, China. Atmospheric Environment 39(20), 3735-3749.

Zhu, T., Melamed, M., Parrish, D., Gauss, M., Klenner, L.G., Lawrence, M., Konare, A. and Liousse, C. (2012) WMO/IGAC Impacts of Megacities on Air Pollution and Climate, World Meteorological Organization, Switzerland.

APPENDIX A

SAMPLE ANALYSIS RESULTS

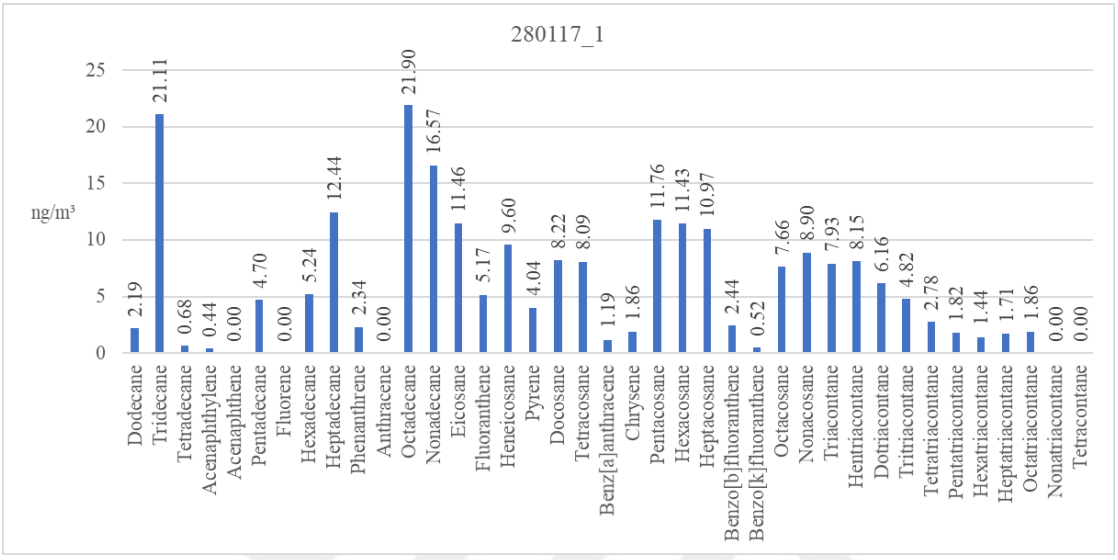

Figure A.1. Concentration of target compounds on 28.01.17 between 07:00-09:00.

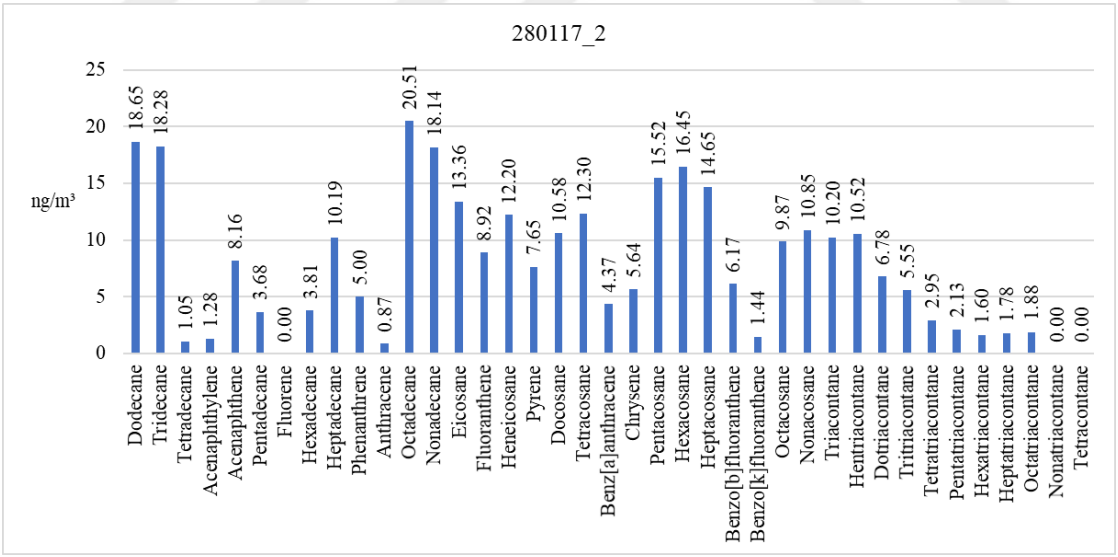

Figure A.2. Concentration of target compounds on 28.01.17 between 09:00-11:00.

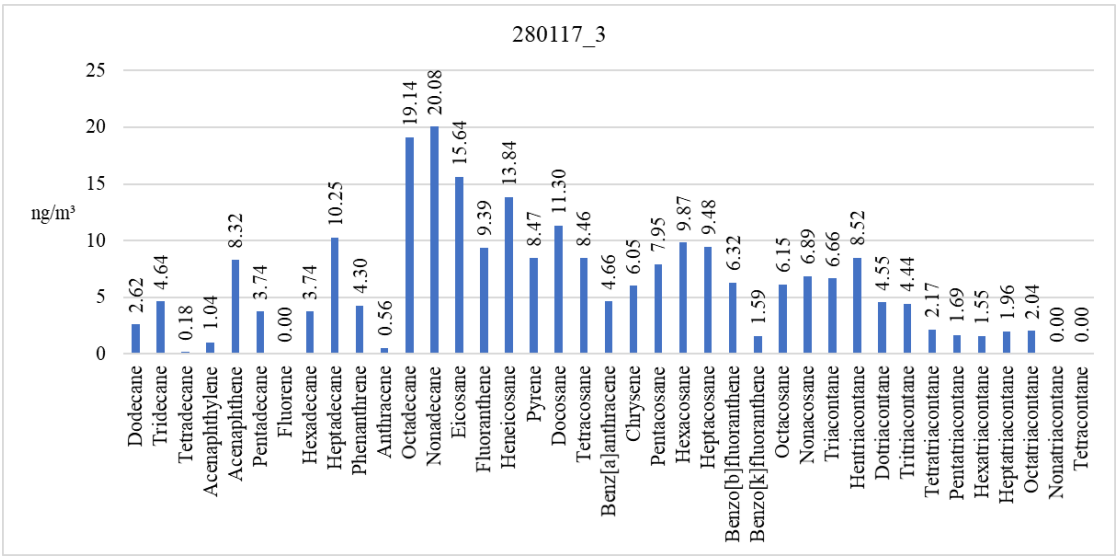

Figure A.3. Concentration of target compounds on 28.01.17 between 11:00-13:00.

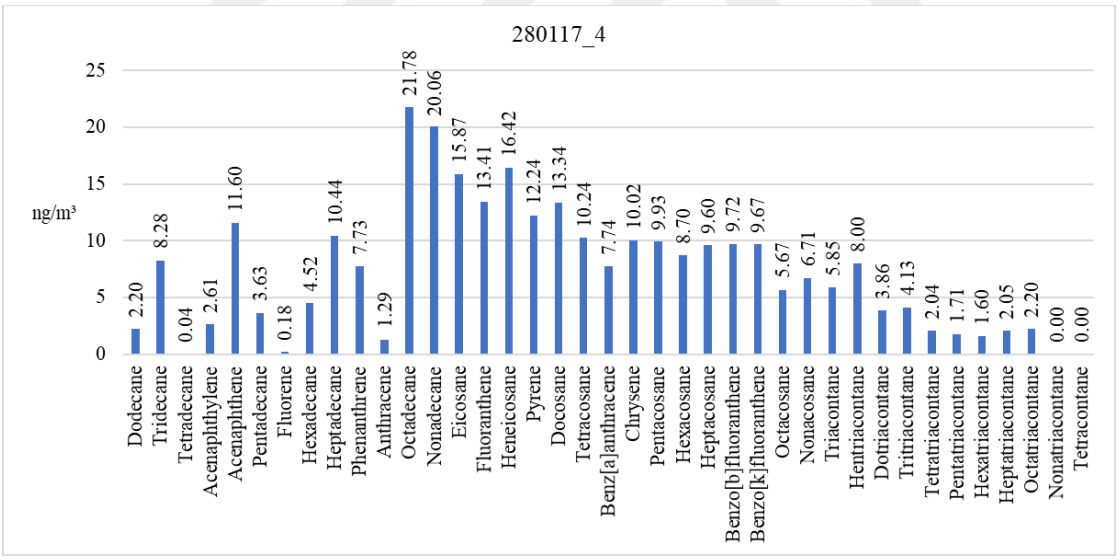

Figure A.4. Concentration of target compounds on 28.01.17 between 13:00-15:00.

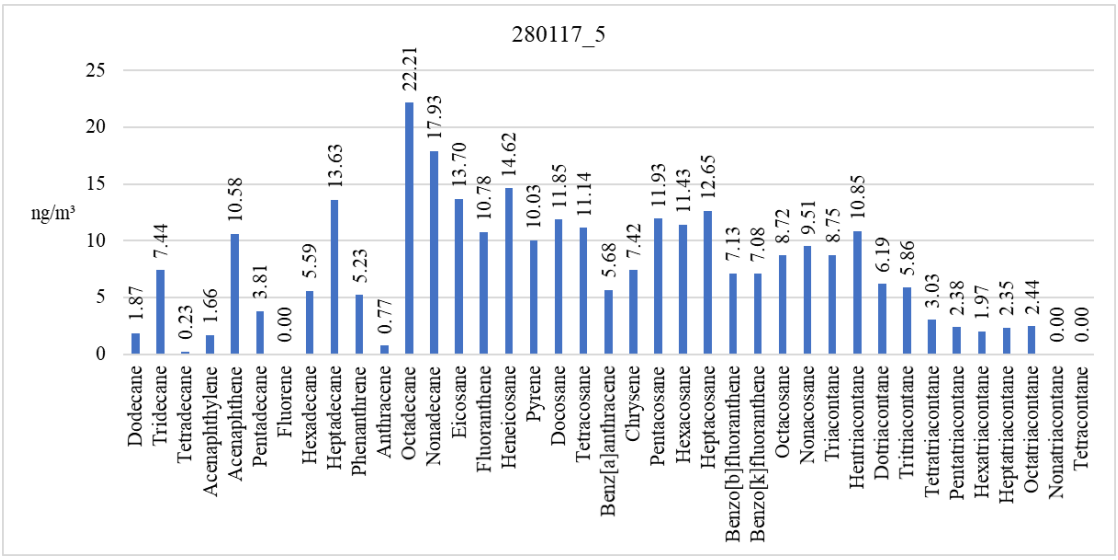

Figure A.5. Concentration of target compounds on 28.01.17 between 15:00-17:00.

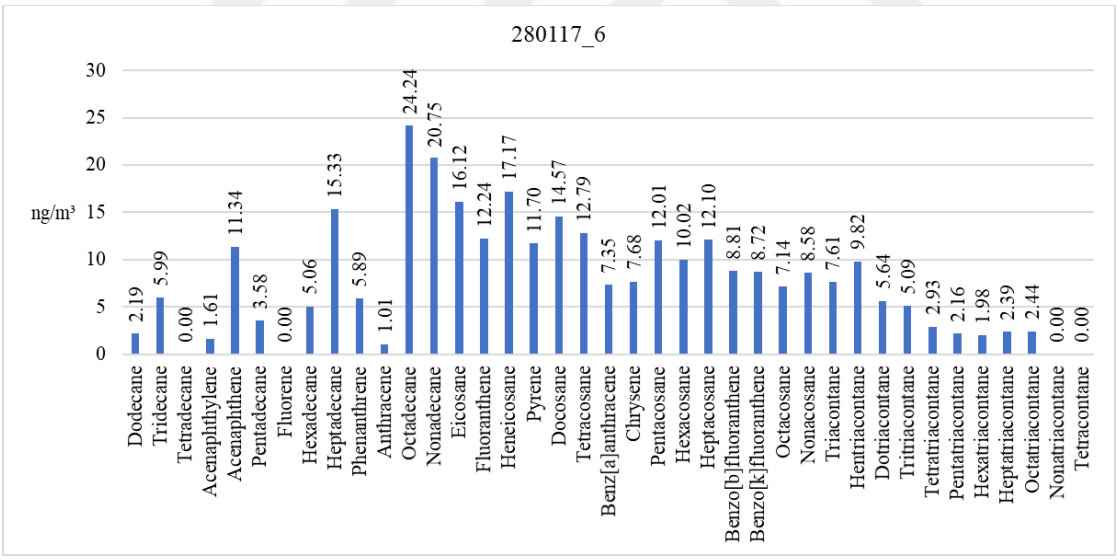

Figure A.6. Concentration of target compounds on 28.01.17 between 17:00-19:00.

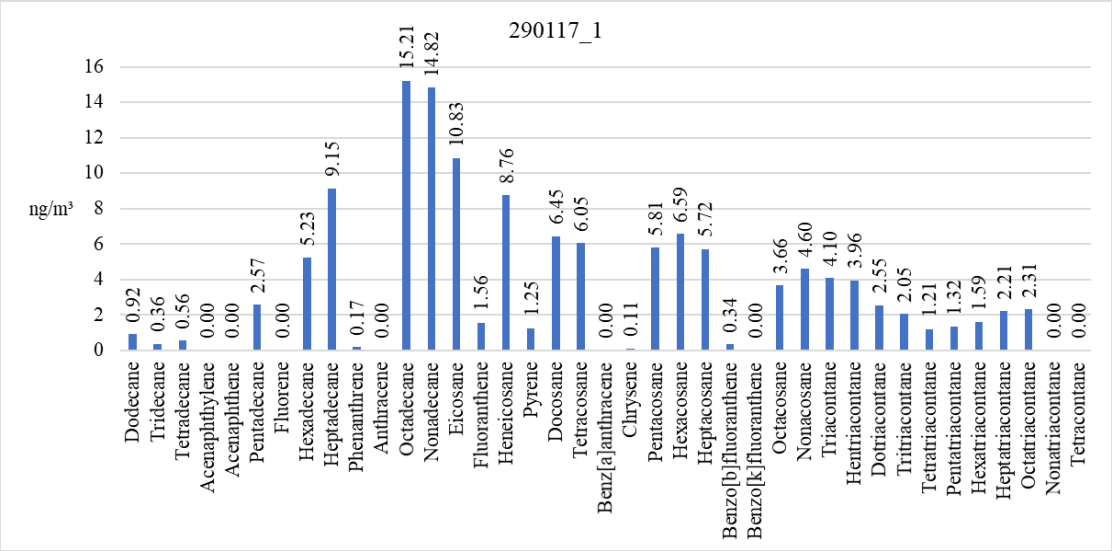

Figure A.7. Concentration of target compounds on 29.01.17 between 07:00-09:00.

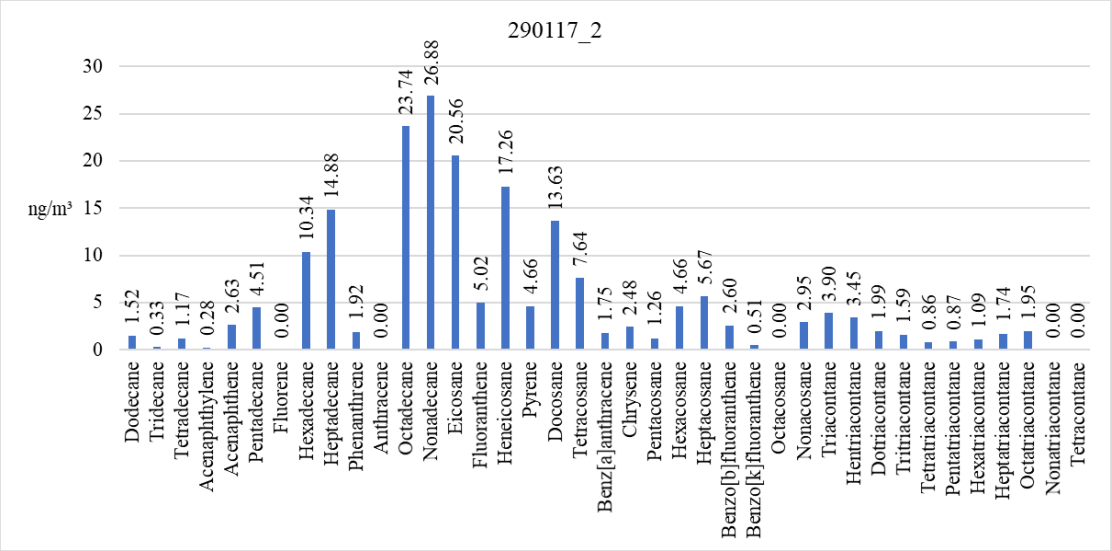

Figure A.8. Concentration of target compounds on 29.01.17 between 09:00-11:00.

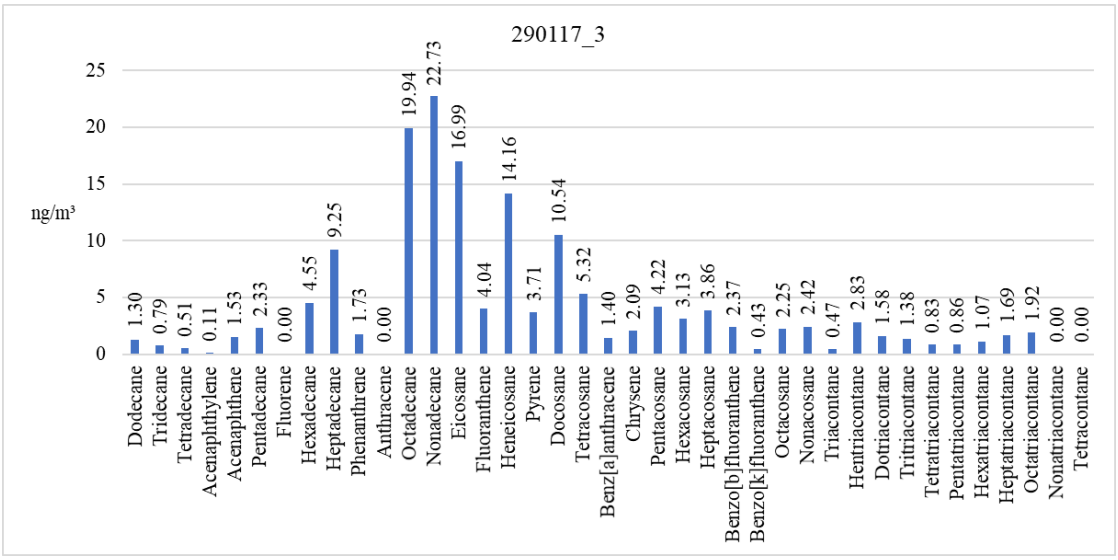

Figure A.9. Concentration of target compounds on 29.01.17 between 11:00-13:00.

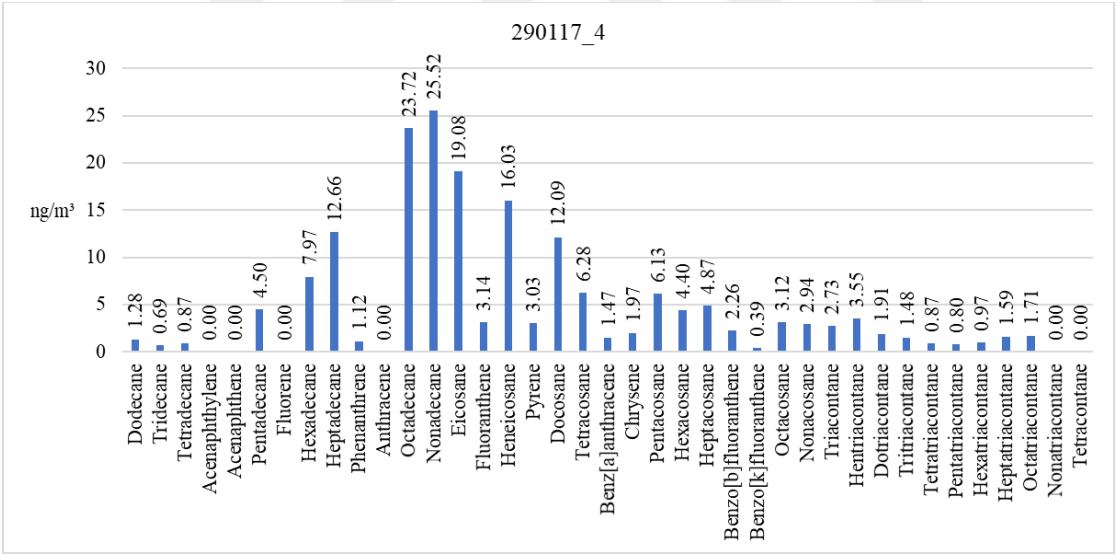

Figure A.10. Concentration of target compounds on 29.01.17 between 13:00-15:00.

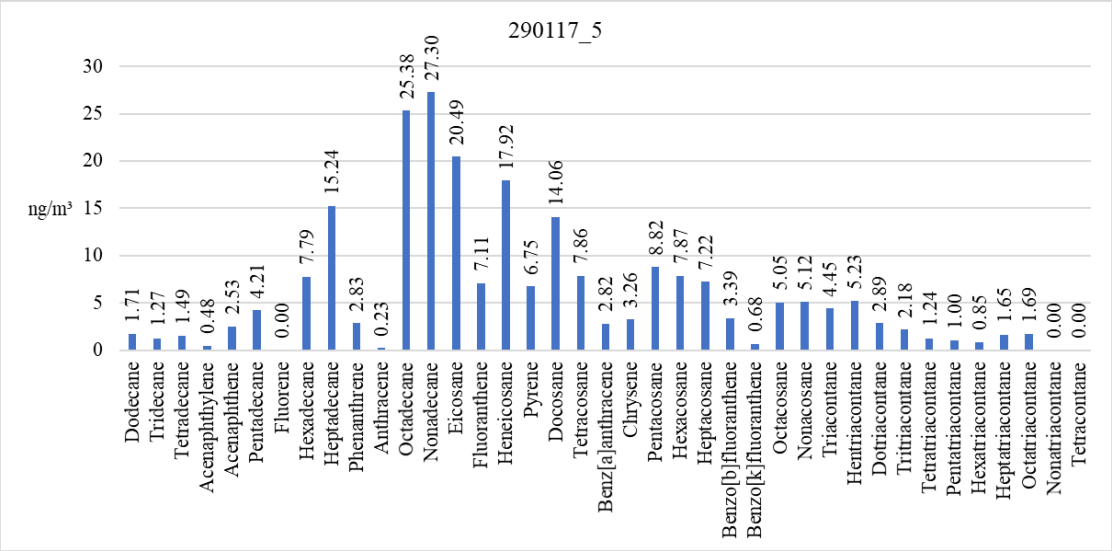

Figure A.11. Concentration of target compounds on 29.01.17 between 15:00-17:00.

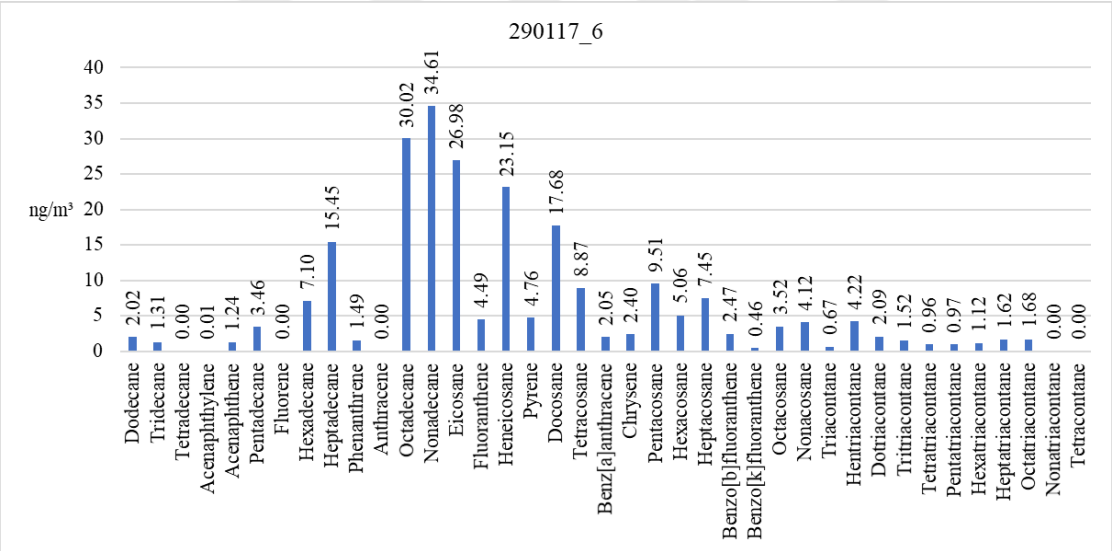

Figure A.12. Concentration of target compounds on 29.01.17 between 17:00-19:00.

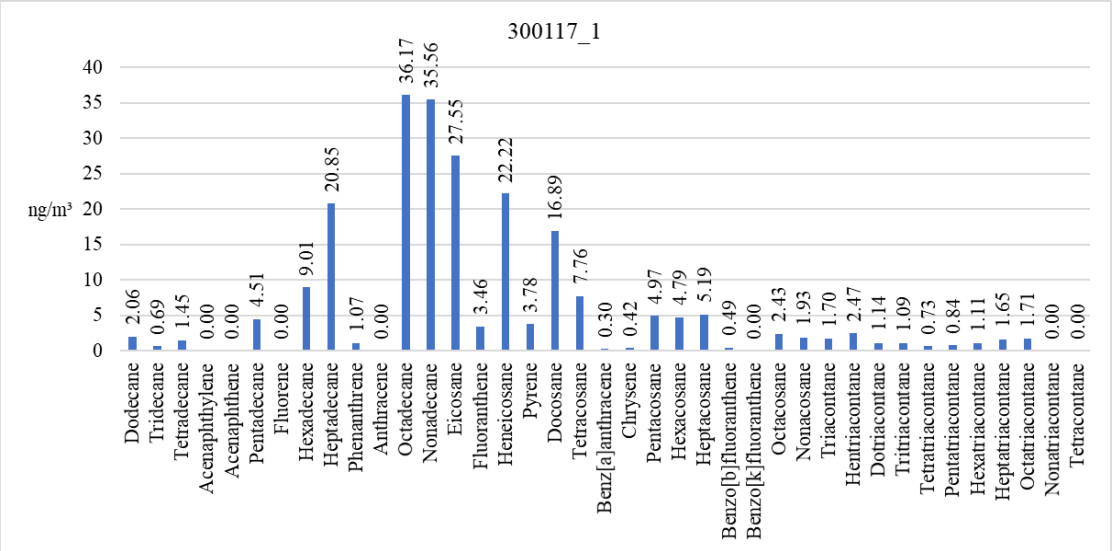

Figure A.13. Concentration of target compounds on 30.01.17 between 07:00-09:00.

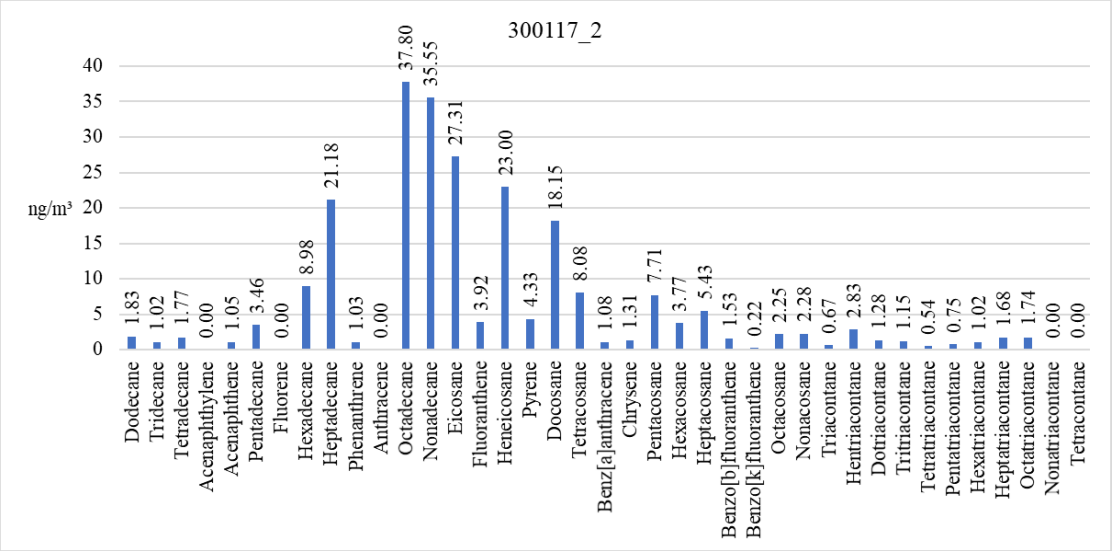

Figure A.14. Concentration of target compounds on 30.01.17 between 09:00-11:00.

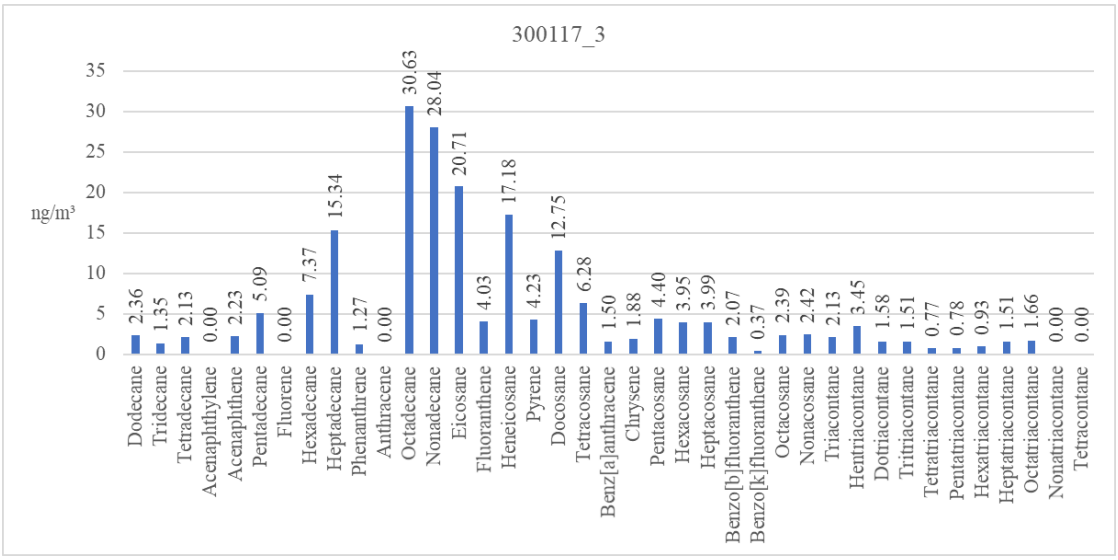

Figure A.15. Concentration of target compounds on 30.01.17 between 11:00-13:00.

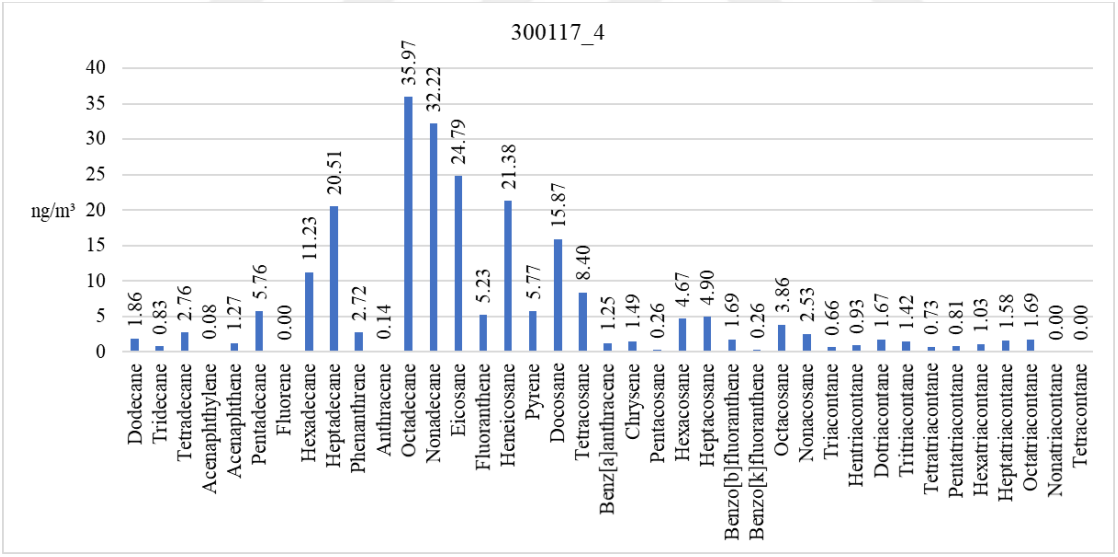

Figure A.16. Concentration of target compounds on 30.01.17 between 13:00-15:00.

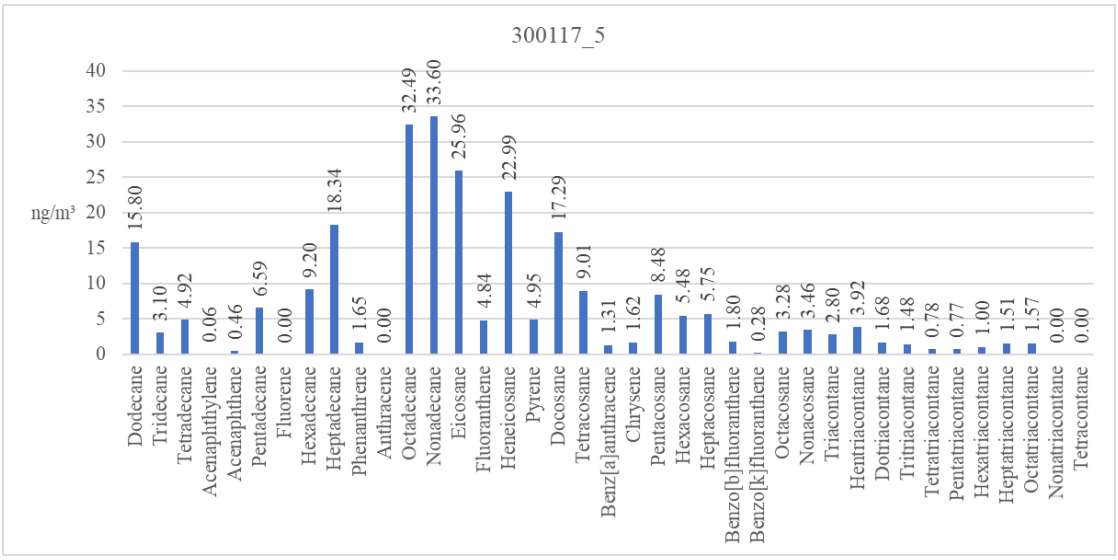

Figure A.17. Concentration of target compounds on 30.01.17 between 15:00-17:00.

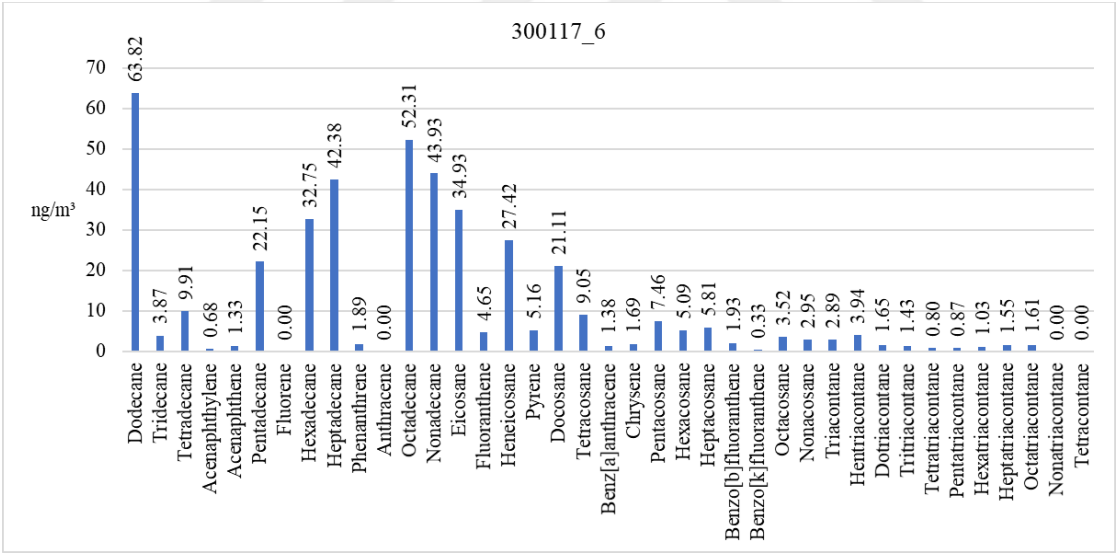

Figure A.18. Concentration of target compounds on 30.01.17 between 17:00-19:00.

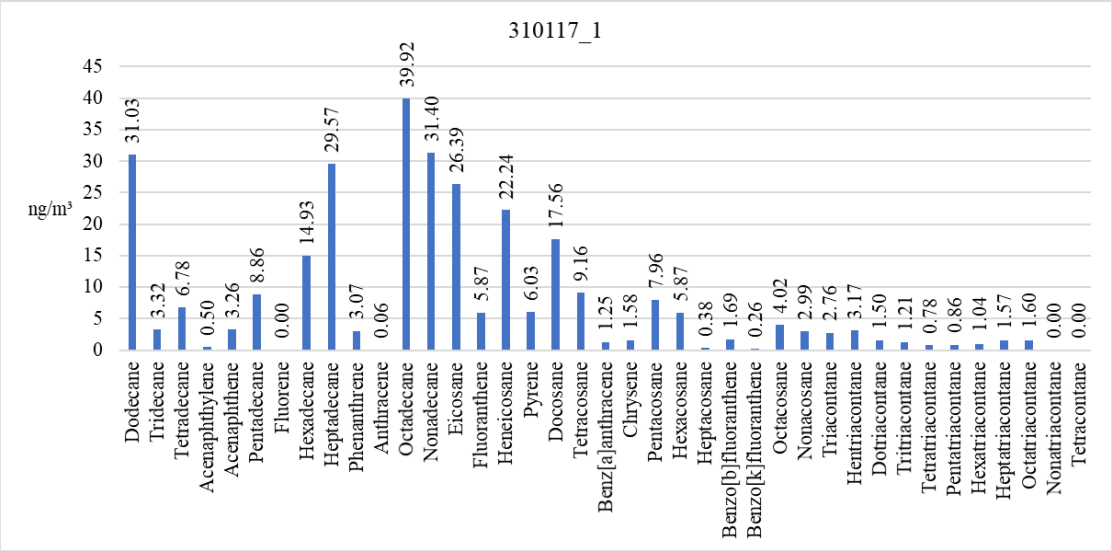

Figure A.19. Concentration of target compounds on 31.01.17 between 07:00-09:00.

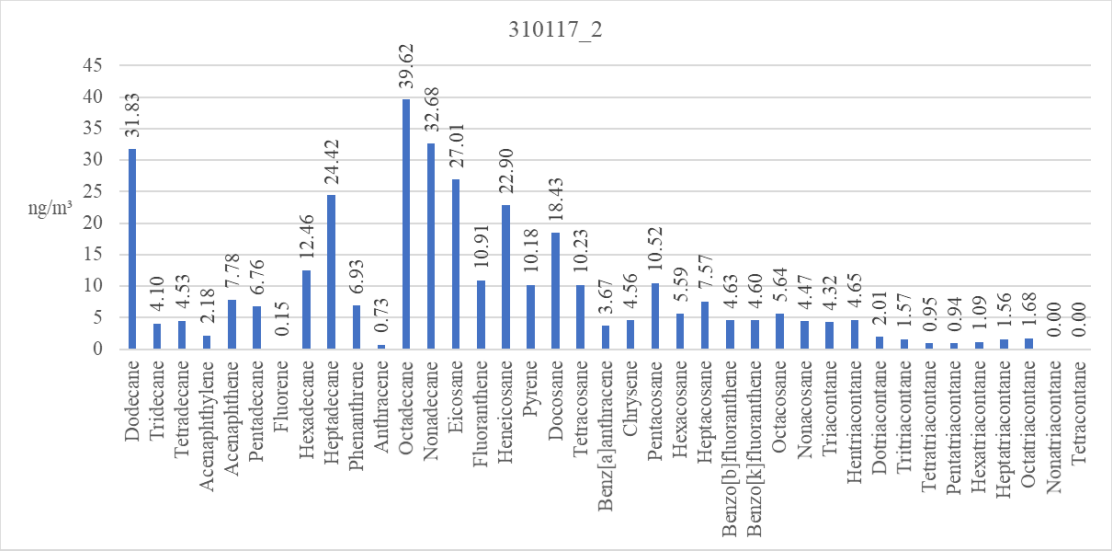

Figure A.20. Concentration of target compounds on 31.01.17 between 09:00-11:00.

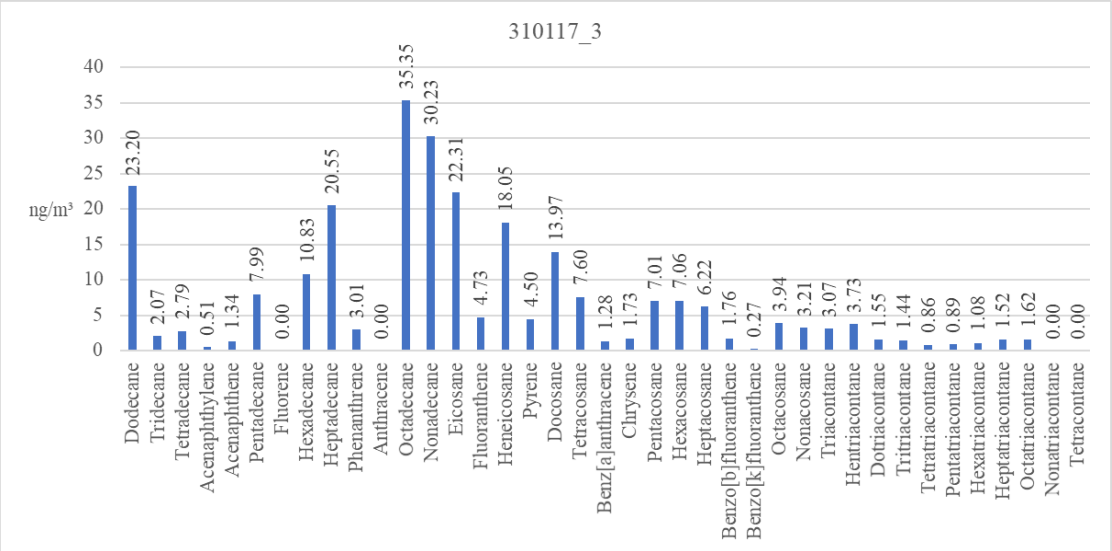

Figure A.21. Concentration of target compounds on 31.01.17 between 11:00-13:00.

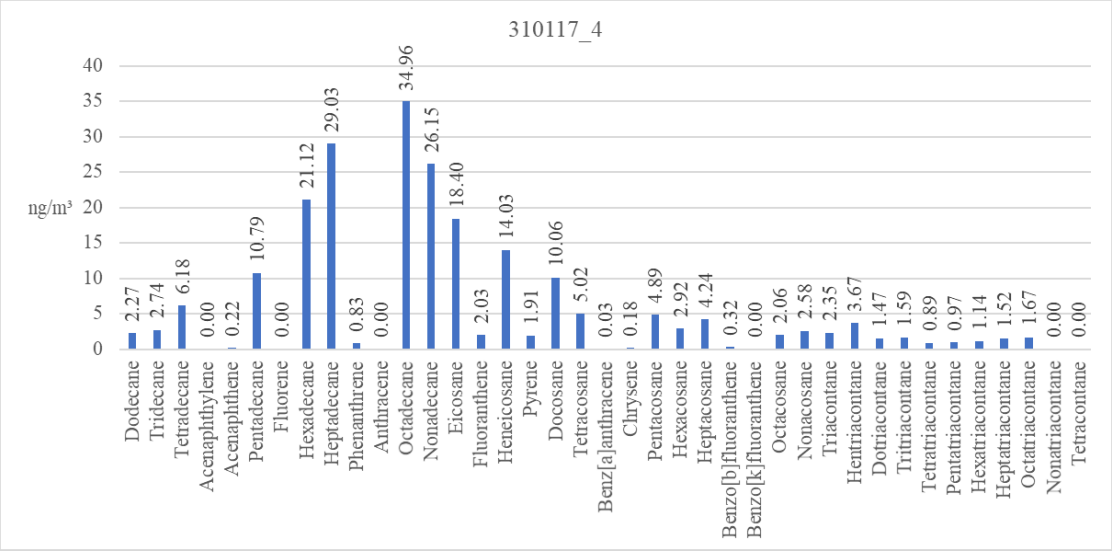

Figure A.22. Concentration of target compounds on 31.01.17 between 13:00-15:00.

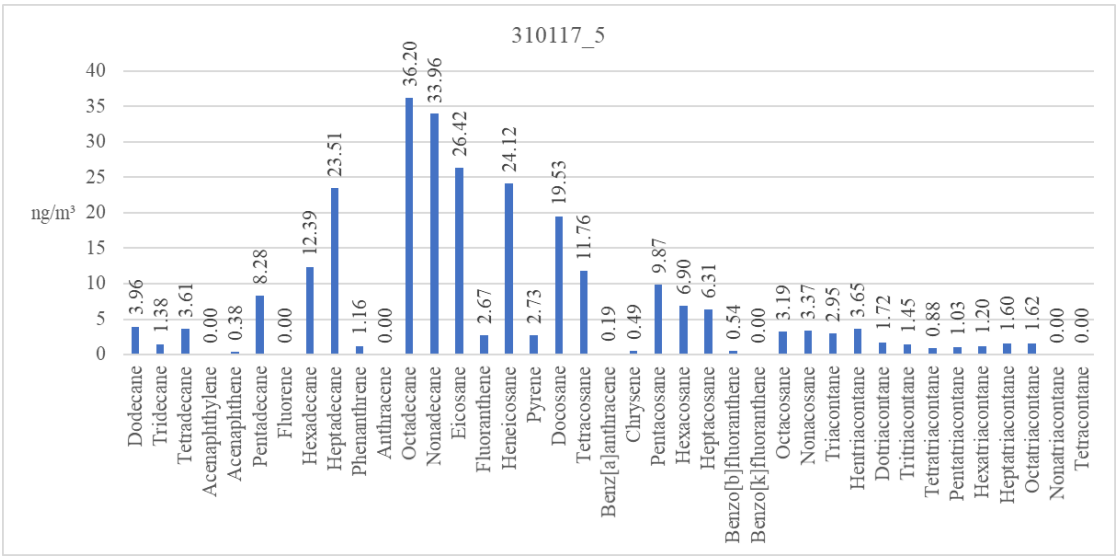

Figure A.23. Concentration of target compounds on 31.01.17 between 15:00-17:00.

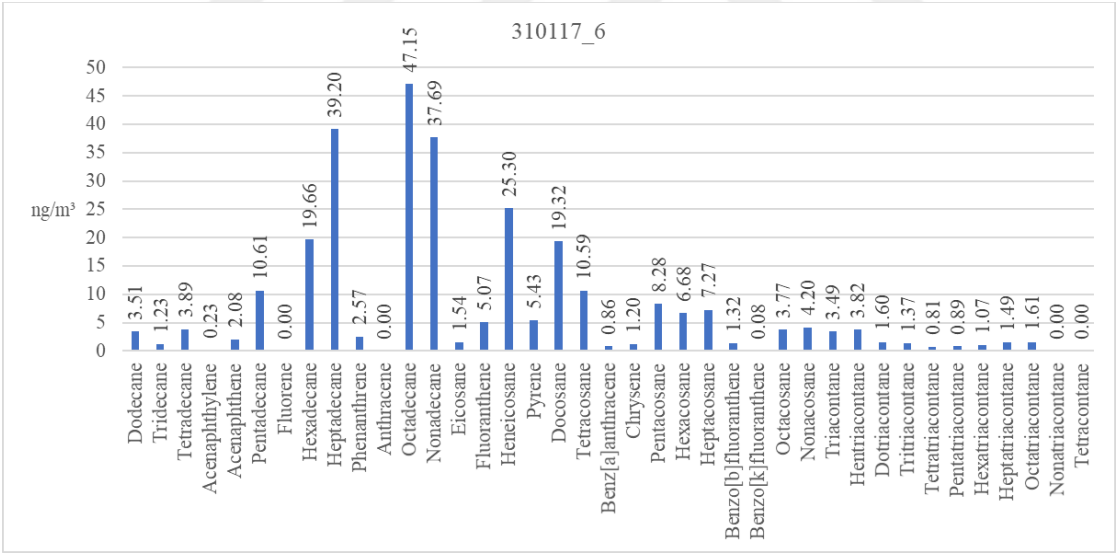

Figure A.24. Concentration of target compounds on 31.01.17 between 17:00-19:00.

CIRRICULUM VITAE

Akın Emrecan GÖK

Environmental Engineer

E-Mail : akingok@marun.edu.tr

: akinegok@gmail.com

EDUCATION

B. Sc.	2013–	Çukurova University, Faculty of Engineering and Architecture, Dept. of Environmental Eng., Adana
High School	2009–	ATO Anatolian High School, Adana
Primary School	2005–	Atatürk Primary School, Adana

LIST OF PUBLICATIONS

Gok, A.E., Flores, R.M., Ozdemir, H., Akkoyunlu, B., Demir, G., Unal, A., Tayanc, M. (November 2017), Evaluation of A Thermal Desorption Method for Complete Characterization of Organic Aerosols. In 8th Atmospheric Sciences Symposium (ATMOS 2017), 01 – 04 November 2017, Istanbul, Turkey.

Gok, A.E., Flores, R.M., Ozdemir, H., Akkoyunlu, B., Demir, G., Tayanc, M. (May 2017), Semi-volatile Organic Aerosol Composition in High-Time Resolved Ambient Air $PM_{2.5}$ Samples: Preliminary Results. In 2nd International Conference on Civil and Environmental Engineering (ICOCEE 2017), 8 – 10 May 2017, Cappadocia, Nevşehir, Turkey.

PROJECTS

Researcher –	Investigation of $PM_{2.5}$ and Hourly Semi Volatile Organic Compounds in Atmospheric Aerosols, Marmara University-TUBITAK, [Project number: TUBITAK-115Y625], 2016 – 2017.
Researcher –	Ortam Havasındaki Yarı Uçucu Organik Bileşiklerin Karakterizasyonu İçin Termal Desorpsiyon GC-MS Metodu Geliştirilmesi ve Validasyonu, BAPKO-C, Institute of Pure and Applied Sciences, Marmara University, [FEN-C-YLP-090217-0060], 2016 – 2017.